Headwater stream network connectivity: biogeochemical consequences and carbon fate

Kristen Alexandra Bretz

Dissertation submitted to the faculty of the Virginia Polytechnic Institute and State University in partial fulfillment of the requirements for the degree of

Doctor of Philosophy
In
Biological Sciences

Erin R. Hotchkiss, Chair
John E. Barrett
Daniel McLaughlin
C. Andrew Dolloff

April 19, 2023
Blacksburg, Virginia

Keywords: streams, biogeochemistry, carbon, climate change, carbon dioxide, methane, greenhouse gas, freshwater ecology

Headwater stream network connectivity: biogeochemical consequences and carbon fate

Kristen Alexandra Bretz

ABSTRACT

Headwaters may be small relative to other aquatic ecosystems, but they are neither simple nor static environments. Heterogeneous stream corridors constitute the majority of river network length and regulate cycling of carbon and oxygen as they expand and contract their connections across the landscape. Though headwater streams integrate many biogeochemical signals from the watersheds they drain and provide important ecosystem services, their diverse habitats and dynamic changes in wet length have been under-examined compared to dendritic, perennial streams. This oversight complicates efforts to identify biogeochemical patterns at larger scales. This dissertation sets out to expand our knowledge of stream biogeochemical responses to variable connections both within the channel and the wider stream corridor. First, I investigated how the presence and arrangement of different habitat patches in the stream corridor affected overall emissions of carbon dioxide (CO_2) and methane (CH_4) from sub-watersheds of a forested mountain stream network. To do this I measured concentration and flux of both gasses along and around 4 streams, including dry reaches and adjacent vernal pools as well as flowing water. I found that emissions were highly variable over space and time; in particular, the presence of a vernal pool enhanced total carbon emissions from the stream corridor. Next, to quantify carbon cycling and export from a non-perennial headwater stream, I monitored concentrations of CO_2 and dissolved organic carbon (DOC) at the stream outlet. I found that CO_2 concentration had a negative relationship with stream discharge, and that exports of both CO_2 and DOC were driven by storms reconnecting isolated surface water reaches. I also found that carbon biogeochemistry of intermediate flow states were unique from driest and highest-flow conditions. Finally, to explore how isolated pools in the stream channel respond to flow decrease and cessation, I measured dissolved oxygen (DO) as well as CO_2 and CH_4 from persistent pools of two non-perennial streams throughout an unusually dry summer and fall. I found that hypoxia was common in all isolated pools, but swings in DO were not consistent between pools even of the same stream. In using diel changes in DO to estimate metabolism, I also found that ecosystem respiration varied by stream, but gross primary production was more driven by stream surface water connectivity. Climate change is inducing many new patterns in stream hydrology with critical implications for biogeochemical activity, from reducing durations of connectivity to causing stronger storms. Improving our understanding of how surface water and landscape connectivity both influence the movement of carbon within and through streams is essential to resolving questions about the contributions of freshwaters to the global carbon cycle.

Headwater stream network connectivity: biogeochemical consequences and carbon fate

Kristen Alexandra Bretz

GENERAL AUDIENCE ABSTRACT

Headwater streams may seem inconsequential to larger ecosystem processes due to their small size. However, the majority of a river's network length, or the total length of all the streams and rivers from spring to ocean, is made up of headwater streams. The widespread presence of headwater streams over all types of land, along with the unique layout of different aquatic habitats near streams and the fact that small streams often grow and shrink in length, mean that studying headwaters can tell us many things about how energy moves through ecosystems. This dissertation explores how we can use changing headwater connectivity to understand how carbon moves through ecosystems. Connectivity in aquatic science refers to how water can move through space in ways that rocks and trees and even many animals cannot. This idea is useful because water carries things around as it moves, and its presence or absence enables reactions that are essential for the cycling of energy and nutrients. For instance, when water moves from high ground to low ground, it navigates through soil and holes in the ground; it may get slowed down at flat spots where little pools form. I measured emissions of carbon dioxide and methane from streams as well as soils, holes, and pools near mountain streams to try to understand how the path water takes influences how much carbon dioxide and methane escapes into the air. My measurements were surprisingly different depending on where and when I took them. I found that if a seasonal pond is connected to a stream channel, the stream will emit more greenhouse gasses than if the pond goes dry. Connectivity can also describe if water moves continuously along a stream, or if the stream goes dry in places and is then disconnected from different parts of itself. I asked how a stream becoming disconnected affected carbon dioxide emissions as well as the movement of dissolved organic carbon, a food source for microorganisms. I found that the less water moving through the stream channel, the higher carbon dioxide concentrations were. I also found that storms move both carbon dioxide and dissolved organic carbon out of streams quickly, even if the stream had been disconnected. Finally, I investigated the water that is left when streams disconnect. I measured dissolved oxygen, carbon dioxide, and methane in isolated pools of two disconnected streams. By tracking how microbes and algae consume and produce oxygen when a stream is not flowing, I can understand how these lifeforms adapt. I found that isolated pools frequently have very low levels of dissolved oxygen. This means that microorganisms in the pools have to use special ways of getting energy, which in turn affects how different forms of carbon move through the stream ecosystems. Headwater stream ecosystems are very sensitive to small changes in flow and precipitation; however, climate change means that streams are going dry more often than they used to. My findings contribute to our understanding of how changes in stream connectivity have many biological effects that are important for water quality and ecosystem health.

Acknowledgements

I would first like to thank Erin Hotchkiss for accepting someone into your lab who was clearly going through a third-of-life crisis. Your mentorship has had a tremendous impact on me as a scientist and as a person. You made my ideas seem interesting and important; few are lucky enough to get to research pretty much whatever they want for 5 years -- thank you for making that possible.

Major thanks to my committee – Daniel McLaughlin, Jeb Barrett, and Andy Dolloff – for their advice and support in many different forms. I've been grateful to have a committee of folks I genuinely enjoy talking to.

Special thanks to Bobbie Niederlehner for her patience in teaching me analytical chemistry techniques as well as for her friendship and humor. Thank you to J.P. Gannon for help with R and fun collaborations.

Thank you to my lab mates Brynn, Carla, Katherine, and Stephen, for your feedback, support, and positivity. Thanks to the many friends in my Virginia Tech communities and in Blacksburg that made me feel at home from the start. Thanks to all the undergraduate researchers who contributed to my projects, especially Jack, AJ, and Natalie.

Thanks to my funding sources: the National Science Foundation, the Virginia Water Resources Research Center, the Virginia Tech Global Change Center, and the Virginia Tech Department of Biological Sciences

Thank you to Heather Allen and Steve Whalen for your mentorship and encouragement over the years that helped me realize I could take on this challenge.

Most of all, thank you to my family for your love and for putting up with me through this process. To my parents, Karl and Debra, who let me wander around streams as a child and continue to teach me about plants against my will: your unwavering support means everything. Thanks to my grandma for keeping my spirits up and sending treats. Thank you to my husband, Graham, for being by my side through this journey; your insights, humor, and patience made the tough parts not so bad. Doing a Ph.D. is the best decision I ever made because it brought me to you.

Table of Contents

List of Figures

Chapter 5

List of Tables

Chapter 2

Chapter 3

Chapter 1: Introduction

Headwaters dominate aquatic network expanse yet undergo dynamic changes in length and connectivity. Headwater streams comprise over 80% of total river length (Downing et al., 2012) and are responsible for draining the vast majority of land cover on earth (Barmuta et al., 2009). Connections between headwater network components are frequently forming, severing, and rerouting. During heavy rainfall, wash paths that cut through terrestrial soils look like streams while wetlands form and merge in new ways. Stream networks also commonly include reaches where surface flow is intermittent or discontinuous. The physical heterogeneity of freshwater ecosystems and adjacent terrestrial landscapes means that biogeochemical activity is spatially variable among reaches and aquatic habitats within networks (Gomes & Wai, 2015). Given the many, overlapping pressures on aquatic ecosystems from climate change, land use change, and withdrawal, it is critical that we continue to improve our understanding of how changing hydrologic connectivity within headwater networks affects various ecosystem fluxes.

First order stream networks are sites of active cycling wherever they appear on the landscape. Streams are important players in the global carbon cycle because they process (i.e., metabolize) organic carbon from both external and internal sources (Battin et al., 2008). Terrestrially-derived organic carbon comes from the adjacent landscape and makes up the majority of headwater carbon substrate, while autochthonous organic carbon is derived from plant and microbial life within the stream's banks (Marx et al., 2017). Metabolism within an ecosystem includes the organic energy fixed from gross primary production (GPP) and its subsequent uptake and mineralization by organisms (ecosystem respiration, ER). The balance between GPP and ER, or net ecosystem production (NEP), tells us whether stream communities

respire more energy than they fix through GPP (Hall & Hotchkiss, 2017). Headwaters are typically heterotrophic (ER>GPP) since ER is subsidized by inputs of terrestrial organic energy sources. Organic matter inputs to streams are then respired via both aerobic and anaerobic pathways. Metabolic transformations are an essential component of the carbon flux through ecosystems (Staehr et al., 2012).

Dissolved oxygen (DO) is an essential variable controlling stream ecosystem functioning and carbon dynamics. Biogeochemical cycling involves microbial catalysis of oxidation-reduction (i.e., redox) reactions where electrons are transferred between chemical compounds to release energy (e.g., organic matter to O_2 or nitrate [NO_3^-]). DO availability drives these processes because microbial heterotrophs in the stream compete for use of terminal electron acceptors with the most favorable energy payoff, with oxygen being the top prize (Schlesinger & Bernhardt, 2013). Since the turbulence of flowing waters typically keeps them well oxygenated (Knapp et al., 2015), DO concentration thus dictates rates of organic carbon (OC) mineralization. When DO is completely consumed or flow disruption halts DO delivery, its absence initiates alternate biogeochemical pathways -- denitrification, metal and sulfate reduction, and methanogenesis -- that change OC mineralization outcomes.

Carbon emissions from streams are integrated signals of terrestrial and aquatic metabolism along with catchment geochemistry (Jones & Mulholland, 1998). Streams are typically sources of carbon dioxide (CO_2) and methane (CH_4) to the atmosphere (Raymond et al., 2013; Stanley et al., 2016); headwaters contribute as much as 30% of CO_2 emissions from all streams and rivers (Marx et al., 2017). Variable concentrations of CO_2 and CH_4 indicate relative importances of different microbial processes within the stream that produce and consume CO_2 and CH_4 (Baker et al., 2000; Stanley et al., 2016). Aerobic respiration of organic carbon in the

benthos and, to a lesser extent, in the water column, results in the production of CO_2. However, some of the CO_2 dissolved in stream water is not produced in the stream but rather was transported there from terrestrial sources (Hotchkiss et al., 2015; Marx et al., 2017). In anaerobic pore spaces of sediments or when oxygen has been depleted within a reach, CH_4 production occurs using CO_2 as a terminal electron acceptor in the oxidation of organic matter (Stumm & Morgan, 1996). Like CO_2, CH_4 may also be imported from hyporheic zones, groundwater, and some soil waters (Jones & Mulholland, 1998; Leith et al., 2014).

Global change is expected to increase both CO_2 (Ran et al., 2021) and CH_4 (Rosentreter et al., 2021) concentrations in headwaters through land use change, greater soil flushing from intense precipitation, and positive temperature feedbacks on metabolic processes. The tight coupling between small streams and their surroundings means that they are sensitive to changes in adjacent ecosystem processes and hydrologic connections, resulting in highly variable fluxes of greenhouse gasses. Spatial and temporal heterogeneity of CO_2 and CH_4 fluxes within headwater networks presents a challenge for developing reliable landscape or regional carbon budgets. The high resolution of data required for large-scale estimates of carbon gas evasion is particularly difficult to meet in headwaters due to their being so numerous and frequently difficult to access. Even with increased attention to constraining variability, studies continue to reveal sources of uncertainty and underestimation in emissions (Drake et al., 2018; Gómez-Gener et al., 2021; Pu et al., 2019; Wallin et al., 2018). Given the intense magnitude of emissions from streams and rivers (Raymond et al., 2013), an improved understanding of local drivers of emissions is essential to building network-scale assessments of carbon movement, metabolism, and fate to understand changes in global-scale carbon cycling (Battin et al., 2023).

The Stream Corridor

Streams are often depicted as simplified continua, facilitating the transport of solutes and reactions along an uninterrupted downhill gradient. However, walking among many headwater networks will reveal channels and flow paths that tangle, pinch, flatten, and dig. Channel physical heterogeneity is the result of catchment topography, geology, and climate, as well as the structure of the surrounding ecosystem. Headwater networks include not just stream channels, but interconnected riparian wetlands, vernal pools, overland flow paths, groundwater flow paths of many depths, and seeps. The stream channel with its surrounding floodplain with associated features, such as those vernal pools and flow paths as well as fluvial deposits and riparian zones, make up a river corridor (Harvey & Gooseff, 2015). The number and shapes of connections between network elements and the stream or river itself influence how the stream processes carbon (Vidon & Serchan, 2016). Additionally, network connectivity is dynamic over time, with storms and seasons influencing the durations of exchange between different parts of the network.

In Chapter 2, I ask how the presence and arrangement of interconnected habitat patches influences stream corridor carbon emissions. I began by searching for patterns of CO_2 and CH_4 concentration and emission in physically heterogeneous stream habitats, and then expanded this search to incorporate changing connectivity to habitats adjacent to the stream. Working at Coweeta Hydrologic Laboratory in western North Carolina, I built a layout of stream corridor components within diverse subcatchments of a mountainous headwater network. From this perspective, I tested how the inclusion of carbon emissions from different patches affects upscaling estimates from stream corridors.

Non-perennial Stream Biogeochemistry and Ecology

Non-perennial streams, comprising many types of streams that do not flow continuously, account for more than half of river and stream networks globally (Messager et al., 2021). Headwaters in particular are highly susceptible to dramatic changes in length and surface water continuity with season, precipitation, and water demand from evapotranspiration as well as human withdrawals and diversions. Traditionally, headwaters were thought to expand in an upstream direction in response to the seasonal rising of the water table (Day, 1978). However, surface water coverage through stream channels may also occur in a downstream direction from springs (Godsey & Kirchner, 2014) or expand from multiple points as isolated pools become linked. Controls including climate, geology, plant community structure, and anthropogenic influence act in different proportions to influence patterns of surface water fragmentation and expansion within watersheds (Shanafield et al., 2021). In the small, mountainous headwaters I have focussed on, discontinuous surface waters have a few common shapes and patterns. Flow is typically highest from late winter to mid-spring. As evapotranspiration ramps up in late spring, streams can form dry patches in a matter of days. If precipitation does not come, dry patches will grow to encompass most of the "riffle" reaches of the stream. From mid-summer to late fall or early winter, small pools of varying width, depth, and temperature will persist within stream channels at groundwater seeps and/or over pockets of bedrock where infiltration of surface water into hyporheic flow paths is impossible.

Flow disruptions are important to stream carbon budgets because they alter carbon transport and reactivity (Hale & Godsey, 2019; von Schiller et al., 2015). Early work on an arid stream, Sycamore Creek, was fundamental to understanding disturbance (Grimm, 1994), succession (Fisher et al., 1982), and the role of the hyporheic zone (Jones, 1995; Jones et al., 1995) on stream carbon cycling. However, the later exclusion of non-perennial streams and

rivers from many quantitative estimates of carbon biogeochemical fluxes (Zimmer et al., 2022) and river conceptual models (Allen et al., 2020) is a major knowledge gap in freshwater research. Many studies of non-perennial streams have been opportunistic and limited to those arid and semi-arid regions. However, flow disruption is both common and variable among humid, forested environments as well (Jensen et al., 2017). Non-perennial streams serve important roles as habitat refugia for aquatic species (Bruno et al., 2022) and flood-control mechanisms for downstream ecosystems (Datry et al., 2018). Further, study of non-perennial systems will likely be increasingly important as they increase in number (Zipper et al., 2021) due to changing precipitation patterns and water draw-down (Jaeger et al., 2014).

Carbon Cycling and Metabolism in Non-perennial Streams

Cycles of drying and rewetting in a non-perennial stream influence the concentrations of CO_2 and DOC in stream water (Hale & Godsey, 2019; Keller et al., 2020). Dry down results in isolated surface water reaches with low DO and high concentrations of CO_2. Storms are key drivers of biogeochemical activity in non-perennial streams when the stream is not fully flowing, because they flush away built up solutes and gasses (Mcdowell & Johnson, 2018) while refreshing supply of DO and organic matter substrates from upstream and terrestrial sources. While non-perennial streams do not exist in binary states of either flowing or non-flowing, many studies have put a spotlight on the most extreme dry phases or moments of brief rewetting (e.g., (Acuna et al., 2004; MacNeille et al., 2020; Meisner et al., 2015; Vazquez et al., 2011). Instead, the channel undergoes constant fluctuations in water level that I predicted would result in concurrent changes in carbon cycling.

My goal in Chapter 3 is to characterize the various flow states and biogeochemistry of a non-perennial stream to better examine the subtleties of carbon transformation and export with changing hydrology. I investigated how discharge affected CO_2 concentration and emissions over time, applying a concentration-discharge analysis to CO_2 in a non-perennial system, thus tracking how CO_2 concentration changed with flow through the stream. I also wanted to find out if DOC-flow relationships would be different from similar perennial systems, and if they changed under different types of flow conditions within a non-perennial stream.

Disruptions in surface water connectivity can alter in-stream rates of GPP and ER (Bernal et al., 2022; Stanley et al., 2004). Previous work in non-perennial systems found wet-dry cycles were associated with laboratory assay respiration pulses from exposed stream channel sediments (Coulson et al., 2022; Keller et al., 2020; Schreckinger et al., 2022; Von Schiller et al., 2019). Little attention has so far been given to the water that remains in the stream through a dry-down event, and how metabolism may respond to flow changes in a non-perennial system. In-stream levels of CO_2 in mountainous headwaters are mostly sourced from outside the channel, as ER is lower in cooler, quicker-flowing waters. Additionally, in perennial forested streams, ER tends to dominate over GPP due to light limitation of GPP by the canopy cover, leading to an even greater surplus of CO_2. These patterns have largely been determined in ecosystems where oxygen is continually available and where groundwater inputs are very small. Thus measuring changes in DO concentration using sensors placed in an open channel has led to a proliferation of metabolism estimates from a wide array of perennial streams. The oxygen dynamics of non-perennial streams are much more unpredictable and less frequently monitored, however, which has ramifications for both metabolic activity as well as how we measure metabolism.

Chapter 4 explores DO and metabolic patterns of persistent pools in two non-perennial streams. This exploration came from what I learned about corridor CO_2 and CH_4 heterogeneity (Chapter 2) together with the biogeochemical responses of surface water isolation (Chapter 3), and I wanted to find out if DO drawdown took on similar patterns in pools within and between two different streams. I asked how CO_2 and CH_4 in pools might follow the behavior of DO in geomorphically distinct pools. I also set out to test if stream metabolism could be estimated in pools without surface water connectivity when DO concentrations are often erratic and extremely low, and how those estimates compare to perennial stream metabolism from headwaters.

Together, the studies included in this dissertation seek to address biogeochemical questions in "messy" headwater stream networks. Heterogeneous and intermittent streams have unique roles in commingling carbon from many sources through biogeochemical processes and sending it down the network or into the atmosphere. The unifying theme of the following chapters is expanding our understanding of biogeochemical processes as stream reaches connect and disconnect from the wider aquatic network and surrounding landscape in varying ways. By piecing together the puzzle of CO_2 and CH_4 fluxes from various parts of a stream corridor, my work is relevant to efforts to understand the contributions of inland waters to the global carbon cycle. My investigations also highlight how climate change-induced changes in hydrology affect the transport and cycling of carbon through aquatic ecosystems, with implications for ecosystem function and management.

References

Acuna, V., Adonis, G., Munoz, I., Uehlinger, U., & Sabater, S. (2004). Flow extremes and benthic organic matter shape the metabolism of a headwater Mediterranean stream. *Freshwater Biology*, *49*, 960–971.

Allen, D. C., Datry, T., Boersma, K. S., Bogan, M. T., Boulton, A. J., Bruno, D., Busch, M. H., Costigan, K. H., Dodds, W. K., Fritz, K. M., Godsey, S. E., Jones, J. B., Kaletova, T., Kampf, S. K., Mims, M. C., Neeson, T. M., Olden, J. D., Pastor, A. V., Poff, N. L., … Zimmer, M. (2020). River ecosystem conceptual models and non-perennial rivers: A critical review. *WIREs Water*, *7*(5), e1473. https://doi.org/10.1002/wat2.1473

Baker, M. A., Valett, H. M., & Dahm, C. N. (2000). Organic carbon supply and metabolism in a shallow groundwater ecosystem. *Ecology*, *81*(11), 3133–3148. https://doi.org/10.1890/0012-9658(2000)081[3133:OCSAMI]2.0.CO;2

Barmuta, L. A., Watson, A., Clarke, A., & Clapcott, J. E. (2009). *The importance of headwater streams. Waterlines report*, National Water Commission, Canberra.

Battin, T. J., Kaplan, L. A., Findlay, S., Hopkinson, C. S., Marti, E., Packman, A. I., Newbold, J. D., & Sabater, F. (2008). Biophysical controls on organic carbon fluxes in fluvial networks. *Nature Geoscience*, *1*(2), 95–100. https://doi.org/10.1038/ngeo101

Battin, T. J., Lauerwald, R., Bernhardt, E. S., Bertuzzo, E., Gener, L. G., Hall, R. O., Jr, Hotchkiss, E. R., Maavara, T., Pavelsky, T. M., Ran, L., Raymond, P., Rosentreter, J. A., & Regnier, P. (2023). River ecosystem metabolism and carbon biogeochemistry in a changing world. *Nature*, *613*(7944), 449–459. https://doi.org/10.1038/s41586-022-05500-8

Bernal, S., Cohen, M. J., Ledesma, J. L. J., Kirk, L., Martí, E., & Lupon, A. (2022). Stream metabolism sources a large fraction of carbon dioxide to the atmosphere in two hydrologically contrasting headwater streams. *Limnology and Oceanography*, *67*(12), 2621–2634. https://doi.org/10.1002/lno.12226

Bruno, D., Hermoso, V., Sánchez-Montoya, M. M., Belmar, O., Gutiérrez-Cánovas, C., & Cañedo-Argüelles, M. (2022). Ecological relevance of non-perennial rivers for the conservation of terrestrial and aquatic communities. *Conservation Biology: The Journal of the Society for Conservation Biology*, *36*(6), e13982. https://doi.org/10.1111/cobi.13982

Coulson, L. E., Weigelhofer, G., Gill, S., Hein, T., Griebler, C., & Schelker, J. (2022). Small rain events during drought alter sediment dissolved organic carbon leaching and respiration in intermittent stream sediments. *Biogeochemistry*, *159*(2), 159–178. https://doi.org/10.1007/s10533-022-00919-7

Datry, T., Boulton, A. J., Bonada, N., Fritz, K., Leigh, C., Sauquet, E., Tockner, K., Hugueny, B., & Dahm, C. N. (2018). Flow intermittence and ecosystem services in rivers of the Anthropocene. *The Journal of Applied Ecology*, *55*(1), 353–364. https://doi.org/10.1111/1365-2664.12941

Day, D. G. (1978). Drainage density changes during rainfall. *Earth Surface Processes and Landforms*, *3*(3), 319–326. https://doi.org/10.1002/esp.3290030310

Downing, J. A., Cole, J. J., Duarte, C. M., Middelburg, J. J., Melack, J. M., Prairie, Y. T., Kortelainen, P., Striegl, R. G., Mcdowell, W. H., & Tranvik, L. J. (2012). *Inland Waters Global abundance and size distribution of streams and rivers*. https://doi.org/10.5268/IW-2.4.502

Drake, T. W., Raymond, P. A., & Spencer, R. G. M. (2018). Terrestrial carbon inputs to inland waters: A current synthesis of estimates and uncertainty. *Limnology and Oceanography Letters*, *3*(3), 132–142. https://doi.org/10.1002/lol2.10055

Fisher, S. G., Gray, L. J., Grimm, N. B., & Busch, D. E. (1982). Temporal succession in a desert stream ecosystem following flash flooding. *Ecological Monographs*, *52*(1), 93–110. https://doi.org/10.2307/2937346

Godsey, S. E., & Kirchner, J. W. (2014). Dynamic, discontinuous stream networks: hydrologically driven variations in active drainage density, flowing channels and stream order. *Hydrological Processes*, *28*(23), 5791–5803. https://doi.org/10.1002/hyp.10310

Gomes, P. I. A., & Wai, O. W. H. (2015). In-stream Physical Heterogeneity, Rainfall Aided Flushing, and Discharge on Stream Water Quality. *Water Environment Research: A Research Publication of the Water Environment Federation*, *87*(8), 758–768. https://doi.org/10.2175/106143015X14362865225997

Gómez-Gener, L., Rocher-Ros, G., Battin, T., Cohen, M. J., Dalmagro, H. J., Dinsmore, K. J., Drake, T. W., Duvert, C., Enrich-Prast, A., Horgby, Å., Johnson, M. S., Kirk, L., Machado-Silva, F., Marzolf, N. S., McDowell, M. J., McDowell, W. H., Miettinen, H., Ojala, A. K., Peter, H., … Sponseller, R. A. (2021). Global carbon dioxide efflux from rivers enhanced by high nocturnal emissions. *Nature Geoscience*, *14*(5), 289–294. https://doi.org/10.1038/s41561-021-00722-3

Grimm, N. B. (1994). Disturbance, succession and ecosystem processes in streams: a case study from the desert. *Aquatic Ecology: Scale, Pattern and Process*, 93–112. http://www.nativefishlab.net/library/textpdf/17783.pdf

Hale, R. L., & Godsey, S. E. (2019). Dynamic stream network intermittence explains emergent dissolved organic carbon chemostasis in headwaters. *Hydrological Processes*, hyp.13455. https://doi.org/10.1002/hyp.13455

Hall, R. O., & Hotchkiss, E. R. (2017). Chapter 34 - Stream Metabolism. In G. A. Lamberti & F. R. Hauer (Eds.), *Methods in Stream Ecology (Third Edition)* (pp. 219–233). Academic Press. https://doi.org/10.1016/B978-0-12-813047-6.00012-7

Harvey, J., & Gooseff, M. (2015). River corridor science: Hydrologic exchange and ecological consequences from bedforms to basins. *Water Resources Research*, *51*(9), 6893–6922. https://doi.org/10.1002/2015WR017617@10.1002/(ISSN)1944-7973.WRR50

Hotchkiss, E. R., Hall, R. O., Jr, Sponseller, R. A., Butman, D., Klaminder, J., Laudon, H., Rosvall, M., & Karlsson, J. (2015). Sources of and processes controlling CO 2 emissions change with the size of streams and rivers. *Nature Geoscience*, *8*(9), 696–699. https://doi.org/10.1038/ngeo2507

Jaeger, K. L., Olden, J. D., & Pelland, N. A. (2014). Climate change poised to threaten

hydrologic connectivity and endemic fishes in dryland streams. *Proceedings of the 22nd International Conference on 3D Web Technology - Web3D '17*, *111*(38), 13894–13899. https://doi.org/10.1073/pnas.1320890111

Jensen, C. K., McGuire, K. J., & Prince, P. S. (2017). Headwater stream length dynamics across four physiographic provinces of the Appalachian Highlands. *Hydrological Processes*, *31*(19), 3350–3363. https://doi.org/10.1002/hyp.11259

Jones, J. B. (1995). Factors controlling hyporheic respiration in a desert stream. *Freshwater Biology*, *34*(1), 91–99. https://doi.org/10.1111/j.1365-2427.1995.tb00426.x

Jones, J. B., Fisher, S. G., & Grimm, N. B. (1995). Vertical hydrologic exchange and ecosystem metabolism in a sonoran desert stream. *Ecology*, *76*(3), 942–952. https://doi.org/10.2307/1939358

Jones, J. B., & Mulholland, P. J. (1998). Influence of drainage basin topography and elevation on carbon dioxide and methane supersaturation of stream water. *Biogeochemistry*, *40*(1), 57–72. https://doi.org/10.1023/A:1005914121280

Keller, P. S., Catalán, N., von Schiller, D., Grossart, H. P., Koschorreck, M., Obrador, B., Frassl, M. A., Karakaya, N., Barros, N., Howitt, J. A., Mendoza-Lera, C., Pastor, A., Flaim, G., Aben, R., Riis, T., Arce, M. I., Onandia, G., Paranaíba, J. R., Linkhorst, A., … Marcé, R. (2020). Global CO2 emissions from dry inland waters share common drivers across ecosystems. *Nature Communications*, *11*(1). https://doi.org/10.1038/s41467-020-15929-y

Knapp, J. L. A., Osenbrück, K., & Cirpka, O. A. (2015). Impact of non-idealities in gas-tracer tests on the estimation of reaeration, respiration, and photosynthesis rates in streams. *Water Research*, *83*, 205–216. https://doi.org/10.1016/j.watres.2015.06.032

Leith, F. I., Garnett, M. H., Dinsmore, K. J., Billett, M. F., & Heal, K. V. (2014). Source and age of dissolved and gaseous carbon in a peatland-riparian-stream continuum: A dual isotope (14C and δ13C) analysis. *Biogeochemistry*, *119*(1-3), 415–433. https://doi.org/10.1007/s10533-014-9977-y

MacNeille, R. B., Lohse, K. A., Godsey, S. E., Perdrial, J. N., & Baxter, C. V. (2020). Influence of Drying and Wildfire on Longitudinal Chemistry Patterns and Processes of Intermittent Streams. *Frontiers in Water*, *2*. https://doi.org/10.3389/frwa.2020.563841

Marx, A., Dusek, J., Jankovec, J., Sanda, M., Vogel, T., van Geldern, R., Hartmann, J., & Barth, J. A. C. (2017). A review of CO2 and associated carbon dynamics in headwater streams: A global perspective. *Reviews of Geophysics* , *55*(2), 560–585. https://doi.org/10.1002/2016RG000547

McDowell, M. J., & Johnson, M. S. (2018). Gas Transfer Velocities Evaluated Using Carbon Dioxide as a Tracer Show High Streamflow to Be a Major Driver of Total CO2 Evasion Flux for a Headwater Stream. *Journal of Geophysical Research: Biogeosciences*, *123*, 2183–2197. https://doi.org/10.1029/2018JG004388

Meisner, A., Rousk, J., & Bååth, E. (2015). Prolonged drought changes the bacterial growth response to rewetting. *Soil Biology & Biochemistry*, *88*, 314–322. https://doi.org/10.1016/j.soilbio.2015.06.002

Messager, M. L., Lehner, B., Cockburn, C., Lamouroux, N., Pella, H., Snelder, T., Tockner, K., Trautmann, T., Watt, C., & Datry, T. (2021). Global prevalence of non-perennial rivers and streams. *Nature*, *594*(7863), 391–397. https://doi.org/10.1038/s41586-021-03565-5

Pu, J., Li, J., Zhang, T., Xiong, X., & Yuan, D. (2019). High spatial and seasonal heterogeneity of pCO2 and CO2 emissions in a karst groundwater-stream continuum, southern China. *Environmental Science and Pollution Research*, *26*(25), 25733–25748. https://doi.org/10.1007/s11356-019-05820-9

Ran, L., Butman, D. E., Battin, T. J., Yang, X., Tian, M., Duvert, C., Hartmann, J., Geeraert, N., & Liu, S. (2021). Substantial decrease in CO2 emissions from Chinese inland waters due to global change. *Nature Communications*, *12*(1), 1730. https://doi.org/10.1038/s41467-021-21926-6

Raymond, P. A., Hartmann, J., Lauerwald, R., Sobek, S., McDonald, C., Hoover, M., Butman, D., Striegl, R., Mayorga, E., Humborg, C., Kortelainen, P., Dürr, H., Meybeck, M., Ciais, P., & Guth, P. (2013). Global carbon dioxide emissions from inland waters. *Nature*, *503*(7476), 355–359. https://doi.org/10.1038/nature12760

Rosentreter, J. A., Borges, A. V., Deemer, B. R., Holgerson, M. A., Liu, S., Song, C., Melack, J., Raymond, P. A., Duarte, C. M., Allen, G. H., Olefeldt, D., Poulter, B., Battin, T. I., & Eyre, B. D. (2021). Half of global methane emissions come from highly variable aquatic ecosystem sources. *Nature Geoscience*, *14*(4), 225–230. https://doi.org/10.1038/s41561-021-00715-2

Schlesinger, W. H., & Bernhardt, E. S. (2013). *Biogeochemistry: An Analysis of Global Change*. Academic Press. https://play.google.com/store/books/details?id=533UOWBU3_AC

Schreckinger, J., Mutz, M., & Mendoza-Lera, C. (2022). When water returns: Drying history shapes respiration and nutrients release of intermittent river sediment. *The Science of the Total Environment*, *838*(Pt 1), 155950. https://doi.org/10.1016/j.scitotenv.2022.155950

Shanafield, M., Bourke, S. A., Zimmer, M. A., & Costigan, K. (2021). An overview of the hydrology of non-perennial rivers and streams. *WIREs Water*, *8*(e1504). https://doi.org/10.1002/wat2.1504

Staehr, P. A., Testa, J. M., Kemp, W. M., Cole, J. J., Sand-Jensen, K., & Smith, S. V. (2012). The metabolism of aquatic ecosystems: history, applications, and future challenges. *Aquatic Sciences*, *74*(1), 15–29. https://doi.org/10.1007/s00027-011-0199-2

Stanley, E. H., Casson, N. J., Christel, S. T., Crawford, J. T., Loken, L. C., & Oliver, S. K. (2016). The ecology of methane in streams and rivers: patterns, controls, and significance. *Ecological Monographs*, *86*(2), 146–171. https://esajournals.onlinelibrary.wiley.com/doi/pdf/10.1890/15-1027

Stanley, E. H., Fisher, S. G., & Jones, J. B. (2004). Effects of water loss on primary production: A landscape-scale model. *Aquatic Sciences*, *66*(1), 130–138. https://doi.org/10.1007/s00027-003-0646-9

Stumm, W., & Morgan, J. J. (1996). *Aquatic chemistry* (3rd ed., p. 1040). Wiley-Interscience.

Vazquez, E., Amalfitano, S., Fazi, S., & Butturini, A. (2011). Dissolved organic matter

composition in a fragmented Mediterranean fluvial system under severe drought conditions. *Biogeochemistry*, *102*(1), 59–72. https://doi.org/10.1007/s10533-010-9421-x

Vidon, P., & Serchan, S. (2016). Impact of Stream Geomorphology on Greenhouse Gas Concentration in a New York Mountain Stream. *Water, Air, and Soil Pollution*, *227*(12), 428. https://doi.org/10.1007/s11270-016-3131-5

Von Schiller, D., Datry, T., Corti, R., Foulquier, A., Tockner, K., Marcé, R., García-Baquero, G., Odriozola, I., Obrador, B., Elosegi, A., Mendoza-Lera, C., Gessner, M. O., Stubbington, R., Albariño, R., Allen, D. C., Altermatt, F., Arce, M. I., Arnon, S., Banas, D., … Zoppini, A. (2019). Sediment respiration pulses in intermittent rivers and ephemeral streams. *Global Biogeochemical Cycles*, *33*(10), 1251–1263. https://doi.org/10.1029/2019gb006276

von Schiller, D., Graeber, D., Ribot, M., Timoner, X., Acuña, V., Martí, E., Sabater, S., & Tockner, K. (2015). Hydrological transitions drive dissolved organic matter quantity and composition in a temporary Mediterranean stream. *Biogeochemistry*, *123*(3), 429–446. https://doi.org/10.1007/s10533-015-0077-4

Wallin, M. B., Campeau, A., Audet, J., Bastviken, D., Bishop, K. H., Kokic, J., Laudon, H., Lundin, E., Löfgren, S., Natchimuthu, S., Sobek, S., Teutschbein, C., Weyhenmeyer, G. A., & Grabs, T. (2018). Carbon dioxide and methane emissions of Swedish low-order streams-a national estimate and lessons learnt from more than a decade of observations. *Limnology and Oceanography Letters*, *3*(3), 156–167. https://doi.org/10.1002/lol2.10061

Zipper, S. C., Hammond, J. C., Shanafield, M., Zimmer, M., Datry, T., Nathan Jones, C., Kaiser, K. E., Godsey, S. E., Burrows, R. M., Blaszczak, J. R., Busch, M. H., Price, A. N., Boersma, K. S., Ward, A. S., Costigan, K., Allen, G. H., Krabbenhoft, C. A., Dodds, W. K., Mims, M. C., … Allen, D. C. (2021). Pervasive changes in stream intermittency across the United States. *Environmental Research Letters: ERL*, *16*(8), 084033. https://doi.org/10.1088/1748-9326/ac14ec

Chapter 2: Integrating Ecosystem Patch Contributions to Stream Corridor Carbon Dioxide and Methane Fluxes

Kristen A. Bretz, Alexis R. Jackson, Sumaiya Rahman, Jonathon M. Monroe, and Erin R. Hotchkiss

Published in *Journal of Geophysical Research: Biogeochemistry* with the citation:
Bretz, K.A., Jackson, A.R., Rahman, S., Monroe, J.M., and Hotchkiss, E.R. 2021. Integrating Ecosystem Patch Contributions to Stream Corridor Carbon Dioxide and Methane Fluxes. *Journal of Geophysical Research: Biogeosciences*, 126, e2021JG006313. https://doi.org/10.1029/2021JG006313.

Key Points:

- Carbon dioxide and methane concentrations and emissions were heterogeneous within streams, even over short distances.
- Year-to-year differences in stream carbon dioxide emissions was greater than monthly variability.
- The presence of vernal pools near a stream elevated overall stream corridor carbon emissions.

Abstract

The heterogeneity of carbon dioxide (CO_2) and methane (CH_4) sources within and across watersheds presents a challenge to understanding the contributions of different ecosystem patch types to stream corridor and watershed carbon cycling. Changing hydrologic connections between corridor patches (e.g., stream, vernal pools, hillslope) can influence stream corridor greenhouse gas emissions, but the spatiotemporal dynamics of emissions within and among corridor patches are not well-quantified. To identify patterns and sources of carbon emissions across stream corridors, we measured gas concentrations and fluxes over two summers at Coweeta Hydrologic Laboratory, NC. We sampled CO_2 and CH_4 along four stream channels (including flowing and dry reaches), adjacent vernal pools, and riparian hillslopes. Stream CO_2

and CH_4 emissions were spatially heterogeneous. All streams were sources of CO_2 to the atmosphere (median = 97.2 mmol $m^{-2}d^{-1}$) but were sources or sinks of CH_4 depending on location (-0.19 to 4.57 mmol $m^{-2}d^{-1}$). CO_2 emissions were lower during the drier of two sampling years but were stable from month to month in the drier summer. CO_2 and CH_4 emissions also varied by both corridor and patch type; the presence of a vernal pool in the corridor had the strongest impact on emissions. Vernal pool patches emitted more CO_2 and CH_4 (246 and 1.95 mmol $m^{-2}d^{-1}$, respectively) than their adjacent streams. High resolution sampling of carbon fluxes from patches within and among stream corridors improves our understanding of the connections between terrestrial, riparian, and aquatic zones in a watershed and their contributions to overall catchment carbon emissions.

Plain Language Summary

Freshwater ecosystems can be sizable sources of greenhouse gases to the atmosphere. Carbon dioxide and methane emissions from fresh waters can be very different depending on where they are measured in a watershed. As distinct areas near a stream become connected by water moving through the watershed, stream greenhouse gas emissions may change in response to new carbon inputs from these connections. We studied carbon emissions from 4 streams and their surrounding patches: temporary pools, hillslopes adjacent to streams, and dry beds in stream channels (when water flowed underground). All streams emitted carbon dioxide and some streams were sources of methane to the atmosphere during our summer measurements, but emission magnitudes for both gases varied within each patch. Temporary pools were an important source of both greenhouse gases and contributed to stream emissions when present. Carbon dioxide emissions were lower in the drier of the two measurement summers, while

methane emissions were similar. Sampling from many patches within and surrounding a stream improves our understanding of landscape-scale carbon emissions.

1 Introduction

As water moves carbon through watersheds and across ecosystem boundaries, stream corridors collect and integrate landscape-scale signals of carbon cycling. Streams metabolize organic carbon and emit carbon dioxide (CO_2) and methane (CH_4) derived from internal metabolism and external sources (Hotchkiss et al., 2015; Stanley et al., 2016). The rates at which streams emit carbon to the atmosphere reflects their importance in local and global carbon cycling. Streams emit CO_2 globally at a rate that surpasses the terrestrial and oceanic carbon sinks (Webb et al., 2018) and emit approximately 5% of yearly global CH_4 to the atmosphere (Flury & Ulseth, 2019; Stanley et al., 2016). As global concentrations of atmospheric greenhouse gases continue to rise, quantifying the relative contributions of different sources and sinks of CO_2 and CH_4 grows ever more important.

The characteristics and gradients of a valley, particularly those in mountainous regions, create heterogeneous stream corridors that regulate the movement of water and carbon. Heterogeneous channel geomorphology and resulting patches within stream corridors offer diverse conditions for microbial metabolic processes. Some patches within stream corridors may disproportionately alter ecosystem carbon budgets, serving as "control points" for biogeochemical activity (Bernhardt et al., 2017; McClain et al., 2003). The path of stream water through pools, riffles, and subsurface connections determines how terrestrial carbon and soil-derived greenhouse gases are received and processed (Bowden & Bormann, 1986). Slower flowing pools allow organic matter to accumulate and be metabolized and oxygen to be depleted,

making them conducive to CH_4 as well as CO_2 production (Sanders et al., 2007). Steeper or pinched reaches with faster flow emit greenhouse gases at a higher rate (Beaulieu et al., 2011). Surface flow continuity and hyporheic exchange may be disrupted because of slope failures, changing soil and bedrock properties, large root systems, lack of precipitation, and other geomorphic features (Boano et al., 2013). Ever-changing connections between patches in corridors, and the subsequent delivery of carbon (Corson-Rikert et al., 2016) and nutrients (Butturini & Sabater, 2000) to streams, affect the spatial and temporal heterogeneity of stream greenhouse gas emissions (Cole & Caraco, 2001). Precipitation and changing flow paths fill and drain ephemeral pools that can be present near streams, even in mountainous regions. Changes in flow create transient connections among features of the watershed that provide sources or loss pathways for dissolved greenhouse gases. Recent advances in river corridor science have pointed to the importance of hyporheic exchange and subsurface biogeochemistry (Stegen et al., 2018; Harvey and Gooseff, 2015) in combination with hydrologic forcing (Schmadel et al., 2017; Ward et al., 2019) to explain variations in ecological function along flowing waters. The biogeochemical signatures of an entire stream corridor are thus a function of how stream, vernal pool, and terrestrial components are formed and connected by variable flows.

One central challenge in estimating stream corridor greenhouse gas emissions is identifying the patterns of carbon emissions within and among corridor patches. To start, there is limited availability of high resolution spatial and temporal pCO_2 and pCH_4 data from geographically and geomorphically diverse stream reaches and nearby freshwater patches. Constraints from low spatial resolution sampling as well as uncertainty around estimates of air-water gas exchange rates often compound upon one another in attempts to upscale from sampling site to landscape carbon budgets (Webb et al., 2018). The consequences of the presence of vernal

pools on carbon emissions from adjacent flowing waters have been particularly understudied, with much work on riparian soil CO_2 contributions to stream carbon fluxes coming from peatland-stream interfaces (A. Campeau et al., 2018; Hope, Palmer, Billett, & Dawson, 2004b; Leith et al., 2015). However, there remains a lack of data from temperate systems to test the influence of multiple freshwater patches on corridor exchange and the consequences for carbon emissions. Since first order streams account for more than 50% of all river networks by length (Downing et al., 2012), inaccurately characterizing their connections to adjacent patches and resulting greenhouse gas contributions to the atmosphere leaves a considerable gap in attempts to upscale emissions estimates.

In this study, we investigated greenhouse gas dynamics of heterogeneous stream corridors within a forested, mountain landscape. We (1) measured the heterogeneity of stream CO_2 and CH_4 concentrations and emissions within and between 4 stream corridors, (2) measured emissions from vernal pools, riparian hillslope, and dry bed patches along streams where available, and (3) tested how integrating different ecosystem patches within a stream corridor affects upscaling CO_2 and CH_4 emissions. By exploring diverse stream corridor and channel patches within subcatchments, we aimed to capture a more representative story of stream carbon emissions and variability from southeastern hardwood forest streams.

2 **Methods**

2.1 Study site

We characterized greenhouse gas dynamics across 4 subwatersheds at Coweeta Hydrologic Laboratory in the Blue Ridge Mountains of North Carolina in the United States (Figure 1). The region is temperate and humid; yearly precipitation averages 179 cm, peaking in the winter and early spring, and snow is infrequent (Laseter et al., 2012). Coweeta received 172

mm of rain during the 2018 summer study period compared to 108 mm during the summer of 2019. Max daily precipitation during summer 2018 was 33 mm and in summer 2019 was 22 mm. Mean summer and annual air temperatures are 21.3 °C and 12.9 °C, respectively (Burt et al., 2018). Vegetation throughout the subwatersheds within the Coweeta basin is approximately 90 year old oak-hickory and northern hardwood forests (Laseter et al., 2012). Soils are shallow but tend to have high organic matter, and the steep, high elevation topography exposes metamorphic rock (granite gneiss and mica schist) (Jensen et al., 2017; Laseter et al., 2012).

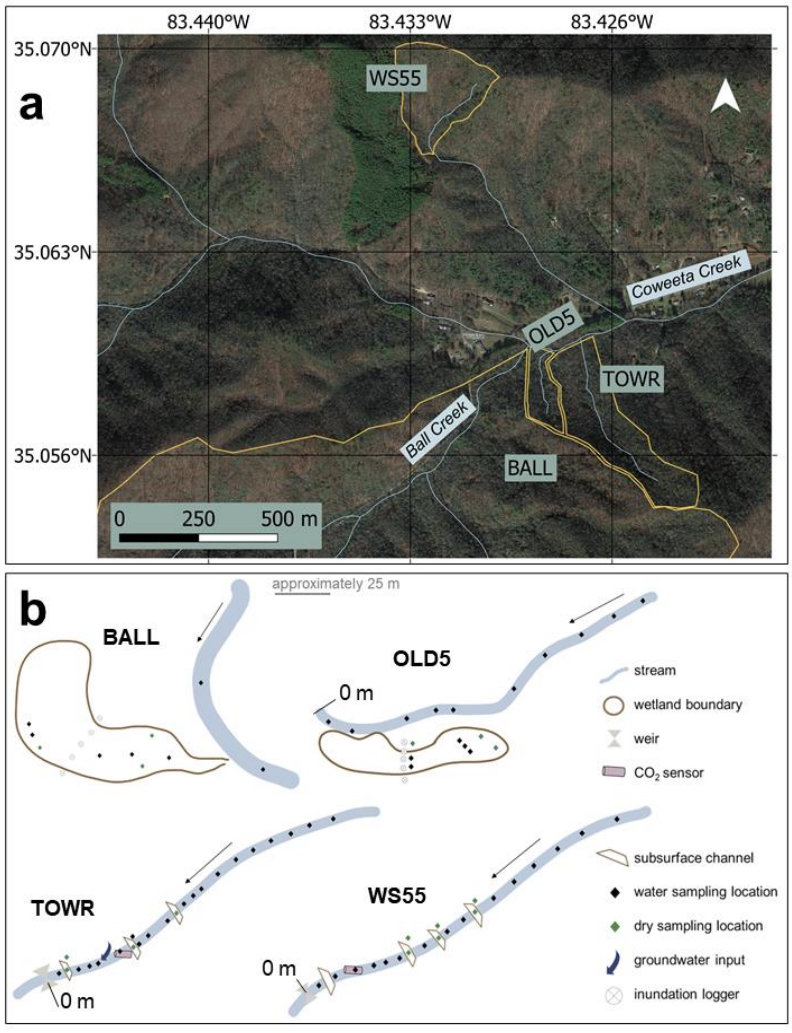

Figure 1. A) Map showing study streams within their subwatersheds: BALL = Ball Creek, OLD5 = Old 5 watershed, TOWR = Watershed 5b, WS55 = Watershed 55 B) Site sketches of each stream corridor showing sampling locations, sensors, and channel features.

Our research took place along 4 stream corridors with distinct ecosystem patches in the Coweeta basin (Table 1, Figure 1). We sampled Watershed 55 (WS55), which had the steepest upstream-downstream channel gradient (24 cm m^{-1}), close to its origin. Watershed 5b (TOWR) and Old 5 (OLD5) streams have shallower slopes, and OLD5 has an adjacent vernal pool near its confluence with Coweeta Creek. TOWR, WS55, and OLD5 are each first order streams with average depths less than 10 cm. Ball Creek (BALL) is a second order stream (10-30 cm deep) that crosses nearly the full length of the Coweeta watershed; near its confluence with Coweeta Creek, the BALL corridor also includes vernal pools. The TOWR stream is part of an ongoing whole-stream warming experiment where the temperature of the stream will be elevated by 3°C above ambient stream water for at least two years. The warming apparatus was not installed in 2018 and ramp-up to the experimental warming started in June 2019. We found no evidence to suggest that early experimental warming altered TOWR greenhouse gas emissions at the corridor scale.

Table 1. Stream corridor characteristics. Elevation and coordinates are for top of the study reach.

Stream corridor (abbreviation)	**Patch types in the corridor**	**Summer studied**	**Elevation (m)**	**Catchment area (km^2)**	**Lat/Long (DD)**
Watershed 55 stream (WS55)	Stream (1st order), dry streambed, hillslope	2018, 2019	819	0.08	35.06829, -83.43224
Watershed 5b stream (TOWR)	Stream (1st order), dry streambed, hillslope	2018, 2019	713	0.07	35.05780, -83.42696
Old 5 stream (OLD5)	Stream (1st order), vernal pool, dry pool	2018, 2019	702	0.19	35.05830, -83.4283
Ball Creek (BALL)	Stream (2nd order), vernal pool, dry pool, hillslope	2019	685	7.28	35.05866, -83.42968

We sampled multiple patches within each stream corridor. A "stream" designation describes flowing surface water. Dry streambed patches refer to locations within the defined stream channel where no surface water was present. In the three first order streams (WS55, TOWR, OLD5) dry streambeds occurred where water preferentially flowed in subsurface channels at the time of sampling. Along approximately 150-200 m study reaches of OLD5, TOWR, and WS55, we selected stream and dry bed sampling sites that captured the diversity of each corridor's channel morphology. Hillslope patches were forest soils adjacent to the stream but within high water marks. Vernal pool patches were areas of ponded water standing over organic-rich soils; two pools were adjacent to the OLD5 and BALL streams (one by each stream). At the beginning of summer 2019, both vernal pools had surface connections to streams; however the BALL stream-pool surface connection dried by July, and the OLD5 stream-pool surface connection was gone in August (Figure 1b). Throughout this paper, we will use "stream" to refer only to our stream patches of flowing surface water, while "corridor" will refer to the collection of patches (stream, dry bed, hillslope, and pool). Not all patch types were present in each corridor (Table 1). For upscaling calculations described below, the corridor includes the stream surface water and dry beds, 1 m of hillslope on either side of the water's edge, and vernal pool wetted area at the maximum observed extent in June.

In summer 2018, we sampled TOWR and WS55 streams and dry streambed sites in June and August. OLD5 stream sites were also sampled only in August of 2018, but during all 3 months of 2019 though at fewer sites. During 2019, all corridors (and patches within them, where present) were sampled once per month in June, July, and August. Vernal pool patches were only sampled in 2019. We also sampled upstream and downstream of a known groundwater input into the TOWR stream. At OLD5 and BALL, we sampled sites upstream and downstream

of ephemeral vernal pools (Figure 1b). Within each of the vernal pools we sampled locations across a transect of different water depths (2-10 cm); in August when standing water in the vernal pools completely receded, we sampled fluxes over smooth sediments across and near the edges of the depressions where airtight chamber seals were possible.

We assembled environmental data from streams and around the catchment. We measured surface water temperature (YSI ProSolo Optical Dissolved Oxygen and Conductivity Meter) and pH (Orion Portable pH Meter) in each stream and vernal pool at every discrete sampling event. We took elevation readings at each sampling site using a GPS unit (Garmin GPSMap 64 Handheld Outdoor). We used precipitation data from Coweeta recording rain gauge 06 (described in Miniat et al. 2017). We measured vernal pool inundation using modified temperature/light loggers (ONSET HOBO Pendant) to detect presence or absence of surface water (Chapin, Todd, & Zeigler, 2014).

2.2 Dissolved gas concentrations

We sampled stream and vernal pool water for dissolved gases using a syringe headspace equilibration method (Halbedel, 2015), taking triplicate samples at each site. We drew 80 mL of bubble-free surface water and 40 mL of ambient air into a 120 mL syringe (JMS JS-S00L) fitted with a 3-way stopcock (DWK Life Sciences Kimble Kontes FlexColumn). We shook each sample for 3 minutes. We injected headspace samples into sealed 20 mL vials (DWK Life Sciences MicroLiter 20mm) filled with ambient air using simultaneous injection and flushing to displace ambient air with our sample volume. Our tests of this sampling method recovered 93% of CH_4 and 101% of CO_2, compared with an analytical error of ±3.1 and ±2.2%, respectively. We analyzed headspace samples and ambient air samples for CO_2 and CH_4 on a gas

chromatograph (Shimadzu Nexis GC-2030) fitted with both a thermal conductivity and flame ionization detector.

We estimated the partial pressure of CO_2 and CH_4 in stream and vernal pool water from GC analyses as (Equation 1):

Equation 1.

$$C_{gas_i}water = BP \cdot \frac{vol_{air}\ (ppmv_{gas_i}eq - ppmv_{gas_i}air)}{\left(R \cdot T \cdot vol_{H_2O}\right) + H^{\Theta} \cdot e^{\left(\frac{-\Delta_{sol} \cdot H}{R}\left(\frac{1}{T} - \frac{1}{298.15}\right)\right)} \cdot ppmv_{gas_i}eq}$$

The concentration of CO_2 or CH_4 dissolved in the water ($C_{gas_i}water$ [where gas_i is either CO_2 or CH_4 throughout], mol m^{-3}) is a function of barometric pressure (BP, kPa), volume of air added for headspace equilibration (vol_{air}, m^{-3}), measured concentration of gas_i in the equilibrated headspace (after mixing air and water, accounting for the volume and temperature of the sample water using Henry's law constant for gas_i at water temperature and partial pressure of the gas_i in the air) ($ppmv_{gas_i}eq$, ppm), the measured concentration of gas_i in the air used as headspace ($ppmv_{gas_i}air$, ppm), the universal gas constant (R, m^3 kPa K^{-1} mol^{-1} [converted from L atm K^{-1} mol^{-1}]), headspace temperature (T, K), the volume of water equilibrated (vol_{H_2O}, m^3, and Henry's law constant H^{Θ} at a standard temperature (298.15 K) for gas_i converted to headspace temperature ($\frac{-\Delta_{sol} \cdot H}{R}$) (Henry's law constants for CO_2 and CH_4 from Sander 2015; method adapted from Demarty, Bastien, and Tremblay 2011).

During the summer of 2019, we deployed one underwater CO_2 sensor (EosGP, Eosense) at fixed points (35 m upstream from the weirs) in each of the TOWR and WS55 streams. We programmed the sensor to log every 30 min using Campbell dataloggers (CR1000) powered by

marine batteries (Optima, Model 034). We used in-stream dissolved CO_2 concentrations from discrete samples and headspace equilibration (Eq. 1) to calibration-correct the sensor measurements assuming linear drift during the sensor deployment period.

2.3 Emission fluxes

We measured the emission flux of CO_2 and CH_4 to the atmosphere from the surface of first order streams and their riparian hillslopes and vernal pools. We connected a portable infrared gas analyzer (Los Gatos Research Ultra-Portable Gas Analyzer) to a small chamber (volume = 214 cm^3, surface area = 38.4 cm^2) with airtight tubing. We placed the floating chamber directly on the surface of the water in stream and vernal pool patches to form a seal atop the water, gently holding it place (Campeau et al., 2014). The small channel width, steep gradients, shallow depth, and the presence of rocks and detritus prevented use of a fully floating chamber technique, but turbulence was low enough to allow for semi-anchored chambers to create an air-tight seal at the water surface. To sample dry bed, dry vernal pool soil, and hillslope patches, we selected sites where chamber placements on the ground were airtight. We monitored flux in real time (5-second intervals) as the chamber was held in place long enough to see a linear change in CO_2 and CH_4 concentration but before concentrations leveled out (up to 5 minutes). We calculated fluxes (Eq. 2) by estimating the slope from a linear regression of chamber concentrations of CO_2 and CH_4 over time, and then we converted each chamber measurement to an areal flux (C flux gas_i, mol m^{-2} d^{-1}):

Equation 2. $$C\ flux\ gas_i = \left(\frac{Flux_{chamber}}{R \cdot T \cdot \frac{1}{BP}}\right) \cdot \frac{V}{SA}$$

where $Flux_{chamber}$ (ppm d^{-1}) is the change in gas concentration over time, and chamber volume (V) and surface area (SA) units are m^3 and m^2, respectively; R, T, and BP are the same as Eq. 1.

At several surface water sampling points in each corridor, we took both dissolved gas flux and concentration measurements at the same location. By rearranging Eq. 3, we calculated the average and range of gas transfer velocity values for a given stream reach or vernal pool sampling location:

Equation 3. $$Emissions_{(i,s)} = [C\ gas_i]_{water} \cdot k_s$$

where i is CO_2 and (k_s; m d^{-1}) is the site-specific gas transfer velocity. We used only paired CO_2 flux and concentration measurements because of the flat slope of CH_4 fluxes we found at many stream sites. We paired flux and concentration measurements at 26 sampling locations. Once we characterized k, we standardized k values to a constant temperature to get gas transfer velocity with a Schmidt number of 600 (k_{600}) after Raymond et al. (2012) using Eq. 4:

Equation 4. $$k_{600} = \left(\frac{600}{Sc_{CO_2}}\right)^{-0.5} \times k_{CO_2}$$

We applied median site-specific k_{600} estimates to measurements of dissolved gas concentrations to convert CO_2 and CH_4 concentration [Cgas_i] or [CO_2 or CH_4]$_{water}$ (mol m^{-3}) to emission fluxes (mol m^{-2} d^{-1}). For Ball Creek stream flux estimates, we estimated k_{600} based on stream channel characteristics, as in Raymond et al. (2012).

2.4 Analyses

To assess the relative importance of the presence of a vernal pool and other stream corridor patches to first order stream corridor emissions, we calculated patch area-weighted fluxes (Equation 5) for the first order corridors: OLD5, TOWR, and WS55.

Equation 5.

$$C\ flux\ gas_{i\ corridor} = \sum_{for\ 1\ to\ x\ patch\ types} C\ flux\ gas_{i\ patch\ x} \cdot \left(\frac{area_{patch\ x}}{area_{corridor}}\right)$$

C *flux gas*$_{i\ \textbf{[patch type]}}$ (where *i* is either CO_2 or CH_4) is the median flux value (mmol m^{-2} d^{-1}) from a specific patch in one corridor from all sampling events, e.g., the OLD5 vernal pool; area$_{\textbf{[patch type]}}$/area$_{\textbf{[corridor]}}$ (m^2/ m^2) is the area occupied by the specific patch divided by the total area of the corridor to get a percent area with which to weight median corridor-specific estimates. The corridor includes the stream surface water and dry beds, 1 m of hillslope on either side of the water's edge, and vernal pool wetted area at the maximum observed extent in June. We did not include the BALL stream corridor in this analysis because we lacked the spatial resolution for BALL samples and because it is a much larger stream. Focusing on first order corridors additionally allowed us to calculate patch area-weighted fluxes for an average first-order stream corridor in the Coweeta basin that included relevant proportions of all 5 patch types, representing their prevalence among all sites. We totaled the full areas and patch type areas of the 3 first order corridors. Using the median emissions values from the different first order patches, we calculated a proportional emissions contribution from first order patch types, and we summed those patch contributions to estimate carbon flux for this average corridor.

We used one-way analyses of variance (ANOVA) to test for differences in the magnitude and variance of fluxes among sampling corridors, time periods (year, month), and patch types. We then used Tukey Honest Significant Differences to compare the means within groups with

significant differences (corridors, year, and patch types). We conducted all statistical analyses using R (version 1.1.463; R Core Team 2018).

3 **Results**

3.1 k_{600} estimations

We found k600 values consistent with first order streams (Raymond et al., 2012) and higher but within range of those for vernal pools (Farr, 2014) (Table S3). WS55 had highesr gas transfer velocities (median 5.93, range 2.41 – 13.6 m d^{-1}) than the TOWR stream (median 3.56, range 0.667 – 9.02 m d^{-1}; $F_{1,22} = 3.59$, $p = 0.04$) as was expected due to its steeper slope. Vernal pool k600 values were lower than both streams (median 1.49, range 1.29 – 4.6 m d^{-1}), but not significantly so ($F_{1, 26} = 3.75$, $p = 0.30$).

3.2 Spatial and temporal heterogeneity of greenhouse gas emissions in streams

CH_4 fluxes varied over space both within streams (Table S4, $p < 0.05$ for each of the 1st order streams) and among corridors ($F_{3,298} = 34.8$, $p < 0.001$): some sampling sites were reliably CH_4 sources, while others were consistently CH_4 sinks (Figure 2). There was no clear correlation of greenhouse gas flux with temperature from any stream ($F_{1,302} = 0.15$ for CH_4 and $F_{1,330} = 0.55$ for CO_2). The WS55 stream was a sink of CH_4 for half of 147 measurements, and the median flux was -0.001, mmol m^{-2} d^{-1}, but on 73 occasions it was a small source of CH_4 to the atmosphere (full range for CH_4 in WS55 stream -0.193 – 0.043 mmol m^{-2} d^{-1}). The TOWR stream was usually a source of CH_4, but individual sampling sites were less likely to be consistent sources or sinks (median=0.021; range -0.092 – 0.443 mmol m^{-2} d^{-1}). The OLD5 stream was a much greater source of CH_4 than the other first order streams, with emissions ranging from 0.006 – 4.57 mmol m^{-2} d^{-1} (median=0.11 mmol m^{-2} d^{-1}; $p_{adj} = 0.00$ compared to TOWR and $p_{adj} = 0.00$ compared to

WS55). While some individual sampling sites were distinctly different from one another within each of the first order streams, there was no longitudinal pattern of CH_4 emission magnitude along any of the 3 first order stream reaches. The 2nd order stream, BALL was a source of CH_4 (median=0.059; range 0.020-0.165 mmol m^{-2} d^{-1}), though significantly less so than the OLD5 stream (p_{adj} = 0.01).

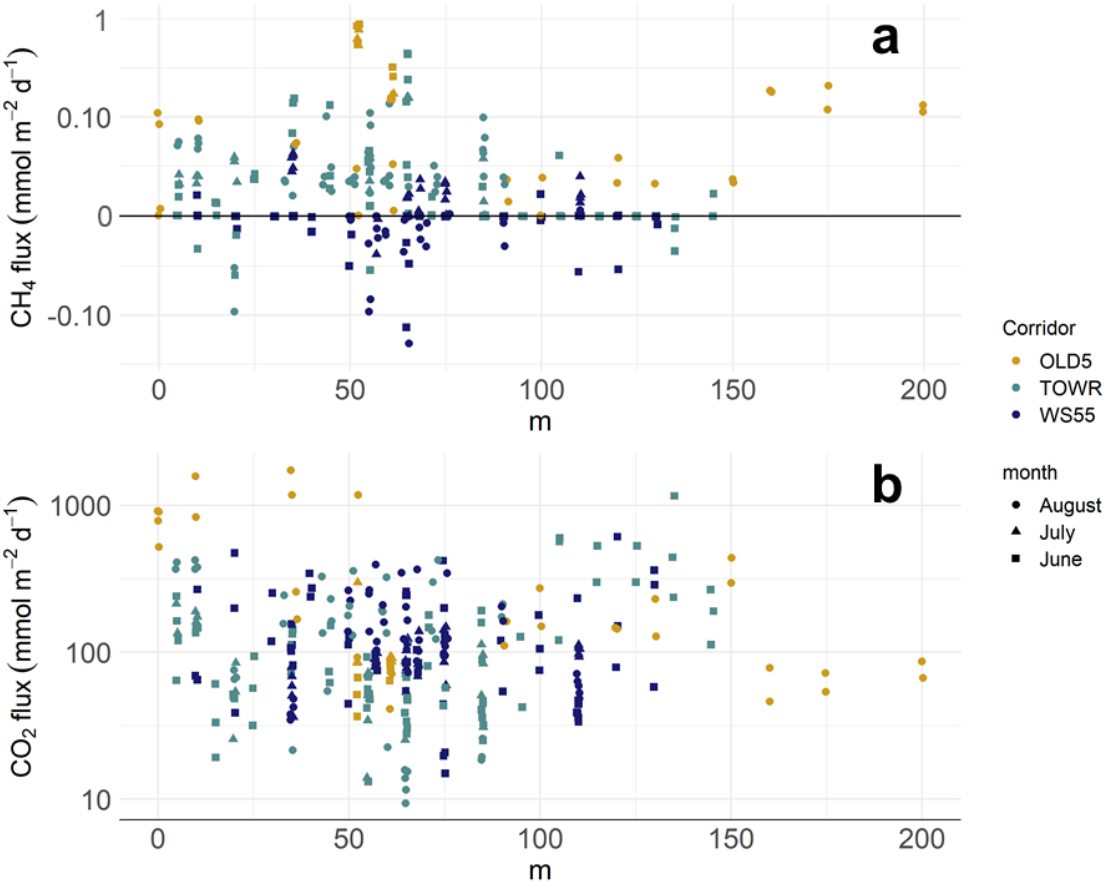

Figure 2. Spatial emission fluxes of CH_4 (A) and CO_2 (B) from first order streams in Coweeta, NC, USA. Emission estimates are organized from downstream (0 m) to upstream (150 m) on the x axis. Sampling months (in 2018 and 2019) are noted with different shapes: squares (June), triangles (July), and circles (August). Shading color corresponds with stream corridor (OLD5, TOWR, WS55). Meter marks denote either distance upstream from a weir (WS55, TOWR) or the farthest downstream point before a confluence with a larger stream (OLD 5) and are intended only as visual aids for longitudinal distance and variability, not to relate distances from different streams to each other. Please note log-transformed y-axes.

Streams were always sources of CO_2 and the magnitude of CO_2 emissions was heterogeneous over the length of each stream (Figure 2b; Table S4, $p < 0.001$ for sampling sites within each stream). Stream CO_2 emissions also differed among the 4 corridors ($F_{3,328}$=12.3, p<0.001). The OLD5 stream was distinct from TOWR and WS55 in that there was a longitudinal pattern with higher CO_2 fluxes near its outlet ($F_{1,27}$=7.90, $p < 0.001$ for sampling sites near the outlet compared to upstream). The OLD5 stream also had higher CO_2 emissions than TOWR and WS55 streams (p_{adj} = 0.000001 and 0.000000, respectively; Table S4). There was no difference between TOWR and WS55 (p_{adj} = 0.94) CO_2 emissions nor was there any spatial pattern in emissions from either of the two streams. Median CO_2 emissions from OLD5, TOWR, and WS55 streams were similar: 110, 78, and 99 mmol m^{-2} d^{-1}, respectively. The ranges of emissions from OLD5 (36–1733 mmol m^{-2} d^{-1}) and TOWR (9–1155 mmol m^{-2} d^{-1}) streams were much greater than WS55 (15–610 mmol m^{-2} d^{-1}). While median CO_2 emissions estimates from BALL were similar to but less variable than the first order streams at 131 mmol m^{-2} d^{-1} (range 9-192 mmol m^{-2} d^{-1}), overall CO_2 emissions from BALL were lower than OLD5 (p_{adj} = 0.0006) but not different than TOWR (p_{adj} = 0.94) or WS55 (p_{adj} = 0.99).

Stream CO_2 and CH_4 concentrations and emissions were less variable over time than they were among different sampling locations within streams. Emissions of CO_2 and CH_4 from streams remained relatively stable despite decreases in flow during summer 2019. There were no differences in CO_2 ($F_{2,259}$ = 0.4, $p > 0.05$) or CH_4 ($F_{2,228}$ = 2.8, $p > 0.05$) emissions when comparing monthly estimates from surface water in 2019 (Figure 3). Interestingly, stream CO_2 emissions were lower in 2019 than in 2018 ($F_{1,331}$ = 14.6, $p < 0.001$; median emissions 76 and 160 mmol m^{-2} d^{-1}, respectively), while CH_4 fluxes were not significantly different in 2018 versus 2019 ($F_{1,296}$ = 2.11 $p > 0.05$; Figure 3b).

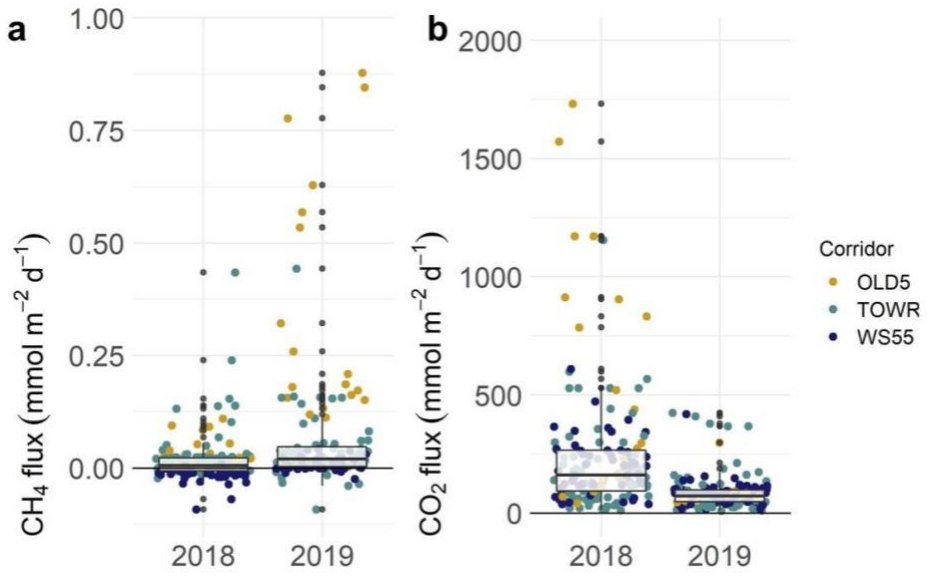

Figure 3. Coweeta stream CH_4 (A) and CO_2 (B) fluxes by year from first-order study streams. Shading color corresponds with stream corridor (OLD5, TOWR, WS55).

The lack of temporal trend in CO_2 emissions estimates over the summer was supported by high-frequency CO_2 sensor data from the TOWR and WS55 streams (Figure 4). In WS55, the variation in sensor dissolved CO_2 over time was comparable to the variation among discrete sampling locations within the 100 m reaches over the same time period (WS55 sensor range: 337-1383 µatm, WS55 discrete: 228-1462 µatm). For the TOWR stream, however, sensor dissolved CO_2 at a single site was less variable than discrete sample concentrations throughout the study reach (TOWR sensor range: 435-587 µatm, TOWR discrete: 247-3503 µatm).

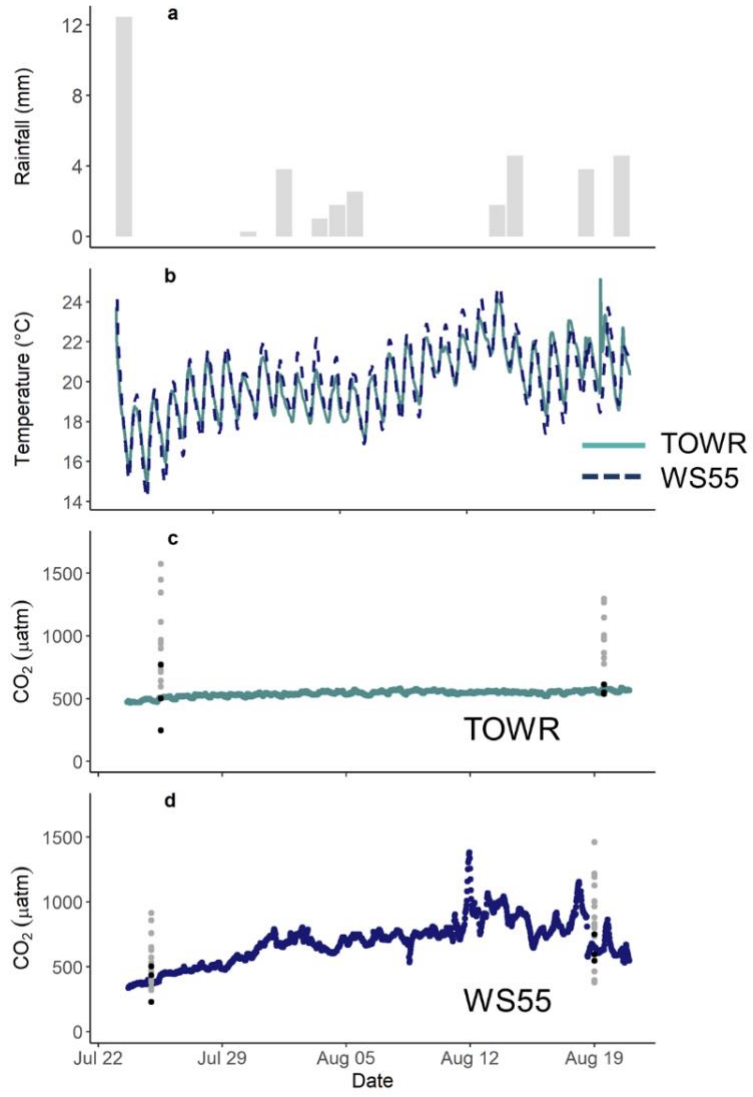

Figure 4. Local precipitation (A; daily, from Coweeta RG06 at the bottom of the basin), water temperature (B, green line TOWR, blue dashed WS55), and dissolved CO_2 concentrations over July and August of 2019 in TOWR (C) and WS55 (D) streams. Colored points are from sensor measurements at one location (35 m mark in each stream), while grey and black points show discrete CO_2 measurements from the locations along the entire sampled reach in for July and August 2019; black points are discrete samples taken at the 35 m mark next to the sensor.

3.3 Patch influences on stream corridor emissions

Patches played distinct roles in corridor CO_2 and CH_4 fluxes across the Coweeta basin (Figure 5; $F_{4,429} = 11.62$ for CO_2, $F_{4,397} = 5.227$ for CH_4, $p < 0.001$ for both; Table S5 and S6). Median CO_2 and CH_4 fluxes to the atmosphere were higher from inundated (246 and 1.95 mmol m^{-2} d^{-1}, for

CO_2 and CH_4 respectively) and dry (277 and 0.239 mmol m^{-2} d^{-1}) vernal pool patches than from stream surface waters (97 and 0.015 mmol m^{-2} d^{-1}) or dry streambeds (78 and -0.009 mmol m^{-2} d^{-1}). The median CO_2 emissions from inundated vernal pools was more than double that of streams (247 and 97 mmol m^{-2} d^{-1}, respectively; p_{adj} = 0.003), while median CH_4 emissions from vernal pools were over 2 orders of magnitude greater than that of streams (37 and 0.067 mmol m^{-2} d^{-1}, respectively; p_{adj} = 0.00008). Only one measurement captured a negative flux (i.e., a CH_4 sink) at a sampling site nearer the edge of one vernal pool. The OLD5 vernal pool had higher CH_4 emissions than the BALL vernal pool (p_{adj}=0.005), but the two pools had similar CO_2 emissions (p_{adj}=0.75). CO_2 emissions from dried vernal pool surfaces were higher than those from inundated vernal pool areas (p_{adj} = 0.008), but CH_4 emissions from dry versus inundated vernal pools were not different (p_{adj} = 0.58). Dry stream bed CH_4 emissions were highest from the TOWR corridor (p_{adj} = 0.05); CO_2 emissions from TOWR and WS55 dry beds were more similar (p_{adj} = 0.06). Riparian hillslopes were typically sinks of CH_4 (median -0.050 mmol m^{-2} d^{-1}, range -0.308–0.434) and sources of CO_2 (259 mmol m^{-2} d^{-1}, range 41–1300), but did not differ significantly from streams (p_{adj} = 0.09 for CO_2 and p_{adj} = 1.0 for CH_4) or vernal pools (p_{adj} = 0.99 for CO_2 and p_{adj} = 0.13 for CH_4). Hillslope CH_4 emissions were higher from the TOWR corridor (p_{adj} = 0.002), but, as with dry beds, the TOWR and WS55 hillslopes had similar CO_2 emissions (p_{adj} = 0.15).

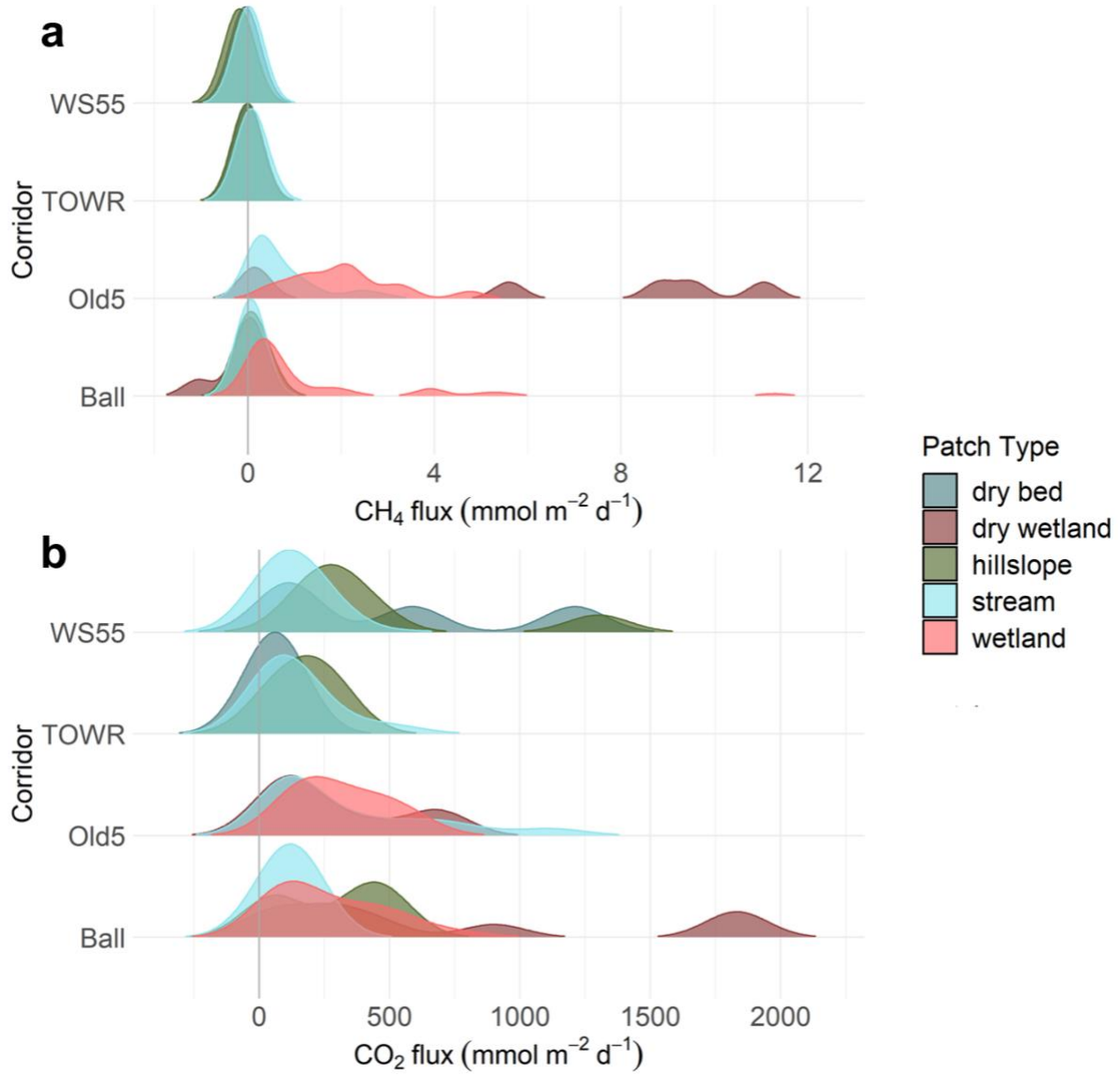

Figure 5. Distributions of patch CH_4 (A) and CO_2 (B) emissions from all 4 stream corridors. Note the different x axis scale. Please see Table S1 for number of measures from each corridor and patch type.

Corridors had unique emissions signatures, and the presence of vernal pools had a significant influence over corridor greenhouse gas emissions. In addition to differences in emission magnitudes from different patch types, there was also a significant difference among the four corridors for both gases ($F_{3,430} = 13.46$ for CO_2, $F_{3,398} = 6.05$ for CH_4, $p < 0.001$ for both). The first order stream corridor with vernal pool patches present, OLD5, had higher CO_2

and CH_4 emissions than corridors without vernal pools ($F_{1,330} = 20.52$ for CO_2, $F_{1,302} = 32.16$ for CH_4, $p < 0.001$ for both; Table S7). Comparing emissions from different first order stream corridors (Tables 2-4) further illustrates the outsized impact of the vernal pools , especially on CH_4 emissions. Within the OLD5 corridor, we can isolate the effect of changing stream-vernal pool connections over summer 2019. Two stream sampling sites on OLD5, 52 and 61 m, were just downstream of where the vernal pool first entered the stream. These sites had higher emissions of CH_4 in June and July than in August of 2019 ($p_{adj} = 0.00008$ for June vs. August and $p_{adj} = 0.001$ for July vs. August). By August 2019, the OLD5 vernal pool had almost completely dried (Supplemental Figure S2), so the surface aquatic connection from stream to vernal pool at those sampling sites was lost. Consequently, August CH_4 emissions from stream sites were more similar to emissions from upstream of the vernal pool sampling sites on OLD5 in 2019 and from the TOWR and WS55 streams.

Table 2. Patch areas (m^2) for Coweeta first order stream corridors: wetted stream study reach, dry stream bed (measured August 2018), vernal pool (measured June 2019), dry pool (measured August 2019), hillslope on 1 m of either side of stream channel, and total corridor area. Dashes indicate no data because that patch type was not present in the corridor.

	Stream	**Dry bed**	**Vernal Pool**	**Dry pool**	**Hillslope**	**Total corridor**
OLD5	200	-	262	58	-	520
TOWR	174	26	-	-	400	600
WS55	189	11	-	-	400	600
All 1st order stream corridors	564	36	262	58	800	1720

Table 3. Median stream corridor CH_4 emissions (mmol m^{-2} d^{-1}; range in parentheses) from patch types in first order stream corridors, including dry stream bed, vernal pool, dry pool, hillslope, and for the full corridor median weighted by patch areas. Data are from all measurements over both study summers.

	Stream	**Dry bed**	**Vernal pool**	**Dry pool**	**Hillslope**	**Weighted corridor by area**
OLD5	0.095 (0.006 – 4.57)	-	2.53 (0.371 – 733)	9.18 (0.044 – 36.7)	-	2.32
TOWR	0.021 (-0.092 – 0.443)	0.003 (-0.039 – 0.007)	-	-	-0.021 (-0.059 – 0.015)	-0.008
WS55	-0.001 (-0.193 – 0.043)	-0.042 (-0.152 – -0.019)	-	-	-0.161 (-0.308– -0.086)	-0.108
All 1st order stream corridors	0.013 (-0.193 – 4.57)	-0.009 (-0.152 – 0.007)	2.53 (0.371 – 733)	9.18 (0.044 – 36.7)	-0.05 (-0.308 – 0.015)	0.679

Table 4. Median stream corridor CO_2 emissions (mmol m^{-2} d^{-1}; range in parentheses) from patch types in first order stream corridors, dry stream bed, riparian ephemeral vernal pool, dry pool, hillslope, and for the full corridor median weighted by patch areas. Data are from all measurements over both study summers.

	Stream	**Dry bed**	**Vernal pool**	**Dry pool**	**Hillslope**	**Weighted corridor by area**
OLD5	111 (36.5 – 1730)	-	247 (114 – 557)	163 (33.2 – 701)	-	178
TOWR	79.4 (9.38 – 1160)	55.2 (44.1 – 81.9)	-	-	187 (41.1 – 288)	150
WS55	99 (15 – 610)	366 (80.9 – 1210)	-	-	301 (164 – 1300)	240
All 1st order stream corridors	94.3 (9.38 – 1730)	78 (44.1 – 1210)	247 (114 – 557)	163 (33.2 – 701)	259 (41.1 – 1300)	186

4 Discussion

We investigated the magnitude and variability of CO_2 and CH_4 emissions within and among stream corridors. We were unable to identify consistent trends in longitudinal spatial variability of CO_2 and CH_4 flux among small streams all nestled within the Coweeta basin. Future work that includes more spatially expansive paired flux and concentration data will help link physical and chemical corridor characteristics when upscaling carbon emissions beyond the reach. Corridor greenhouse gas emissions were variable over space, particularly when comparing emissions from different patches. Emissions of CO_2 and CH_4 from stream surface waters in particular were heterogeneous along our study reaches, even over distances of less than 10 m. We conducted this research over two summers in 2018 and 2019, the latter of which was unusually dry for the humid southeastern Appalachians. The dryness of 2019 provided an interesting opportunity to measure stream corridor CO_2 and CH_4 flux under diminished water levels. Stream water CO_2 emissions from all corridors were lower in 2019 but did not vary much within either summer. There was no effect of temperature on greenhouse gas fluxes within summer months. Finally, the first order stream with an adjacent vernal pool in its corridor had elevated carbon emissions compared to the first order streams without vernal pools, with highest emissions downstream of adjacent vernal pools. Streams and riparian vernal pools both contributed substantially to corridor carbon emissions, while hillslope and dry bed sites were sources of CO_2 but not always CH_4. Our integrated corridor emissions estimates reflect the diversity of ecosystem patches surrounding fresh waters.

All streams were sources of CO_2 to the atmosphere, and all but one were CH_4 sources. Stream CO_2 emissions were comparable to values reported for other forested first order streams in the southeastern United States (146 mmol m^{-2} d^{-1} in Jones & Mulholland, 1998a compared to

our median of 94.3 mmol m^{-2} d^{-1}). Our median CH_4 estimate was 0.013 mmol m^{-2} d^{-1}, which was lower, though within range, of those of global forested streams (range 0.001-100 mmol m^{-2} d^{-1} in Stanley et al., 2016). The WS55 corridor was unusual in its undersaturation of CH_4 compared to the atmosphere. While not unprecedented for fluvial ecosystems (Stanley et al., 2016), CH_4 sinks on the landscape are more commonly associated with forest soils. The valley and channel gradient of the WS55 subcatchment may be responsible for stream CH_4 undersaturation: with lower organic matter and fewer sources of CH_4, water flowing over steep gradients remains well oxygenated allowing CH_4 oxidation to use what little CH_4 is available. In reaches of small streams with high spatial variability in CH_4 production and oxidation, sediment nitrogen content was positively correlated with CH_4 production and oxidation (Bodmer, Wilkinson, & Lorke, 2020). Because stream nitrogen concentrations vary among subwatersheds at Coweeta and over time, with forested streams typically having low stream nitrogen (Knoepp & Swank, 1997; Webster et al., 2016), future work characterizing differences in sediment nutrient contents may provide valuable insights into drivers of CH_4 from our study streams.

CO_2 and CH_4 emissions were heterogeneous within stream reaches. Spatial differences in emissions have been previously attributed to geomorphic controls, especially when channel geomorphology creates surface water and groundwater connections (Crawford et al., 2017; Lupon et al., 2019; Smits et al., 2017). While our first order study reaches had high overall variability of CO_2 and CH_4 emissions, we did not see consistent patterns of certain sampling points as sources or sinks of a particular magnitude. For example in the TOWR stream, one sampling location at 65 m featured a bowl-like area of slower-moving water and sediment buildup. This location usually had higher CH_4 emissions than anywhere else along the stream; sometimes they were comparable to the high-emitting OLD5 stream sites nearest the vernal pool.

However, it was not always significantly higher than other individual TOWR sampling sites, nor was it significantly higher than all other sampling locations in that stream put together. We do not believe in-stream primary production altered local CO_2 heterogeneity because light and primary productivity are consistently low along first order forested streams in this region (e.g., Benstead et al., 2009; Greenwood & Rosemond, 2011). The lack of emission pattern based on geomorphic features may result from the mechanisms that are at odds with one another acting on carbon emissions at an individual site. Slope effects (Jones & Mulholland, 1998b; Smits et al., 2017), weathering (Johnson et al., 2007; Jones & Mulholland, 1998a), and terrestrial inputs (Dinsmore et al., 2013) all contribute to the biogeochemical and physical processes acting on carbon fluxes. It is notable that CO_2 emissions from the second order stream, Ball Creek, were less variable than those from the first order streams, indicating that the signals of mechanisms creating higher spatial heterogeneity in first order streams may become diluted in higher order streams.

Stream CO_2 emissions did not vary within summer months but differed between the two sampling years. We did not observe short term summer changes in emissions in response to lower precipitation periods, which contrasts with some previous work from streams (Crawford et al., 2017; Wallin et al., 2020) and adjacent habitats (Hope et al., 2004; Jacinthe et al., 2015) where emissions tracked precipitation more closely. We expected that the lack of precipitation would deprive the stream of more soil-derived carbon (Dinsmore et al., 2013; Johnson et al., 2008). Groundwater connections among riparian soils and stream channels can support stable greenhouse gas emissions over time (Lupon et al. 2019). Organic matter and dissolved gas inputs from terrestrial sources and subsurface flow paths at our sites appear to have been sufficiently stable to minimize variability in patch-scale biogeochemical activity and emissions within a

certain range during the summer months. Given that our sampling times were during peak terrestrial productivity, when high rates of evapotranspiration may reduce hydrologic connections between soils and streams, less soil-derived CO_2 may enter stream water, and stream flow and pCO_2 levels are likely maintained by groundwater from deeper subsurface flow paths (Jones & Mulholland, 1998b). Our finding of lower CO_2 emissions in the dryer summer of 2019 compared to summer 2018 are in agreement with work that has connected annual precipitation and fluvial CO_2 emission (Butman & Raymond, 2011; Öquist et al., 2014; Winterdahl et al., 2016). Lower CO_2 emissions during longer-lasting dry spells may have resulted from the lower rates of outgassing we observed in 2019, which can control emissions in steep mountain streams (Marx et al., 2017). While wet-dry cycles can control carbon flux (Looman et al., 2017; McClain et al., 2003), our results provide additional evidence that year-to-year differences in precipitation may be more important drivers in some small streams than changes within a season.

Interestingly, the combination of in-stream logging CO_2 sensors and monthly CO_2 grab samples highlights three pivotal considerations when quantifying patterns of CO_2 emissions from headwater streams. First, isolated sampling events may bias stream CO_2 emissions because the timing of grab samples relative to storms or short term drying will sway resulting analyses (as noted by Crawford et al., 2017). We found that nearby first order streams can have contrasting patterns of spatiotemporal variability: WS55 grab samples along the length of the study reach had a smaller range in CO_2 concentrations than the sensor captured at a single location, but the TOWR sensor concentrations were remarkably constrained over time relative to the spatial variability along that stream. This brings us to the next consideration, which is that the contrasting CO_2 emissions patterns for headwater streams may not be limited to streams from different climatic zones or geographic provinces since we can see divergent patterns from

streams less than 2 km apart. Finally, any single sampling location along a geomorphically heterogeneous stream reach may be a poor representative of the full stream's contributions to carbon flux.

The presence of vernal pools in a stream corridor had an outsized impact on corridor-scale carbon emissions. Vernal pool CO_2 and CH_4 emissions were high, but not different from the range of values reported for other freshwater wetlands and vernal pools (e.g., Bolpagni et al. 2017; Boon et al., 1997; Kifner et al. 2018). Riparian zones accumulate organic matter along streams, directly influencing the size (Ledesma et al., 2015) and arrangement (Leith et al., 2015; Teodoru et al., 2009) of connections between corridor patches and the stream channel, and thus shape corridor carbon fluxes. OLD5 was the only first order stream in our study that had an impermanent surface water connection to a vernal pool, but ephemeral pools are not uncommon in mountain or humid landscapes (Blackman, 2019; Lathrop et al., 2005; Wu et al., 2014). While there is little flat land for vernal pools to form upon in this region, not much riparian area is needed to effectively slow down water and retain soil moisture and organic matter in a way that steeply carved streams cannot. Our vernal pools share many characteristics with pools from other temperate regions, which are demonstrated hotspots of organic matter processing (Capps et al., 2014).

As vernal pools dried, we were able to observe higher CO_2 emissions from both vernal pools but different patterns in CH_4 emissions from OLD 5 and BALL. Surprisingly, some of our highest CH_4 emissions estimates came from dry vernal pool patches in OLD5, while BALL dry vernal pool patches more predictably emitted less CH_4. While there was a diminished area of standing water in the vernal pools during our August sampling trip in 2019, we did happen to sample after small rain showers (<5 mm). It is also of note that we never observed the sediments

of vernal pool patches to be completely desiccated, likely due to the brief rain showers, humid climate, and heavy canopy shading of the patches. The OLD5 vernal pool area was particularly well covered by rhododendron compared to BALL. While aeration from drying should reduce methanogenesis due to changes in dissolved oxygen and redox state, it is possible to see brief surges of CH_4, before eventual longer term decreases in emissions, as water tables drop (e.g., as reported by Sturtevant et al., 2016 for a freshwater restored vernal pool). Small vernal pools are sensitive to changes in hydrology (Blackman, 2019), and climate change is likely to increase incidence of extreme weather phenomena that could influence the formation and longevity of ephemeral waterbodies. The climate of the southeastern United States is predicted to shift closer to a Mediterranean climate (Karl et al., 2009), with mild, wet winters and dry summers that promote vernal pool formation (Keeley & Zedler, 1998). Given the impact of vernal pool patches on both stream reach and stream corridor carbon emissions, along with climatic changes that will create conditions conducive to their formation, mountain riparian vernal pools could become a more important component of freshwater ecosystem carbon emissions in the future.

Cycles of drying and rewetting control the flow and transformation of carbon within, through, and among patches along a stream corridor. The movement of water between patches transports resources across patch boundaries; ecosystem functions change as cross-patch connections are lost or fundamentally altered (Crawford et al., 2014; Schiff et al., 1990). The timing, quantities, and qualities of resource exchanges between patches have important consequences for biogeochemical cycling and greenhouse gas emissions (Abril & Borges, 2019; Tockner, Malard, & Ward, 2000). Our study found that stream-vernal pool linkages can be significant contributors to stream corridor carbon emissions. Our results also point to a future avenue of research in that the area of a vernal pool relative to an adjacent stream may predict

how much the pool contributes to stream carbon emissions when connected—of our two similarly sized vernal pools, we only found that the vernal pool contributed emissions to the first order stream. However, many unknowns linger surrounding patterns of patch connectivity and comparisons among catchments. How distinct pathways and timings of resource movement among patches change with flow is an increasingly large knowledge gap given new precipitation patterns that are being observed due to climate change.

This project provides unique insights into the spatial and temporal complexities of estimating freshwater greenhouse gas emissions from stream corridors. Our results also highlight ongoing challenges for future studies on this topic. Firstly, the use of chambers to estimate emissions from flowing waters may introduce a positive bias to our emissions estimates (Lorke et al., 2015). We acknowledge that fixed chambers may alter turbulent outgassing, thus adding uncertainty to our estimates. Prior studies have tried to overcome this using options that were not well suited to first order streams at Coweeta because of their geomorphology, such as tapered chamber ends (Crawford et al., 2013 or freely floating chambers (Looman et al., 2017). Our k_{600} calculations from paired flux and dissolved gas measurements are not higher than we would expect from headwater streams (Raymond et al., 2012), which would be the case if the chamber was exerting a strong bias on emissions. Some of our fluxes estimated indirectly using calculated k_{600} values were the highest (for CO_2) or among the highest (for CH_4), of all our flux estimates, especially in the vernal pool patches (Figure S1). However, none of those higher estimates were far from a directly measured flux within a similar patch. Finally, prioritizing using high spatial resolution measurements to inform patch and corridor greenhouse gas emissions estimates across a few forested headwater catchments, we were unable to delve more into temporal changes to linkages among different patches within corridors.

We found that the stream corridor structure had a strong influence on carbon emissions, as patch types indicated interesting linkages between channel features or hydrologic conditions. We measured heterogeneous stream emissions over small spatial scales, which improves our understanding of how carbon enters, moves through, and exits ecosystems. Higher resolution sampling is impractical in many studies, but where possible it can shed light on unique control points for biogeochemical activity over changing terrain and hydrology (Crawford et al., 2017; Horgby et al., 2019). Connectivity between patches will affect carbon emissions and export by distributing or restricting different sources of dissolved gases and organic matter. The presence of a riparian vernal pool influenced carbon emissions from a stream corridor, supporting the need to better integrate biogeochemical measurements across ecosystem types to advance our perspectives on carbon fluxes and fate as materials move within and beyond ecosystem boundaries. To assess carbon flux from all surface water in a large basin, knowing that the basin contains some subwatersheds with ephemeral vernal pools and intermittent streams, we would be remiss to only sample stream surface water near a catchment outlet. Without searching for patterns in terrestrial-riparian-aquatic connectivity and carbon flux, we will not be able to fully tackle questions around the global freshwater carbon budget.

Acknowledgments

This work was supported by the National Science Foundation (DEB-1655996, 1918584, and 1820563). We would like to thank everyone at Coweeta Hydrologic Laboratory (United States Forest Service) for accommodating this project. Many thanks to Bobbie Niederlehner for her assistance with analytical chemistry as well as to Stephen Plont and Brynn O'Donnell for their

help in early field sampling. We also appreciate the two anonymous reviewers who provided helpful feedback on the manuscript.

Data Availability Statement

Data are available through HydroShare at the following link:

http://dx.doi.org/10.4211/hs.ab2b33f27b3b4a0ca9a8ce4b8936753f

References

Abril, G., & Borges, A. V. (2019). Ideas and perspectives: Carbon leaks from flooded land: do we need to replumb the inland water active pipe? *Biogeosciences*, *16*(3), 769–784. https://doi.org/10.5194/bg-16-769-2019

Beaulieu, J. J., Tank, J. L., Hamilton, S. K., Wollheim, W. M., Hall, R. O. D., Mulholland, P. J., … Thomas, S. M. (2011). Nitrous oxide emission from denitrification in stream and river networks. *Proceedings of the National Academy of Sciences*, *108*(1), 214–219. https://doi.org/10.1073/pnas.1011464108

Benstead, J. P., Rosemond, A. D., Cross, W. F., Wallace, J. B., Eggert, S. L., Suberkropp, K., … Tant, C. J. (2009). Nutrient enrichment alters storage and fluxes of detritus in a headwater stream ecosystem. *Ecology*, *90*(9), 2556–2566. https://doi.org/10.1890/08-0862.1

Bernhardt, E. S., Blaszczak, J. R., Ficken, C. D., Fork, M. L., Kaiser, K. E., & Seybold, E. C. (2017). Control Points in Ecosystems: Moving Beyond the Hot Spot Hot Moment Concept. *Ecosystems*, *20*(4), 665–682. https://doi.org/10.1007/s10021-016-0103-y

Blackman, T. (2019). Vernal pool mapping and gepmorphology in the Appalachian mountains of Pennsylvania. *Master's Thesis, Virginia Polytechnic State University*, 68. Retrieved from http://hdl.handle.net/10919/89930

Boano, F., Revelli, R., & Ridolfi, L. (2013). Modeling hyporheic exchange with unsteady stream discharge and bedform dynamics. *Water Resources Research*, *49*(7), 4089–4099. https://doi.org/10.1002/wrcr.20322

Bodmer, P., Wilkinson, J., & Lorke, A. (2020). Sediment Properties Drive Spatial Variability of Potential Methane Production and Oxidation in Small Streams. *Journal of Geophysical Research: Biogeosciences*, *125*(1), e2019JG005213. https://doi.org/10.1029/2019JG005213

Bolpagni, R., Folegot, S., Laini, A., & Bartoli, M. (2017). Role of ephemeral vegetation of emerging river bottoms in modulating CO 2 exchanges across a temperate large lowland river stretch. *Aquatic Sciences*, *79*, 149–158. https://doi.org/10.1007/s00027-016-0486-z

Boon, P. I., Mitchell, A., & Lee, K. (1997). *Effects of wetting and drying on methane emissions*

from ephemeral floodplain wetlands in south-eastern Australia. *Hydrobiologia* (Vol. 357). Kluwer Academic Publishers.

Bowden, W. B., & Bormann, F. H. (1986). Transport and loss of nitrous oxide in soil water after forest clear-cutting. *Science*, *233*(4766), 867–869. https://doi.org/10.1126/science.233.4766.867

Burt, T. P., Ford Miniat, C., Laseter, S. H., & Swank, W. T. (2018). Changing patterns of daily precipitation totals at the Coweeta Hydrologic Laboratory, North Carolina, USA. *International Journal of Climatology*, *38*(1), 94–104. https://doi.org/10.1002/joc.5163

Butman, D., & Raymond, P. A. (2011). Significant efflux of carbon dioxide from streams and rivers in the United States. *Nature Geoscience*, *4*, 839–842. https://doi.org/10.1038/ngeo1294

Butturini, A., & Sabater, F. (2000). Seasonal variability of dissolved organic carbon in a Mediterranean stream. *Biogeochemistry*, *51*(3), 303–321. https://doi.org/10.1023/A:1006420229411

Campeau, A., Bishop, K., Nilsson, M. B., Klemedtsson, L., Laudon, H., Leith, F. I., … Wallin, M. B. (2018). Stable Carbon Isotopes Reveal Soil-Stream DIC Linkages in Contrasting Headwater Catchments. *Journal of Geophysical Research: Biogeosciences*, *123*(1), 149–167. https://doi.org/10.1002/2017JG004083

Campeau, Audrey, Lapierre, J.-F., Vachon, D., & Del Giorgio, P. A. (2014). Regional contribution of CO2 and CH4 fluxes from the fluvial network in a lowland boreal landscape of Québec. *Global Biogeochemical Cycles*, *28*, 57–69. https://doi.org/10.1002/2013GB004685

Capps, K. A., Rancatti, R., Tomczyk, N., Parr, T. B., Calhoun, A. J. K., & Hunter, M. (2014). Biogeochemical Hotspots in Forested Landscapes: The Role of Vernal Pools in Denitrification and Organic Matter Processing. *Ecosystems*, *17*(8), 1455–1468. https://doi.org/10.1007/s10021-014-9807-z

Chapin, T. P., Todd, A. S., & Zeigler, M. P. (2014). Robust, low-cost data loggers for stream temperature, flow intermittency, and relative conductivity monitoring. *Water Resources Research*, *50*(8), 6542–6548. https://doi.org/10.1002/2013WR015158

Cole, J. J., & Caraco, N. F. (2001). Carbon in catchments: connecting terrestrial carbon losses with aquatic metabolism. *Marine and Freshwater Research*, *52*, 101–110. https://doi.org/10.1071/MF00084

Corson-Rikert, H. A., Wondzell, S. M., Haggerty, R., & Santelmann, M. V. (2016). Carbon dynamics in the hyporheic zone of a headwater mountain stream in the Cascade Mountains, Oregon. *Water Resources Research*, *52*, 7556–7576. https://doi.org/10.1002/2016WR019303

Crawford, J. T., Loken, L. C., West, W. E., Crary, B., Spawn, S. A., Gubbins, N., … Stanley, E. H. (2017). Spatial heterogeneity of within-stream methane concentrations. *Journal of Geophysical Research: Biogeosciences*, *122*(5), 1036–1048. https://doi.org/10.1002/2016JG003698

Crawford, J. T., Lottig, N. R., Stanley, E. H., Walker, J. F., Hanson, P. C., Finlay, J. C., & Striegl, R. G. (2014). CO2 and CH4 emissions from streams in a lake-rich landscape: Patterns, controls, and regional significance. *Global Biogeochemical Cycles*, *28*(3), 197–210. https://doi.org/10.1002/2013GB004661

Crawford, J. T., Stanley, E. H., Dornblaser, M. M., & Striegl, R. G. (2017). CO2 time series patterns in contrasting headwater streams of North America. *Aquatic Sciences*, *79*, 473–486. https://doi.org/10.1007/s00027-016-0511-2

Crawford, J. T., Striegl, R. G., Wickland, K. P., Dornblaser, M. M., & Stanley, E. H. (2013). Emissions of carbon dioxide and methane from a headwater stream network of interior Alaska. *Journal of Geophysical Research: Biogeosciences*, *118*(2), 482–494. https://doi.org/10.1002/jgrg.20034

Demarty, M., Bastien, J., & Tremblay, A. (2011). Annual follow-up of gross diffusive carbon dioxide and methane emissions from a boreal reservoir and two nearby lakes in Québec, Canada. *Biogeosciences*, *8*, 41–53. https://doi.org/10.5194/bg-8-41-2011

Dinsmore, K. J., Wallin, M. B., Johnson, M. S., Billett, M. F., Bishop, K., Pumpanen, J., & Ojala, A. (2013). Contrasting CO2 concentration discharge dynamics in headwater streams: A multi-catchment comparison. *Journal of Geophysical Research: Biogeosciences*, *118*(2), 445–461. https://doi.org/10.1002/JGRG.20047@10.1002/(ISSN)2169-8961.SYNTHESIS1

Downing, J. A., Cole, J. J., Duarte, C. M., Middelburg, J. J., Melack, J. M., Prairie, Y. T., … Tranvik, L. J. (2012). Inland Waters Global abundance and size distribution of streams and rivers. https://doi.org/10.5268/IW-2.4.502

Flury, S., & Ulseth, A. J. (2019). Exploring the Sources of Unexpected High Methane Concentrations and Fluxes From Alpine Headwater Streams. *Geophysical Research Letters*, *46*(12), 6614–6625. https://doi.org/10.1029/2019GL082428

Greenwood, J. L., & Rosemond, A. D. (2011). Periphyton response to long-term nutrient enrichment in a shaded headwater stream. *Canadian Journal of Fisheries and Aquatic Sciences*, *62*(9), 2033–2045. https://doi.org/10.1139/F05-117

Halbedel, S. (2015). Updates of the Headspace Equilibration Technique often used for CO2 Sampling in water : Protocol Exchange Updates of the Headspace Equilibration Technique often used for CO Sampling in water. *Protocol Exchange*. https://doi.org/10.1038/protex.2015.085

Harvey, J., & Gooseff, M. (2015). River corridor science: Hydrologic exchange and ecological consequences from bedforms to basins. *Water Resources Research*, *51*(9), 6893–6922. https://doi.org/10.1002/2015WR017617@10.1002/(ISSN)1944-7973.WRR50

Hope, D., Palmer, S. M., Billett, M. F., & Dawson, J. J. C. (2004a). Variations in dissolved CO 2 and CH 4 in a first-order stream and catchment: an investigation of soil-stream linkages. *Hydrological Processes*, *18*, 3255–3275. https://doi.org/10.1002/hyp.5657

Hope, D., Palmer, S. M., Billett, M. F., & Dawson, J. J. C. (2004b). Variations in dissolved CO2 and CH4 in a first-order stream and catchment: An investigation of soil-stream linkages. *Hydrological Processes*, *18*(17), 3255–3275. https://doi.org/10.1002/hyp.5657

Horgby, Å., Boix Canadell, M., Ulseth, A. J., Vennemann, T. W., & Battin, T. J. (2019). High-Resolution Spatial Sampling Identifies Groundwater as Driver of CO2 Dynamics in an Alpine Stream Network. *Journal of Geophysical Research: Biogeosciences*, *124*(7), 1961–1976. https://doi.org/10.1029/2019JG005047

Hotchkiss, E. R., Hall Jr, R. O., Sponseller, R. A., Butman, D., Klaminder, J., Laudon, H., … Karlsson, J. (2015). Sources of and processes controlling CO 2 emissions change with the size of streams and rivers. *Nature Geoscience*, *8*(9), 696–699. https://doi.org/10.1038/ngeo2507

Jacinthe, P. A., Vidon, P., Fisher, K., Liu, X., & Baker, M. E. (2015). Soil Methane and Carbon Dioxide Fluxes from Cropland and Riparian Buffers in Different Hydrogeomorphic Settings. *Journal of Environmental Quality*, *44*(4), 1080–1090. https://doi.org/10.2134/jeq2015.01.0014

Jensen, C. K., McGuire, K. J., & Prince, P. S. (2017). Headwater stream length dynamics across four physiographic provinces of the Appalachian Highlands. *Hydrological Processes*, *31*(19), 3350–3363. https://doi.org/10.1002/hyp.11259

Johnson, M. S., Lehmann, J., Riha, S. J., Krusche, A. V., Richey, J. E., Ometto, J. P. H. B., & Couto, E. G. (2008). CO2 efflux from Amazonian headwater streams represents a significant fate for deep soil respiration. *Geophysical Research Letters*, *35*(17), L17401. https://doi.org/10.1029/2008GL034619

Johnson, M. S., Weiler, M., Couto, E. G., Riha, S. J., & Lehmann, J. (2007). Storm pulses of dissolved CO $_2$ in a forested headwater Amazonian stream explored using hydrograph separation. *Water Resources Research*, *43*(11). https://doi.org/10.1029/2007WR006359

Jones, J. B., & Mulholland, P. J. (1998a). Carbon dioxide variation in a hardwood forest stream: An integrative measure of whole catchment soil respiration. *Ecosystems*, *1*(2), 183–196. https://doi.org/10.1007/s100219900014

Jones, J. B., & Mulholland, P. J. (1998b). Carbon dioxide variation in a hardwood forest stream: An integrative measure of whole catchment soil respiration. *Ecosystems*, *1*(2), 183–196. https://doi.org/10.1007/s100219900014

Jones, J. B., & Mulholland, P. J. (1998c). Influence of drainage basin topography and elevation on carbon dioxide and methane supersaturation of stream water. *Biogeochemistry*, *40*(1), 57–72. https://doi.org/10.1023/A:1005914121280

Karl, T. R., Melillo, J. M., & Peterson, T. C. (2009). *Global Climate Change Impacts in the United States*. *Cambridge University Press*. Retrieved from http://publications.lib.chalmers.se/records/fulltext/245180/245180.pdf%0Ahttps://hdl.handle.net/20.500.12380/245180%0Ahttp://dx.doi.org/10.1016/j.jsames.2011.03.003%0Ahttps://doi.org/10.1016/j.gr.2017.08.001%0Ahttp://dx.doi.org/10.1016/j.precamres.2014.12

Kaufman, M. H., Ghosh, R. N., Grate, J., Shooltz, D. D., Freeman, M. J., Ball, T. M., … Stegen, J. (2020, February 2). Dissolved oxygen dynamics reveal biogeochemical tipping points driven by river corridor hydrology. *BioRxiv*. bioRxiv. https://doi.org/10.1101/2020.01.31.929505

Keeley, J. E., & Zedler, P. H. (1998). Characterization and global distribution of Vernal Pools. In C. Witham, E. Bauder, D. Belk, W. Ferren Jr., & R. Ornduff (Eds.), *Ecology, Conservation, and Management of Vernal Pool Ecosystems – Proceedings from a 1996 Conference* (p. 14). Sacramento, CA: California Native Plant Society. Retrieved from papers://cdef7b8f-a3fb-4ba8-9a44-baea6fa39920/Paper/p539

Kifner, L. H., Calhoun, A. J. K., Norton, S. A., Hoffmann, K. E., & Amirbahman, A. (2018). Methane and carbon dioxide dynamics within four vernal pools in Maine, USA. *Biogeochemistry*, *139*(3), 275–291. https://doi.org/10.1007/s10533-018-0467-5

Knoepp, J. D., & Swank, W. T. (1997). Forest Management Effects on Surface Soil Carbon and Nitrogen. *Soil Science Society of America Journal*, *6*(3).

Laseter, S. H., Ford, C. R., Vose, J. M., & Swift, L. W. (2012). Long-term temperature and precipitation trends at the Coweeta Hydrologic Laboratory, Otto, North Carolina, USA. *Hydrology Research*, *43*(6), 890–901. https://doi.org/10.2166/nh.2012.067

Lathrop, R. G., Montesano, P., Tesauro, J., & Zarate, B. (2005). Statewide mapping and assessment of vernal pools: A New Jersey case study. *Journal of Environmental Management*, *76*, 230–238. https://doi.org/doi: 10.1016/j.jenvman.2005.02.006.

Ledesma, J. L. J., Grabs, T., Bishop, K. H., Schiff, S. L., & Köhler, S. J. (2015). Potential for long-term transfer of dissolved organic carbon from riparian zones to streams in boreal catchments. *Global Change Biology*, *21*(8), 2963–2979. https://doi.org/10.1111/gcb.12872

Leith, F. I., Dinsmore, K. J., Wallin, M. B., Billett, M. F., Heal, K. V., Laudon, H., … Bishop, K. H. (2015). Carbon dioxide transport across the hillslope–riparian–stream continuum in a boreal headwater catchment. *Biogeosciences*, *12*(6), 1881–1892. https://doi.org/10.5194/bg-12-1881-2015

Looman, A., Maher, D. T., Pendall, E., Bass, A., & Santos, I. R. (2017). The carbon dioxide evasion cycle of an intermittent first-order stream: contrasting water–air and soil–air exchange. *Biogeochemistry*, *132*(1–2), 87–102. https://doi.org/10.1007/s10533-016-0289-2

Lupon, A., Denfeld, B. A., Laudon, H., Leach, J., Karlsson, J., & Sponseller, R. A. (2019). Groundwater inflows control patterns and sources of greenhouse gas emissions from streams. *Limnology and Oceanography*. https://doi.org/10.1002/lno.11134

Marx, A., Dusek, J., Jankovec, J., Sanda, M., Vogel, T., Geldern, R. van, … Barth, J. A. C. (2017). A review of CO2 and associated carbon dynamics in headwater streams: A global perspective. *Reviews of Geophysics*, *55*(2), 560–585. https://doi.org/10.1002/2016RG000547

McClain, M. E., Boyer, E. W., Dent, C. L., Gergel, S. E., Grimm, N. B., Groffman, P. M., … Pinay, G. (2003). Biogeochemical Hot Spots and Hot Moments at the Interface of Terrestrial and Aquatic Ecosystems. *Ecosystems*, *6*(4), 301–312. https://doi.org/10.1007/s10021-003-0161-9

Öquist, M. G., Bishop, K., Grelle, A., Klemedtsson, L., Köhler, S. J., Laudon, H., … Nilsson, M. B. (2014). The Full Annual Carbon Balance of Boreal Forests Is Highly Sensitive to Precipitation. *Environmental Science and Technology Letters*, *1*(7), 315–319.

https://doi.org/10.1021/ez500169j

Raymond, P. A., Zappa, C. J., Butman, D., Bott, T. L., Potter, J., Mulholland, P., … Newbold, D. (2012). Scaling the gas transfer velocity and hydraulic geometry in streams and small rivers. *Limnology and Oceanography: Fluids and Environments*, *2*(1), 41–53. https://doi.org/10.1215/21573689-1597669

Sanders, I. A., Heppell, C. M., Cotton, J. A., Wharton, G., Hildrew, A. G., Flowers, E. J., & Trimmer, M. (2007). Emission of methane from chalk streams has potential implications for agricultural practices. *Freshwater Biology*, *52*(6), 1176–1186. https://doi.org/10.1111/j.1365-2427.2007.01745.x

Schiff, S. L., Aravena, R., Trumbore, S. E., & Dillon, P. J. (1990). *Dissolved Organic Carbon Cycling in Forested Watersheds' A Carbon Isotope Approach*. *WATER RESOURCES RESEARCH* (Vol. 26). Retrieved from https://agupubs-onlinelibrary-wiley-com.ezproxy.lib.vt.edu/doi/pdf/10.1029/WR026i012p02949

Schmadel, N. M., Ward, A. S., & Wondzell, S. M. (2017). Hydrologic controls on hyporheic exchange in a headwater mountain stream. *Water Resources Research*, *53*(7), 6260–6278. https://doi.org/10.1002/2017WR020576

Smits, A. P., Schindler, D. E., Holtgrieve, G. W., Jankowski, K. J., & French, D. W. (2017). Watershed geomorphology interacts with precipitation to influence the magnitude and source of CO_2 emissions from Alaskan streams. *Journal of Geophysical Research: Biogeosciences*, *122*(8), 1903–1921. https://doi.org/10.1002/2017JG003792

Stanley, E. H., Casson, N. J., Christel, S. T., Crawford, J. T., Loken, L. C., & Oliver, S. K. (2016). The ecology of methane in streams and rivers: patterns, controls, and significance. *Ecological Monographs*, *86*(2), 146–171. Retrieved from https://esajournals.onlinelibrary.wiley.com/doi/pdf/10.1890/15-1027

Stegen, J. C., Johnson, T., Fredrickson, J. K., Wilkins, M. J., Konopka, A. E., Nelson, W. C., … Zachara, J. (2018). Influences of organic carbon speciation on hyporheic corridor biogeochemistry and microbial ecology. *Nature Communications*, *9*(1), 585. https://doi.org/10.1038/s41467-018-02922-9

Sturtevant, C., Ruddell, B. L., Knox, S. H., Verfaillie, J., Matthes, J. H., Oikawa, P. Y., & Baldocchi, D. (2016). Identifying scale-emergent, nonlinear, asynchronous processes of wetland methane exchange. *Journal of Geophysical Research: Biogeosciences*, *121*(1), 188–204. https://doi.org/10.1002/2015JG003054

Teodoru, C. R., del Giorgio, P. A., Prairie, Y. T., & Camire, M. (2009). Patterns in pCO_2 in boreal streams and rivers of northern Quebec, Canada. *Global Biogeochemical Cycles*, *23*(2), n/a-n/a. https://doi.org/10.1029/2008GB003404

Tockner, K., Malard, F., & Ward, J. V. (2000). An extension of the flood pulse concept. *Hydrological Processes*, *14*, 2861–2883. https://doi.org/10.1002/1099-1085

Wallin, M. B., Audet, J., Peacock, M., Sahlée, E., & Winterdahl, M. (2020). Carbon dioxide dynamics in an agricultural headwater stream driven by hydrology and primary production. *Biogeosciences*, *17*(9), 2487–2498. https://doi.org/10.5194/bg-17-2487-2020

Ward, A. S. ;, Wondzell, S. M. ;, Schmadel, N. M. ;, Herzog, S. ;, Zarnetske, J. P. ;, Baranov, V. ;, … Wells, J. (2019). Spatial and temporal variation in river corridor exchange across a 5th-order mountain stream network. *ETH Library Hydrol. Earth Syst. Sci*, *23*, 5199–5225. https://doi.org/10.3929/ethz-b-000387385

Webb, J. R., Santos, I. R., Maher, D. T., & Finlay, K. (2018). The Importance of Aquatic Carbon Fluxes in Net Ecosystem Carbon Budgets: A Catchment-Scale Review. *Ecosystems*, 1–20. https://doi.org/10.1007/s10021-018-0284-7

Webster, J. R., Knoepp, J. D., Swank, W. T., & Miniat, C. F. (2016). Evidence for a Regime Shift in Nitrogen Export from a Forested Watershed. *Ecosystems 2016 19:5*, *19*(5), 881–895. https://doi.org/10.1007/S10021-016-9974-1

Winterdahl, M., Wallin, M. B., Karlsen, R. H., Laudon, H., Öquist, M., & Lyon, S. W. (2016). Decoupling of carbon dioxide and dissolved organic carbon in boreal headwater streams. *Journal of Geophysical Research: Biogeosciences*, *121*(10), 2630–2651. https://doi.org/10.1002/2016JG003420

Wu, Q., Lane, C., & Liu, H. (2014). An effective method for detecting potential woodland vernal pools using high-resolution LiDAR data and aerial imagery. *Remote Sensing*, *6*, 11444–11467. https://doi.org/10.3390/rs61111444

Chapter 3: Carbon Biogeochemistry and Export Governed by Flow in a Non-Perennial Stream

Kristen A. Bretz, Natalie N. Murphy, and Erin R. Hotchkiss

In revision at *Water Resources Research*

Key Points:

- Surface water disconnection led to high CO_2 concentrations and emissions.
- DOC was low, except when storm pulses first reconnected surface water fragments with C sources within and beyond the stream channel.
- Interim flows generated distinct C dynamics; focusing on only flowing or fragmented states likely misses key biogeochemical transitions.

Abstract

Non-perennial headwaters experience extremes in flow conditions that likely influence carbon fate. As surface waters contract through dry periods, reconnect during storms, and re-expand or dry again, there is a great deal of variability in carbon emissions and export. We measured discharge, dissolved oxygen (DO), carbon dioxide (CO_2), and dissolved organic carbon (DOC) continuously in a persistent pool at the base of a non-perennial, forested headwater stream in the southeastern United States to characterize how flow changes affect carbon emissions and export as the stream expands and shrinks. We also compared carbon concentrations and export during different stream flow categories before and after fall wet-up. CO_2 concentrations were high when discharge was lowest (median = 10.2 mg L^{-1}) and low during high flows (3.2 mg L^{-1}) and storms (1.1 mg L^{-1}). High CO2 concentrations led to high emissions on a per area basis during low flow times, but w hole-channel stream CO_2 emissions were limited by the small surface area of the stream during periods of surface water disconnection. DOC concentration varied by season (range = 0.1 - 16.2 mg L^{-1}) with large pulses during smaller summer storms. We found that CO_2 and DOC concentrations differed among binned stages of stream flow. As non-perennial

streams become more prevalent across the southeastern United States due to shifts in climate, the relationships between flow and carbon movement into and out of stream networks will become increasingly critical to understanding stream carbon biogeochemistry.

Plain Language Summary

Non-perennial streams lack continuously flowing surface water. We studied the movement of carbon through a forested non-perennial headwater stream in the mountains of the southeastern United States. The stream channel was nearly empty at certain times in summer and early fall, when surface water was reduced to small pools, but storms could briefly cause the stream to flow again. These cycles of drying and rewetting influence concentrations of carbon dioxide gas and organic carbon dissolved in the stream water. As the stream dried up, oxygen decreased and carbon dioxide increased. When a storm occurred, much of the carbon dioxide in the stream was emitted into the atmosphere as water turbulence increased. Dissolved organic carbon was almost always very low, but storms sent large amounts of carbon downstream very quickly. Categorizing different levels of stream flow also helped explain how carbon cycles through a non-perennial stream because distinct low flow phases varied in carbon concentration and transfer to downstream ecosystems. Non-perennial streams are predicted to become more common as climate change affects precipitation patterns, so tracking how carbon moves into and out of streams that dry up and rewet will improve our understanding of freshwater contributions to the global carbon cycle.

1 Introduction

Streams are settings for dynamic biogeochemical processes where flow regulates exchanges of carbon between the water, land, and atmosphere. Stream waters bring in carbon from upstream and terrestrial sources and transport it to many possible fates. The fate of a dead leaf or a molecule of groundwater CO_2 entering a stream depends on many factors, including flow, which are interdependent

and ever-changing with the environment. Stream carbon inputs may depend on stream geomorphology (Alin et al., 2011), water sources (Dinsmore et al., 2013; Jones & Mulholland, 1998), phenology (Johnson et al., 2018; Liu et al., 2021), and more. Fluvial networks outgas 1.8 Pg of carbon per year and transport 0.43 Pg of dissolved and particulate organic carbon to the ocean, making them major players in the global carbon cycle (Battin et al., 2008; Raymond et al., 2013).

Flow organizes lotic ecosystems by controlling the delivery and residence time of chemical constituents important for biogeochemical reactions. Dissolved oxygen (DO) may be generated from primary producers within the channel or, more often in forested headwaters, mixed in through turbulent gas exchange depending on how fast the water loses elevation (Guasch et al., 1998). When flow slows, stream biota are hit with hypoxic conditions, as diminished turbulent mixing brings in little new DO, inputs may be dominated by low-DO groundwater, and what DO remains is quickly used by microbes in aerobic respiration (Ice et al., 2021). Streams are typically supersaturated with CO_2 relative to the atmosphere (Raymond et al. 2013). Stream CO_2 concentrations result from external inputs and the internal uptake and mineralization of organic matter (Hotchkiss et al., 2015), including dissolved organic matter (DOM; Battin et al., 2008). The duration for which both the OM substrates and respired CO_2 remain in a given reach along the network is subject to flow velocity as well as the legacies of past flows (Schreckinger et al., 2022; Zhang et al., 2021). The movement of carbon through streams remains an understudied area, especially since fluxes can be heterogeneous over space and time even within a single stream (Crawford et al., 2017; Bretz et al., 2021). Further, the carbon biogeochemistry of different fluvial ecosystems is not equally well-represented in the literature.

Flow governs the delivery and residence time of carbon in a stream, so drastic flow changes in non-perennial streams should result in accordingly drastic biogeochemical carbon fluxes. In perennial streams, CO_2 and DOC dynamics are sensitive to flow changes (Gómez-Gener et al., 2021; Koenig et al., 2017; Leith et al., 2015). Sustained movement of water through a catchment not only connects a stream longitudinally, but continuously delivers solutes from the terrestrial ecosystem surrounding the stream

through runoff and groundwater inputs. Surface water persists at baseflow where the channel is locally fed by groundwater and thus accumulates terrestrially-derived CO_2 from soil respiration flowing through underground flowpaths (Lupon et al., 2019). Contrastingly, streams can receive DOM from near- or in-stream processes (Buffam et al., 2001). Storm inputs of carbon may be lost to rapid downstream transport and turbulent outgassing, while also flushing pools and flowing reaches of built-up solutes and refreshing oxygen. Thus drying-rewetting cycles in non-perennial streams give rise to surges in respiration as changes in water content, DO, and redox conditions affect carbon biogeochemistry.

Limited information exists on how flow changes influence the balance of carbon constituents moving into, through, and out of non-perennial streams. Non-perennial streams appear frequently across landscapes (Costigan et al., 2015; Messager et al., 2021; Nadeau & Rains, 2007), and their occurrence is increasing with climate change across much of the continental United States (Zipper et al., 2021). Many prior works on non-perennial streams focus on arid and semi-arid regions; for example, following DOM quality through a drying event in the Mediterranean (Granados et al., 2020) or carbon gas evasion from wet-dry cycles in Australia (Looman et al., 2017). However, non-perennial streams also occur widely in temperate, humid landscapes. In the southeastern United States where our study took place, predictions indicate that precipitation regimes will shift to more severe but less frequent storms (Burt et al., 2018), further intensifying the transitions between no or low flow and higher flow storm conditions in streams. Jensen et al. (2017) found frequent and variable wet reach expansion and contraction from many streams in the eastern, temperate United States, including the stream studied for this project. Further, e missions from sediments have to date been a central focus in overall carbon emissions from fluvial networks (Gómez-Gener et al., 2016; Keller et al., 2020; Marcé et al., 2019). However, little knowledge exists of biogeochemical processes in the water that remains, if ever so diminished in area, and knowledge gaps persist in our understanding of how carbon may build up and flush away in patterns that differ from perennially flowing streams.

In this study, we quantified the fluctuations of CO_2 and DOC in a non-perennial, first order stream over six months as surface flow fragmented and reconnected. We captured high-frequency, continuous observations of a small, temperate stream for 6 months of drying and rewetting to expand our knowledge of non-perennial systems beyond a few wet-dry cycles. Our objectives were to (1) determine how flow variability affects non-perennial stream CO_2 concentration; (2) identify how discharge changes DOC concentration and export; and (3) describe the role of storms in lateral and atmospheric fluxes of carbon. To monitor fine-scale temporal changes in CO_2 and DOC, as well as relevant environmental parameters like DO, water temperature, and stage, we deployed sensors in a contracting and expanding stream pool near our study stream outlet to record high-frequency measurements. We predicted that CO_2 and DOC would build up in remaining isolated pools while DO declined as the stream fragmented. We also predicted that lengthy drying periods preceding a storm pulse would influence carbon export as flow reconnected during a storm. We use these data to provide a framework for characterizing carbon biogeochemistry during different flow stages.

2 Methods

2.1 Study Site

The study stream, Beast Stream, drains an 82 ha catchment of the Jefferson National Forest near Blacksburg, VA, USA (Figure 1A). Beast Stream flows down the north side of Brush Mountain, and the total wetted stream network length of all channels in the catchment undergoes considerable expansion and contraction (Jensen et al. 2019). Our project focused on the main stem of the network, a channel 1.4 km long beginning at 830 m elevation (37.25498 N, -80.48104 W) before descending to join Poverty Creek at ~640 m (37.26598 N, -80.48658 W). Local air temperatures range from January lows around 1ºC to July highs around 22ºC, and annual precipitation is 98-103 cm (Arguez et al. 2010). The catchment lies in the Valley and Ridge physiographic province with bedrock made up of Devonian shales, siltstones, and sandstones (Virginia Division of Mineral Resources, 1993). The stream valley is entirely forested with

mostly mature (>60 y) hardwood; these are predominantly oaks (*Quercus coccinea, Quercus prinus, Quercus velutina*), but red maple (*Acer rubrum*), pines (*Pinus rigida, Pinus virginianam, Pinus pungens*), and eastern hemlock (*Tsuga canadensis*) are also present. Rhododendrons (*Rhododendron catawbiense, Rhododendron maximum*) are common in the Poverty Creek watershed but are relatively sparse in the study catchment.

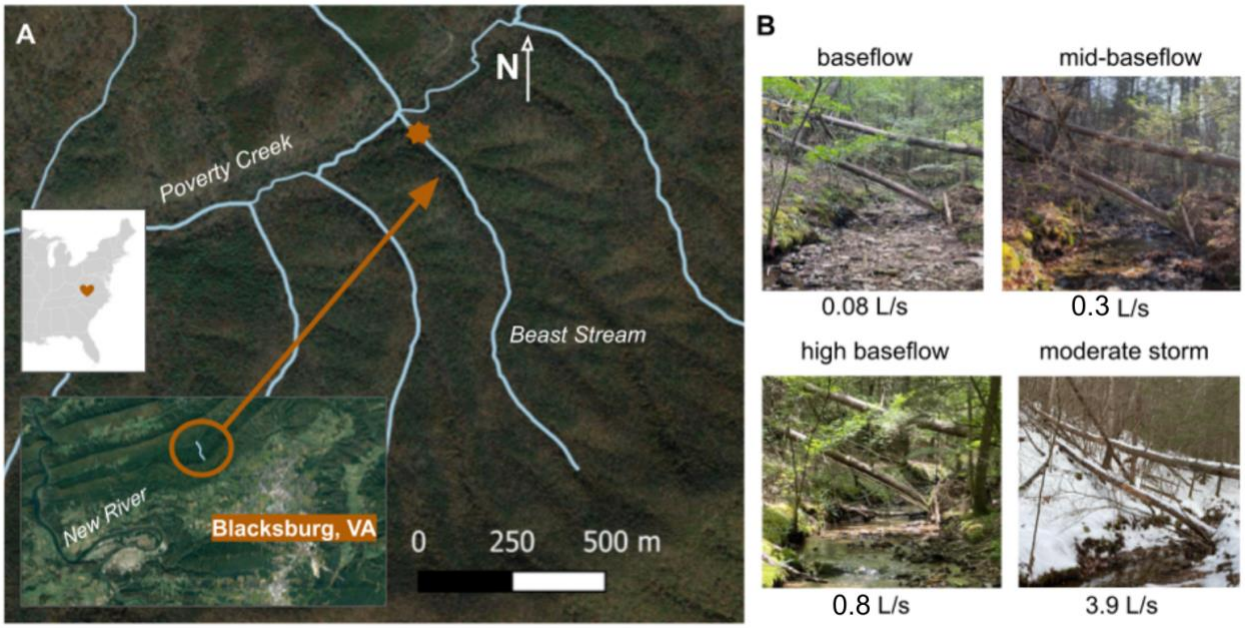

Figure 1. (A) Map showing Beast Stream (our study stream) relative to Poverty Creek and the New River in southwestern Virginia, USA; the orange star shows the location of the sensor pool site on Beast Stream (37.265 N, 80.48549 W). The stream line shows longest upstream extent of surface water when the stream is fully flowing. (B) Photos of the Beast Stream sensor pool during different flow stages categorized for this study: low baseflow (17 July), mid-baseflow (22 September), high baseflow (22 June) and moderate storm (6 December). We do not have a site photo from one of the few "large storm" days.

We focused our sampling on the late summer dry period through the early winter rewetting season (July-December 2020). We visited sites at least every other week in the summer and early fall, and at least monthly in late fall and winter. Our primary monitoring site was located 150 m upstream from the confluence of Beast Stream and Poverty Creek. A series of persistent step pools separated by variably inundated runs extends approximately 65 m upstream of the main sampling pool. Beyond the first 215 m lie alternating longer, more frequently dry reaches and sets of step pools for another 500 m, after which valley gradient increases sharply. We measured elevation every 50 m up the main channel using a GPS unit (Garmin GPSMap 64). We measured surface water temperature and DO (YSI ProSolo Optical

Dissolved Oxygen Meter) as well as pH (Oakton 150 pH Meter) from available pools below 1000 m at every visit (Table S1). We measured turbidity in the field at every site visit with a handheld sensor (NTU, Turner Designs AquaFluor). Rainfall data is from a local weather station (Blacksburg NWSO, VA US USC00440766, approximately 8 km from the stream).

2.2 Stream discharge and surface water inundation

We installed a pressure transducer (Onset HOBO U20L-04) near the catchment outlet to record surface water stage at 30 min intervals from June 2020 to December 2020. We conducted salt (NaCl) dilution gauging to estimate stream travel time and discharge six times during a variety of flow conditions (Moore, 2005). We used pulse additions of NaCl to measure stream velocity and discharge along 60-300 m stream reaches where we had deployed two conductivity sensors (Onset HOBO U24-001) recording every 10 sec; we used shorter reach lengths during lower flows because extended dry channel sections created very slow travel times. We measured wetted channel width every 5 m along salt addition reaches to estimate depth from discharge, velocity, and width; above salt addition reaches, we recorded wetted width every 100 m as well as flowing reach lengths on 10 days along the entire stream channel to estimate how surface water area changed over the study period. We were not able to directly measure discharge at higher flows, but we used channel cross sectional dimensions and wetted stream widths observed during higher flows to estimate discharge using Manning's equation. Combining our measured salt addition and Manning's-estimated discharge values, we established a rating curve to estimate continuous discharge from stage data over the study period ($R^2 = 0.76$; Figure S1).

To characterize flow across our high-frequency measurements, we binned discharge estimates into four groups based on baseflow separation calculations (after Piggott et al., 2005) throughout the study period. The ***Low Baseflow*** category includes discharge up to the median baseflow value for the drier July - September study window (22% of all discharge observations). ***Mid-Baseflow*** covers low to overall median baseflow range (29% of observations); this bin includes the median discharge value for the entire high-frequency discharge dataset. Discharge values in the ***High Flow*** category range from the

median overall baseflow to the median baseflow for the wetter portion of the study period (October-December; 28%, of observations). ***Storms*** (20% of observations) are discharge values above the wet-period median baseflow. Because we were interested in the effects of our most extreme, rare storm events (and to disentangle them from more common high flow storms), we created two sub-bins within ***Storms***: ***Moderate Storms*** include 19% of high-frequency discharge values and the ***Large Storms*** category represents the top 1% of discharge values (Figure S2). We also estimated the average surface water extent in the channel to match with the flow bins. We assessed average stream channel surface area coverage for each of our flow categories using wetted width measurements every 20 m along the entire stream from 11 different days. We checked our assumptions about the change in wet stream length based on outlet flow using the relationship for this catchment established by Jensen et al. (2018).

2.3 Dissolved carbon dioxide and oxygen

From June 2020 to December 2020, we deployed one underwater CO_2 sensor (eosGP, Eosense) at the farthest downstream persistent pool. The sensor recorded a measurement every 30 min using a Cambpell datalogger (CR1000) that was powered by a marine battery (Optima, Model 034). We deployed a logging DO and temperature sensor (miniDOT, PME) in the farthest downstream pool with the CO_2 sensor. Sensors logged a measurement every 10 min and were cleaned monthly. We checked the calibration of DO sensors in the lab before and after deployment using bubbling, yeast, and Winkler titrations to check our high and low calibration points (Hall & Hotchkiss, 2017). We corrected miniDOT field measurements using instrument-specific calibration curves and assumed linear drift between our calibration checks.

We took discrete samples of dissolved CO_2 from 4 persistent pools along the lower 1000 m of the stream, including the sensor deployment pool above the Beast-Poverty confluence. We used discrete stream dissolved CO_2 concentrations measured from the sensor deployment pool to calibration-correct the sensor measurements, assuming linear drift occurred during deployment (as in Bretz et al., 2021). We

sampled stream water for CO_2 using the syringe headspace method (Halbedel, 2015), approximately monthly in fall and winter, and twice per month in summer, at the downstream sensor monitoring site. We also collected CO_2 samples from pools 100, 300, and 1000 m upstream of the sensor pool at monthly intervals for comparison with the sensor pool. There are often more pools in this lower 1000m section of the channel, but from previous observation we knew we could reliably find enough water to sample at these four pools during driest conditions. We took triplicate samples at each site, drawing 80 mL of bubble free water and 40 mL of ambient air into a 120 mL syringe (JMS JS-S00L) fitted with a 3-way stopcock valve (Kimble). We shook each sample vigorously for 3 min, then pushed the water out of the syringe and injected the headspace into sealed 20 mL vials (Wheaton MicroLiter 20 mm), displacing ambient air with sample volume using a vent needle (Bretz et al., 2021). We measured the headspace concentrations of CO_2 on a gas chromatograph (Shimadzu Nexis GC-2030) fitted with a thermal conductivity and flame ionization detector. Using Equation 1, we estimated the partial pressure of CO_2 in stream water:

Eq. 1

$$C_{gas_i}\ water = BP \cdot \frac{vol_{air}\ (ppmv_{gasi}\ eq - ppmv_{gasi}\ air)}{\left(R \cdot T \cdot vol_{H_2O}\right) + H^{\theta} \cdot e^{\left(\frac{-\Delta_{sol} \cdot H}{R}\left(\frac{1}{T} - \frac{1}{298.15}\right)\right)} \cdot ppmv_{gas_i}eq}$$

The concentration of CO_2 dissolved in water is a function of barometric pressure (*BP*, kPa), volume of air added to the headspace for equilibration (vol_{air}, m^{-3}), measured concentration of CO_2 in the equilibrated headspace (after mixing air and water, accounting for the volume and temperature of the sample water using Henry's law constant for CO_2 at water temperature and partial pressure of the CO_2 in the air) ($ppmv_{gas\ eq}$, ppm), the concentration of CO_2 in the air used as headspace ($ppmv_{gas\ air}$, ppm), the universal gas constant (*R*, m^3 kPa K^{-1} mol^{-1} [converted from L atm K^{-1} mol^{-1}]), headspace temperature (*T*, K), the volume of water equilibrated (vol_{H20}, m^3), and Henry's law constant H^{Θ} at a standard temperature

(298.15 K) for CO_2 converted to headspace temperature ($-\Delta_{sol} \cdot H/R$) (Henry's law constants for CO_2 and CH4 from Sander, 2015; method adapted from Demarty et al., 2011).

We calculated CO_2 emissions from the stream surface to the atmosphere based on measured CO_2 and modeled air-water gas exchange:

Eq. 2

$$Emissions\ CO_2 = ([CO_2]_{water} - [CO_2]_{air}) \cdot k_{600}$$

where $[CO_2]_{water}$ is the dissolved CO_2 concentration (μatm) from the sensor and $[CO_2]_{air}$ is local atmospheric concentration. The gas transfer velocity (k_{600}; m d^{-1}) was estimated using stream velocity and slope from a physical model (Eq. 5 in Table 2 of Raymond et al., 2012). Because estimating k_{600} using equations derived from log-transformed datasets come with high uncertainty, we compared calculated k_{600} estimates with k_{600} derived from measured k_{CO2} at the same sampling location in 2019, when flux was measured using a portable infrared gas analyzer (Los Gatos UGGA) attached to a small chamber atop the water's surface (as in Bretz et al., 2021). While we did not use direct chamber measurements of k_{CO2} made at a single site to estimate emissions, they confirmed that our calculated k_{600} estimates from a physical model were reasonable for Beast Stream across all four of our main flow categories. To calculate emissions from the whole stream channel, we multiplied areal emissions rates (mg m^{-2} d^{-1}) by the average wetted area of the stream (m^2) specific to each flow category.

2.4 Dissolved organic matter

We deployed a submersible fluorescent dissolved organic matter sensor (fDOM; Turner Cyclops-7 with PME logger) in the same farthest downstream persistent pool from July 2020 to December 2020. The fDOM sensor logged at 30 min intervals. We corrected the sensor fDOM estimates for temperature, turbidity, and light attenuation (Downing et al., 2012). We collected grab samples at the fDOM sensor site

for DOC analysis to convert high-frequency fluorescent sensor data to DOC using a stream-specific conversion. We filtered stream water through pre-ashed filters (Whatman GF/F) into acid-washed, ashed 40 mL amber vials. Ashed filters and vials were combusted at 500 °C for four hours. We added 2N HCl to the filtered samples and stored samples in a refrigerator for a maximum of one month until analyzing for non-purgeable organic carbon (Elementar varioTOC). We then constructed a stream-specific rating curve to convert corrected fDOM measurements into DOC concentrations using the grab samples (R^2 = 0.72; Figure S3); we calculated error for the fDOM-DOC relationship using prediction intervals (Wilson et al., 2013). We calibrated the fDOM sensor in the lab before and after field deployment (as in Plont et al., 2022). We upscaled DOC concentration to DOC flux by multiplying concentration by stream discharge. We generated error estimates around DOC flux by multiplying the prediction interval upper and lower bounds for DOC and discharge.

2.5 Statistical Analyses

We performed all statistical analyses using base R (version 3.6.1; R Core Team, 2021). To examine the relationship between high-frequency DO, CO_2, or DOC and discharge we used regression analysis (*lm()*). We used the output of the regression model to characterize the relationships between concentration and discharge. We also used regression output to determine the slopes of the DOC concentration to discharge relationships within different storm events. We compared median values of CO_2 and DOC from different flow categories using the Kruskal-Wallis test (*kruskal.test()*), with multiple pairwise comparisons among flow categories (*pairwise.wilcox.test()*). To test differences in the DOC-discharge slope values from different times in the study period, we used repeated measures analysis of variance (ANOVA; *anova_test()*). We also used repeated measures ANOVA to test whether storm C export was different depending on whether or not there had been a storm in the previous 2 days.

3 **Results**

3.1 Stream flow, temperature, and dissolved oxygen

Stream discharge ranged from 0.07 to 31.4 L s^{-1} over the study period, with a median of 0.37 L s^{-1} (Fig. 2). Our study began during the summer dry season, and excluding storm pulses, discharge remained under 1 L s^{-1} until November. We observed a gradual increase in stream flow starting around late September. The largest summer storm peaked at 4.9 L s^{-1} on August 15. After a significant late October storm (19.6 L s^{-1}; 28 Oct), the stream had noticeably increased and continuous flow. Only two storms induced flows over 15 L s^{-1} and were associated with the two largest rainfall events (each a multi-day event with peaks on 28 October and 12 November). Flow bins established using quantiles of discharge measurements plus the largest of storms were bounded as follows: low baseflow 0.07-0.23 L s^{-1}, mid-baseflow 0.23-0.37 L s^{-1}, high baseflow 0.37- 0.98 L s^{-1}, moderate storm flow 0.98 -7.3 L s^{-1}, and large storms (top 1%) 7.3-31 L s^{-1}.

Beast Stream was at least partially surface disconnected from July to mid-November, except during storms. Surface connections were variable, and depended on local factors like temperature, shading, channel slope, and substrate, in addition to responding to precipitation. Surface water covered approximately 3% of the stream channel at low baseflow, 36% at mid-baseflow, 47% during high flow, 100% during moderate storms when the stream was fully connected (total area 2601 m^2) , and 104% during rare large storms when the stream would overflow its banks.

Median water temperature was 14.1°C, peaking at 19.8°C in July with a low of 4.6 in December (Figure 2). Stream temperatures were steady above 15°C until mid-September, after which they declined throughout the study period. Water temperature decreased with increasing discharge, especially after the September cooling of the stream began. Stream pH was always neutral (range 6.9-7.2).

DO was low, with a median of 4.0 mg L^{-1} (range 0.1 - 11.4 mg L^{-1}; Figure 2). DO increased with higher flows ($R^2 = 0.08$, $F_{(1, 7683)} = 704$, $p < 1^{-10}$); Figures 2, 3A). Diel patterns of DO tracked opposite to stream temperature with early morning DO peaks and late afternoon valleys. Summer DO concentrations consistently hovered around the first quartile of all measurements (2.3 mg L^{-1}), but the stream briefly reoxygenated during summer storms. DO concentration increased to stay near or above the 3rd quartile

(8.6 mg L^{-1}) after the same late October storm event that led to more continuous stream flow. Median DO values for baseflow and mid-baseflow categories were 2.0 and 2.8 mg L^{-1}, respectively. High flow median DO was 9.3 mg L^{-1}, while storm medians were 9.3 for moderate and 9.8 mg L^{-1} for large storms, respectively.

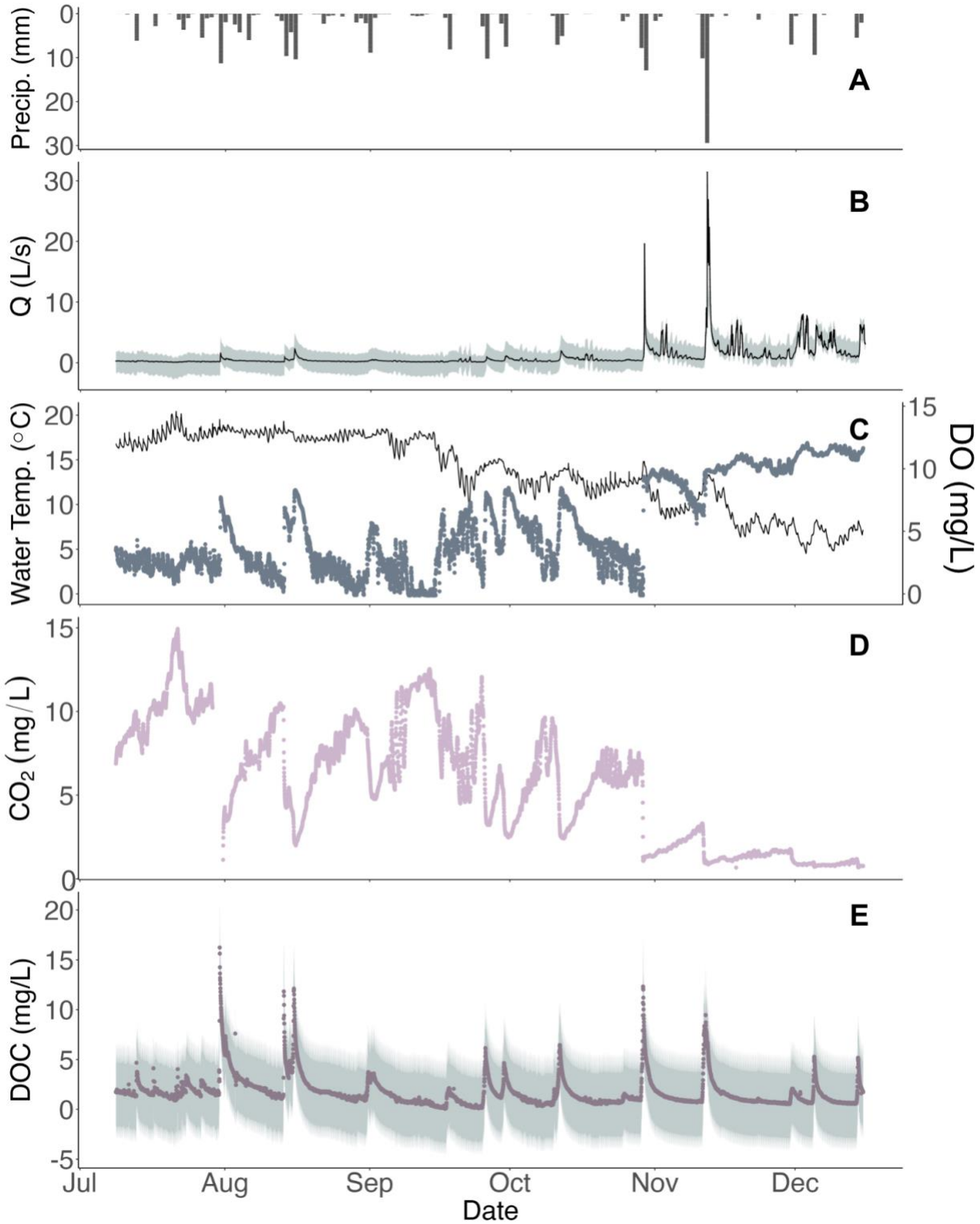

Figure 2. Time series of (A) local precipitation, (B) stream discharge (Q), (C) water temperature (Temp.) and dissolved oxygen (DO), (D) carbon dioxide (CO_2) concentration, and (E) dissolved organic carbon (DOC) concentrations as measured at the sensor pool (150 m) near the outlet of a non-perennial forested stream in southwest VA, USA.

3.2 CO_2 concentrations, emissions, and export

Stream CO_2 concentrations were variable over time but consistently decreased with increasing discharge (Figure 3B). From July to November, we observed repeated gradual accumulation of dissolved CO_2 during dry times followed by abrupt flushing and dilution when a rainfall event occurred (Figure 2). In early November, a CO_2 increase was observed to a lesser extent for one more storm event cycle, but concentrations were no longer dramatically responsive to hydrological fluctuations; in fact, median CO_2 concentration declined in November and December (1.26 mg L^{-1}) compared to previous months (6.9 mg L^{-1}, $p = 0.04$). CO_2 concentrations decreased with increasing stream flow throughout the summer and fall ($R^2 = 0.09$, $F_{(1, 7577)} = 709$, $p < 1^{-10}$; Fig. 2). CO_2 concentrations also decreased with increasing DO ($R^2 = 0.83$; Fig. 3C). CO_2 concentrations also differed among all flow categories (Kruskal-Wallis significance value $H_4 = 6251$, $p < 1^{-10}$), with the highest CO_2 concentrations when stream discharge was lowest (median = 10.2, range 4.6-14.9 mg L^{-1}; Table 1). CO_2 concentrations measured at sampling sites upstream of the sensor pool showed the same pattern of lower concentrations with discharge, and were usually less variable than or fell along a similar range to sensor measurements from the lowest pool (three upstream sites, range 0.5-7 mg L^{-1}; lowest site with sensors, 0.8-16 mg L^{-1}).

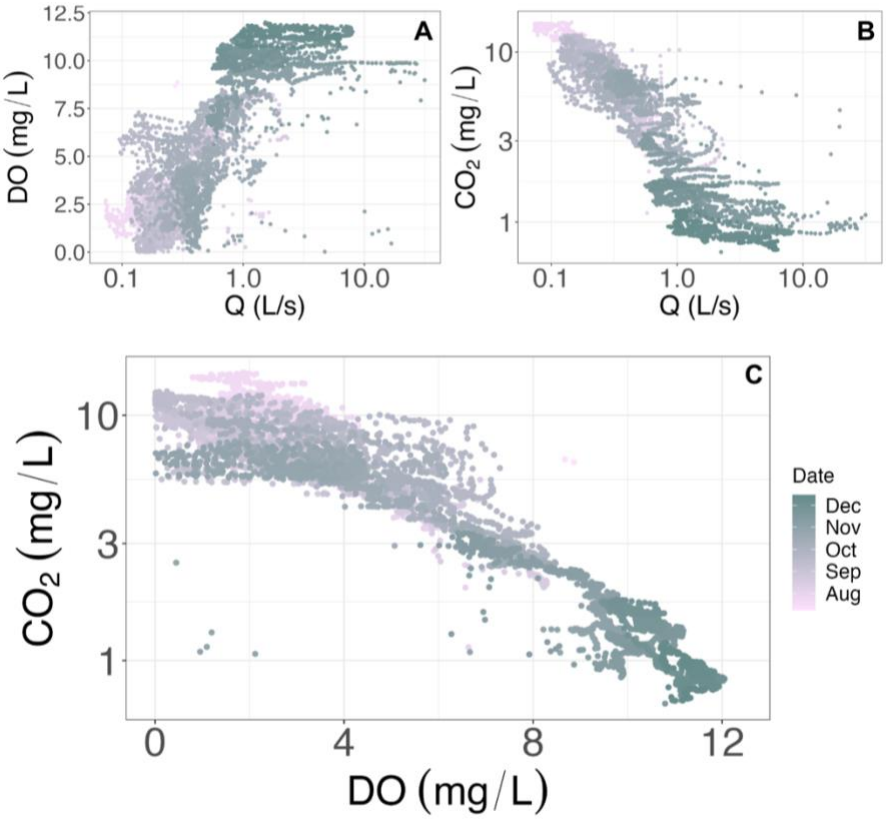

Figure 3. Changes in (A) dissolved oxygen (DO) and (B) carbon dioxide (CO_2) with stream discharge (Q) in Beast Stream, VA. (C) CO_2 was negatively related to DO. In all panels, color is ramped by date, with earlier dates represented by lighter shades. Note the log-transformed x- axis in panels A and B and log-transformed y-axis in panels B and C.

Table 1. *Stream discharge, expansion, and biogeochemical parameters across flow categories*

Flow category (% distribution of discharge, days in each category)	Discharge ($L\ s^{-1}$)	Stream surface area (m^2)	k_{600} ($m\ d^{-1}$)	CO_2 concentration ($mg\ L^{-1}$)	CO_2 export ($g\ d^{-1}$)	CO_2 emissions ($g\ m^{-2}\ d^{-1}$)	CO_2 emissions from entire stream ($kg\ d^{-1}$)	DOC concentration ($mg\ L^{-1}$)	DOC export at stream outlet ($g\ d^{-1}$)
1. Low baseflow (22%, 35 days)	0.17 (0.07-0.23)	78	3.2 (2.6-4.3)	10.2 (4.6-14.9)	151 (58-221)	32.9 (17.9-44.4)	2.6 (1.4 – 3.5)	1.2 (0.1-4.1)	0.20 (0.01-0.9)
2. Mid-baseflow (29%, 46 days)	0.29 (0.23-0.37)	936	3.8 (3.4-4.9)	7.1 (3.4-11.6)	182 (56-765)	27.4 (14.9-42.8)	27 (14-40)	1.6 (0.1-7.6)	0.46 (0.4-2.6)
3. High baseflow (28%, 44.5 days)	0.58 (0.37-0.99)	1222	5.2 (3.9-7.6)	3.2 (0.8-10.3)	863 (535-7,707)	18.1 (5.1-52.9)	22 (6-65)	1.1 (0.3-12.9)	0.71 (0.14-11)
4A. Storms - Moderate (19%, 30 days)	3.03 (0.99-7.16)	2601	9.4 (5.5-22)	1.1 (0.7-10.3)	179 (93-300)	12.3 (6.56-76.4)	32 (17 - 198)	1.3 (0.5-16.2)	2.8 (0.4-65)
4B. Storms - Large (1%, 1.5 days)	10.04 (7.25-31.44)	2705	22 (17-40)	0.9 (0.9-5.6)	221 (76 -2,358)	20.1 (15.5-135)	55 (42-366)	6.4 (0.7-12.3)	73 (5.5-2)

Note. Median values (range in parentheses) for discharge (Q), stream channel surface area, gas transfer (k_{600}), carbon dioxide (CO_2), and dissolved organic carbon (DOC) parameters across different flow categories from low baseflow to large storms in Beast Stream, VA.

Emissions of CO_2 on a per area basis usually declined with flow (Fig. 5A, Table 1). Estimated k_{600} values based on discharge and channel morphometry (Raymond et al., 2012) ranged from 2.6 to 40.1 m d^{-1} with a median of 4.4 m d^{-1}. Median measured flux chamber k_{600} from the previous year (2019), used to bound our estimated k_{600}, was 2.3 m d^{-1} (range 1.5 to 7.2 m d^{-1}) over 5 sampling events representing flow conditions similar to low baseflow, mid-baseflow, and moderate storm categories (Table S2). Emissions from the study period (derived from estimated k_{600}) decreased with increasing flow (R^2 = 0.32, $F_{1,7577}$ = 3717, $p < 1^{-10}$) and varied by flow category (Table 1; H_4 = 3258, $p < 1^{-10}$); only the high flow and moderate storm categories were not different from each other (p = 0.85, medians = 18.1 and 12.2 g m^{-2} d^{-1}, respectively). The low baseflow flow category had the highest estimated emissions on a per area basis (median = 33.2, range = 17.8 - 44.4 g m^{-2} d^{-1}) compared to other flow categories (median = 15.2, range = 5.1-135 g m^{-2} d^{-1}) (Table 1). Emissions were positively correlated with concentration ($p < 0.001$, R^2 value (0.83); variability in this relationship was driven by times of greater discharge and lower CO_2 concentration. While emissions did decrease after November (11.8 compared to 28.7 g m^{-2} d, p = 0.10), it was to a lesser extent than CO_2 concentration declines (p = 0.04). CO_2 emissions were higher during storms (median = 19.38 g m^{-2} d) if there had been no prior storms within 4 days (if prior storms, median = 13.29 g m^{-2} d^{-1}; $F_{1,1136}$ = 68.77, $p < 1^{-10}$). Gas transfer velocities, however, were higher if a storm had occurred within the prior 4 days (median = 5.7 compared to 2.9 m d^{-1}, as calculated from changes in velocity.; $p < 0.01$)

Considering the entire stream as it contracted and expanded in surface water area over the study period, areal CO_2 emissions scaled by stream area varied with flow category (H_4 = 4842, $p < 1^{-10}$). Scaling up sensor-based emission rates using our observations of surface water area coverage during different flow categories revealed that landscape emissions from our study stream were highest when the stream covered the full channel (moderate storm and large storm categories, medians = 32.0 and 54.5 kg d^{-1}, respectively; Table 1). Given the small stream water surface area during the driest parts of the study time (less than 100 m^2 on average), total stream emissions were accordingly quite small during the low flow periods (2.6 kg d^{-1}).

3.3 DOC concentrations and export

DOC was consistently low throughout the study period (median = 1.3 mg L^{-1}, range 0.08 - 16.2 mg L^{-1}), and only peaked briefly during storm events (Figure 1). DOC concentration increased with discharge ($R^2 = 0.7$, $F_{1,7683} = 1934$, $p < 1^{-10}$; Fig. 4A). We found that the slope of DOC concentration versus discharge during 37 individual storms differed by season; summer and early fall storms prior to October 10 had higher slopes than late fall storms (median = 3.2 compared to -0.03, respectively; $F_{1,35} = 26.3$, $p < 0.001$, $\eta^2 = 0.43$ [effect size]; Fig. 4B). DOC concentration also usually varied by flow category ($H_4 = 368$, $p < 1^{-10}$; Table 1), however, the extreme categories drove this difference ($p < 1^{-10}$ comparing low baseflow and large storm categories to all other bins), while the mid-baseflow, high flow and moderate storm categories had similar DOC concentrations ($p = 0.08$ for mid-baseflow - high flow and $p = 1$ for high flow - moderate storm). Antecedent conditions also had an effect on DOC concentration, where concentrations were 50% more during a storm if no storm had occurred during the prior 2 days than if storms occurred close together (medians = 1.5 and 1.0 mg L^{-1}, respectively; $F_{1, 1193} = 22.3$, $p < 0.001$, $\eta^2 = 0.02$).

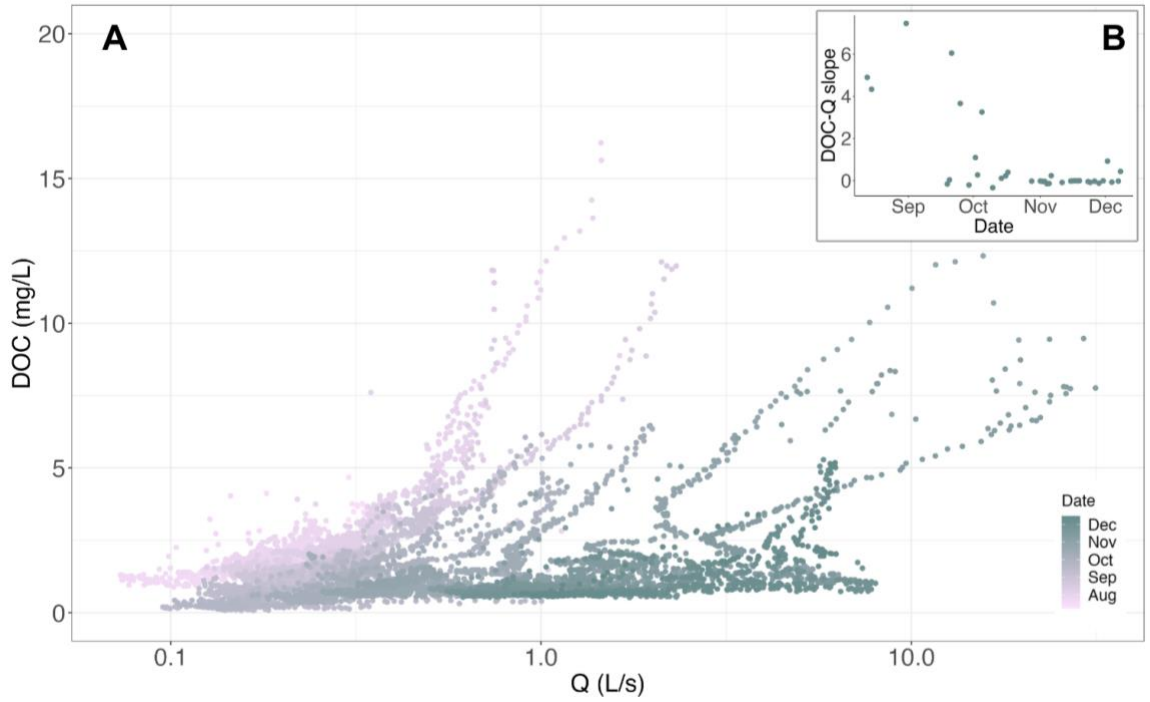

Figure 4. (A) Dissolved organic carbon (DOC) concentration at the sensor monitoring location near the Beast Stream outlet, color-ramped by date. Note log-transformed x-axis. (B) Change in slope of the increase in DOC concentration with rising discharge over time.

Export of DOC ranged over several orders of magnitude during the study period (median = 0.53, range 0.01-277, g d^{-1}; Figure 5b). Export was highest during the large storm flow category (median = 73.2 g d^{-1}) and differed significantly among every flow category ($H_4 = 5458$, $p < 1^{-10}$; Table 1). Comparing export before and after the October 10 shift in DOC-discharge storm slopes, we found that export was higher in the late fall, with a median flux of 136 up from 23 g d^{-1} in summer ($F_{1, 35} = 26$, $p < 0.01$). However, we found that during individual storms, drier antecedent conditions led to higher storm export loads, or 1.5 g d^{-1} compared to 1.2 g d^{-1} ($F_{1, 1193} = 74$, $p < 0.01^{-}$).

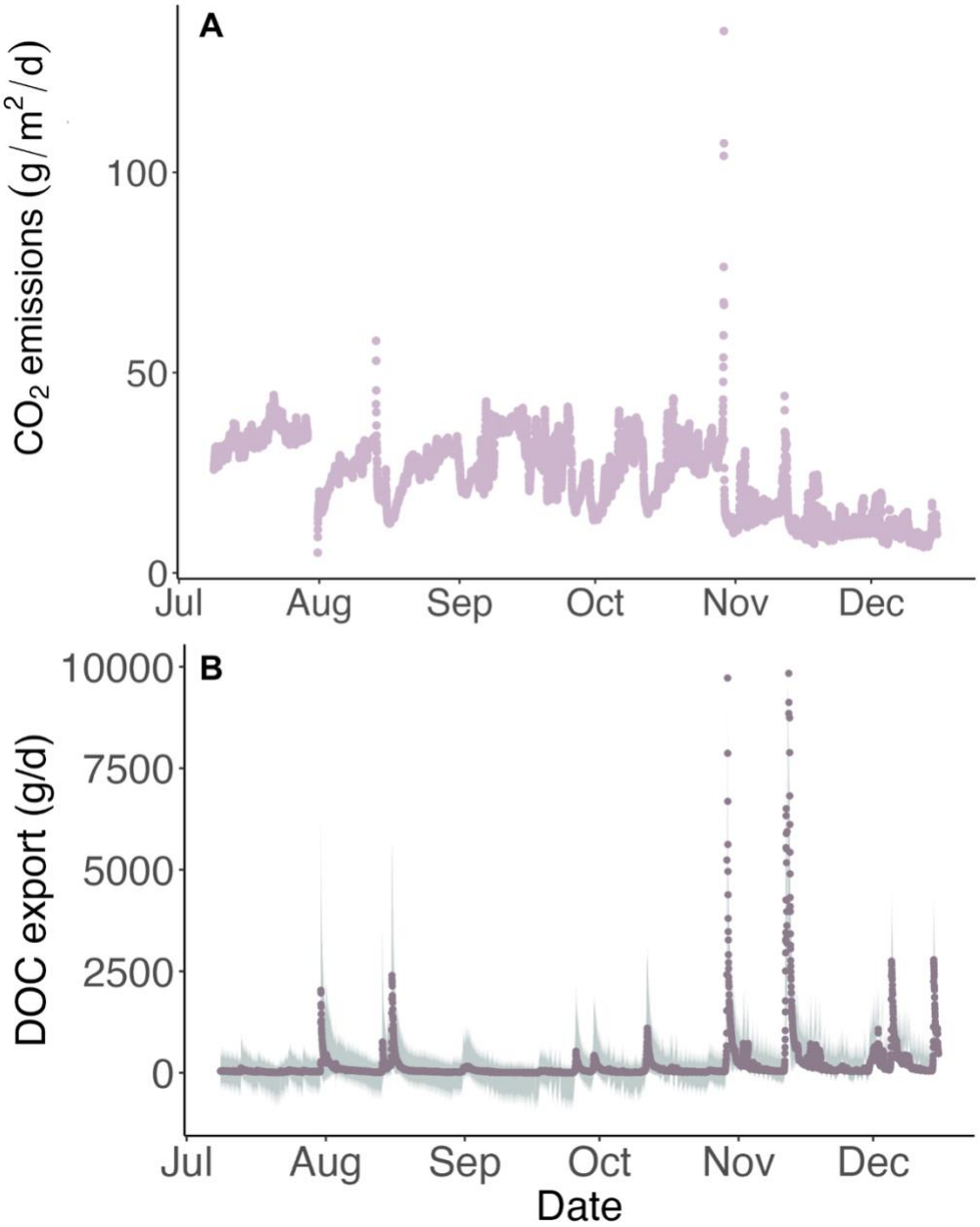

Figure 5. (A) Carbon dioxide (CO_2) emissions and (B) dissolved organic carbon (DOC) export at the sensor pool at the outlet of the non-perennial Beast Stream for the duration of the study period. Shaded area in (B) represents product of 5 and 95% prediction intervals for discharge and DOC concentration.

4 Discussion

We characterized high-frequency CO_2, DOC, discharge, temperature, and DO dynamics over a seasonal drying and rewetting cycle of a temperate, forested non-perennial tributary stream in southwest

Virginia, USA. During the study period, we observed that the stream rarely had continuous surface flow, especially during the summer and early fall. These periods of very low flow, where surface water could be limited to a few isolated pools along a mostly dry channel, were responsible for the highest concentrations of CO_2 and lowest DO. The highest concentrations of DOC occurred when a storm interrupted a low flow period to briefly reconnect pools. Both short- and longer-term increases in stream discharge led to higher DO and lower CO_2 concentrations; however, DOC and Q had the strongest positive correlations during brief moments on the rising limb of storm flood pulses.

High-frequency flow and DO data revealed surprising gradations in concentration at intermediate flow levels along with the more expected contrasts between DO at flow extremes. We found that low DO conditions persisted not only through the driest periods included in the baseflow category, but stream segments were frequently at or near hypoxia (i.e., DO < 3 mg L^{-1}) during mid-baseflow as well. Together the baseflow and mid-baseflow categories represent 51% of observations and 42% of days during our 6-month study period. Low DO during intermediate flow levels can result from DO-poor groundwater and an aerobically active hyporheic and benthic zone (Triska et al., 1990; Valett et al., 1990). A flowing mountain stream would be expected to continuously re-aerate from turbulence, sustaining aerobic respiration in surface waters and shallow sediments (Ward, 1994). We found that dry season flow frequently may not have been sufficient to mix surface waters with the atmosphere. As such, respiration in non-perennial streams shifts towards anaerobic processes across many stream habitats with sustained low DO, which supports methane production and emissions as well (Gómez-Gener et al., 2021). Higher temperature extremes in the future may exacerbate low DO conditions, as warmer waters hold less dissolved gasses and may also induce higher rates of DO-consuming metabolic processes. Microbial biomass and activity are suppressed under low oxygen conditions, which can lead to lower leaf litter degradation (Romani et al., 2017). Further, humid, temperate streams that increasingly experience drying are more likely to have community assemblages and invertebrate taxa that are not well-adapted to sustained low oxygen environments (Crabot et al., 2021).

Surface water disconnection caused CO_2 concentrations to build up when the stream was at low flow. High concentrations of CO_2 and solutes may be typical of pools (Gómez-Gener et al., 2016; Looman et al., 2017) and sediments (Arce et al., 2021; Martinsen et al., 2019; von Schiller et al., 2019) in intermittent streams, and our measurements of concentration and emissions at low flow are within ranges of CO_2 reported for both perennial and intermittent small streams. Soils and dry sediments of non-perennial streams often have an uptick in respiration with rewetting (Arce et al., 2019; Schimel et al., 2011; Yu et al., 2014), consistent with the Birch effect (Birch, 1958). Our results point out potential challenges in observing CO_2 concentration increases in the context of expanded stream surface water. After every recorded rainfall, we saw declines in pool CO_2 concentration, likely due to dilution from rainwater and degassing that exceeds new CO_2 inputs. We were surprised thatmodest rain events did not generate a pulse in CO_2 from rewetted sediments in expanded surface water of the isolated pool. It may be that severe drying caused a delay in the respiration pulse in some sediments (Schreckinger et al., 2022). While rain events were associated with a drop in CO_2, concentrations would rise again when the rain stopped and stream surface water again contracted. If respiration lagged rewetting, we may have captured that CO_2 pulse as part of the redrying effect, but further study is required to assess if these results would be observed during dry phases of other temperate streams.

CO_2 emissions at the scale of the entire wetted stream channel were dominated by storm periods, as emissions during other flow states were spatially limited by fragmentation of surface water area. The stream was fragmented during low and mid-baseflow, which together account for 81 days of the 159-day study period; however, we estimate that the stream as a whole emitted 1271 kg of CO_2 from its wetted surface during those 81 days, compared to 985 kg from the 44.5 high flow days, and 960 kg from the 30 moderate storm days. It may be that the elevated times of CO_2 concentration in the fragmented stream created antecedent conditions that enabled storms to push large quantities of CO_2 both into the atmosphere and downstream. Our finding that emissions during storms were greater if no storms had

previously occurred for 4 days supports the idea that fleeting transitions between desiccated and inundated sediments may have an outsize impact on overall stream CO_2 emissions (Looman et al., 2017). Our data come from a tributary that has notable surface flow variability even for an intermittent stream, and even compared to another non-perennial stream in the same Poverty Creek watershed. Jensen et al. (2017) mapped wet length dynamics of our study stream as well as of one other stream within the Poverty Creek Basin, finding that wet drainage density could vary sixfold over 4 seasons (winter 2015-summer 2016) during which local precipitation totals were higher than during our study (NOAA, 2023) . Since nearby non-perennial streams from Jensen's work in temperate forest streams all maintained greater flow permanence than our study stream, it may be that total reach emissions scaled up for stream surface water area are frequently higher than we estimated.

Data from storm pulses support the idea that intermittent stream channels could be significant sources of DOC. With increasing water residence time in pools, the accumulated DOC in both inundated and dry patches becomes less available as a substrate, and organic matter degradation subsides with less favorable metabolic conditions associated with lower DO (Catalán et al., 2017). Accordingly, many previous studies show that stream drying increases DOC concentration (Granados et al., 2020, 2022; Vazquez et al., 2011); however, we found that DOC did not build up in the sensor-monitored pool. Channel sections of low flow may also accumulate particulate organic carbon (POC), which leaches DOC that is then sitting and waiting to be flushed when the stream reconnects (Wondzell & Ward, 2022). The spatially-frequent flow breaks of a non-perennial stream have ample opportunity to obstruct the export of DOC and POC. Our findings support the idea that storm DOC export can decrease in winter for forested streams due to more frequent scouring and depletion of dissolved sources (i.e., the channel source hypothesis; Wondzell & Ward, 2022). Fragmentation of our study stream may have enhanced channel sources of DOC similarly to how fragmentation enhances bacterial respiration and carbon leaching in sediments as drying shifts redox condition and alters community composition (Casas-Ruiz et al., 2016; Harjung et al., 2018; von Schiller et al., 2015). However, sources from the channel alone may not produce these larger summer concentrations. In intermittent Canadian shield streams, small summer storms

produced higher DOC/Q slopes by sourcing OM from shallower soil as well as rewetted channel sediments, while winter storms generated low DOC/Q slopes due to sourcing from deeper, OM-poor soils (Turmel et al., 2005). Warmer summer and early fall temperatures are favorable for the accumulation of a larger pool of available DOC (Strohmeier et al., 2013). With disrupted flow in a non-perennial stream, DOC may be stranded in the hyporheic zone (Harjung et al, 2019), tiny pockets of stream water (Granados et al., 2020), and shallow OM-rich soils adjacent to the stream (Blaurock et al., 2022). Summer storms occurring after disconnected conditions not only briefly reconnect channel sources but also increase hydrologic connectivity to accumulated DOC in wetter pockets of the riparian zone (Blaurock et al., 2022). Drying-rewetting cycles occurring during summer and early fall then provide small flushes that gather up stored DOC, whether from in-channel pools or more distal terrestrial sources, and stimulate new biogeochemical transformations with changing DO and redox conditions. DOC/Q relationships in non-perennial streams are likely subject to the interplay of both seasonal and hydrologic causes, as we saw the largest DOC concentrations in summer but the second largest during fall storms at the height of leaf fall. The extent to which a fragmented stream may truly isolate from its valley, in different regions and seasons, would be helpful context to have for examining DOC storm pulses.

Non-perennial streams experience not only drastic hydrologic extremes but also a wide variety of intermediate flow states that experience unique biogeochemical conditions. As the channel transitioned from fragmented to connected waters, the flow categories representing in-between states emerged as having unexpected contributions to carbon cycling. Median discharge almost doubled between low baseflow to mid-baseflow and mid baseflow to high flow; however, median carbon concentrations and fluxes usually did not follow suit in incrementally increasing or decreasing at the same proportions. For example, DOC concentration increased from low baseflow to mid-baseflow, then dropped again in the high flow category. Some of these differences in concentration or flux by category, especially between high flow and other categories, likely also reflect seasonal changes in addition to flow increase. Because high flows occurred mostly later in the study period, they coincide more with autumn leaf fall and lower stream temperature. However, low baseflows and mid-baseflows occurred often within the same season,

i.e., there was a 70% increase in discharge between low and mid flows but a 30% decrease in median CO2 concentration. Much prior work on non-perennial systems has been about transitions from dry to flowing or vice versa (e.g., Arce et al., 2014; Bernal et al., 2013; Harjung et al., 2018; Von Schiller et al., 2015), where the transition can be treated as either a single homogenous phase or considered only in the sense of "time-to-drying" when looking to quantify antecedent conditions. However, our work introduces the idea that biogeochemical subtleties may exist in this transitional period. We found no relationship between CO_2 and DOC concentration (Figure S5). This was surprising, as past studies have typically found negative relationships where CO_2 dilutes and DOC increases during storms (Peter et al., 2014; Drake et al., 2018), and we certainly found that storms had a flushing effect on CO_2 concentrations. Because the bulk of our data were not from storms, but rather from varying transition flow states between dry and stormy, the intermediate flow stages blunt the effect of storms on the CO_2-DOC relationship. DOC, having such a low background concentration in Beast Stream (and throughout the region), may be metabolized rapidly upon entering the stream during or after a storm. We observed that when CO_2 began to increase during the post-event phase, DOC had already returned to lower baseline concentrations. Ecosystem respiration is typically higher in small streams like ours (Hotchkiss et al., 2015), potentially indicating more reactive DOC in similar streams where inputs from the landscape may be more recently mobilized and less metabolized than DOC further downstream (Marin-Spiotta et al., 2014). However, the limited nature of our study and the lack of DOC reactivity data from studies in similar streams precludes meaningful speculations on DOC biological availability. Since most of our higher flows occurred in one season, it is also possible that seasonal changes drove differences in CO_2 and DOC responses to intermediate flow states along with hydrologic and connectivity changes. More attention is owed to relationships between inorganic and organic carbon fluxes, especially as emerging long-term trends show uncoupling of CO_2 and DOC concentration in many ecosystems (e.g., Nydahl et al., 2017).

Tracking both wet and dry reaches through hydrologic phase transitions would augment understanding of non-perennial stream carbon biogeochemistry. We were not able to reliably map surface water coverage continuously at frequencies to correspond to our sensor datasets, but increased resolution

of stream spatial contraction and expansion would provide a crucial next step for fine-tuning our estimates of whole-stream carbon emissions and export over different flow states. If we enhance spatial resolution along with including the potential contributions of dry reaches to overall channel emissions, we may find that baseflow conditions contribute the greatest delivery of CO_2 from stream to atmosphere. Linking high-frequency surface water coverage estimates with frequent discrete estimates of dry sediment emissions, to capture subtle and shorter-term flow phase changes, would enable creation of a more robust non-perennial stream CO_2 budget. It is also likely that precipitation falling on dry sediments during highly fragmented periods (when a small to moderate storm would not be enough to reconnect isolated surface water reaches) would stimulate a non-trivial respiration pulse in the sediments and/or hyporheic zone (Arce et al., 2021). CO_2 and DOM generated by brief rewetting of dry reaches, and not exported or emitted, may add to carbon pools temporarily stored in the stream; the next wet-up even may be large enough to degas dissolved CO_2 or be a storm more capable of scouring stored material. The intense flushing of this non-perennial headwater stream points towards the value of future work that will capture hillslope and upstream carbon export along with downstream dynamics and network-scale biogeochemistry.

As the length and duration of non-flowing stream channels increase with changes in climate and anthropogenic flow modifications, understanding the biogeochemical implications of network drying is a priority. This study identified the effects of both extreme flows and intermediate flow stages on carbon emissions and export from a non-perennial stream. Low baseflow and mid-baseflow conditions differed from each other for each carbon parameter we tested, indicating that transitions among intermediate flow states in fragmented streams should be investigated along with droughts and floods. Storms also differed from lower flow conditions for all parameters and dominated CO_2 and DOC export. Non-perennial headwater streams transform from beads of isolated pools to continuous strands of flowing waters multiple times per year and can contain both fragmented and flowing sections at the same time.

Understanding how carbon flux is affected by modulations among different flow states enables us to better approach questions surrounding the freshwater carbon cycle.

Acknowledgements

This work was supported by NSF DEB-1655996, the Virginia Water Resources Research Center, and the Department of Biological Sciences at Virginia Tech. We would like to thank Bobbie Niederlehner for her invaluable assistance in laboratory analyses and thoughtful advice. Thank you to the U.S. Forest Service for access to our field site. Thanks to Stephen Plont for assistance with fDOM sensor calibration and data analysis; to JP Gannon for helpful discussions about storms and DOC; and to Jack Monroe, Kelly Crum, and Rooster Snyder for assistance in the field.

Data Availability

The discharge, DO, CO_2, and DOC data used to characterize changing C dynamics with stream flow in the study are available at the following link:
Bretz, K. (2023). C_Biogeo&Export_NonPStream_Data, HydroShare, http://www.hydroshare.org/resource/47aceb6573e8423da98ca3ba7a13f401. Upon acceptance, data will be published with a DOI.

References

Alin, S. R., Rasera, M. de F. F. L., Salimon, C. I., Richey, J. E., Holtgrieve, G. W., Krusche, A. V., & Snidvongs, A. (2011). Physical controls on carbon dioxide transfer velocity and flux in low-gradient river systems and implications for regional carbon budgets. *Journal of Geophysical Research, 116*(G1). https://doi.org/10.1029/2010jg001398

Arguez, A., Durre, I., Applequist, S., Squires, M., Vose, R., Yin, X., & Bilotta, R. (2010). *NOAA's U.S. Climate Normals (1981-2010)*. National Centers for Environmental Information. doi:10.7289/V5PN93JP

Arce, M. I., Bengtsson, M. M., von Schiller, D., Zak, D., Täumer, J., Urich, T., & Singer, G. (2021). Desiccation time and rainfall control gaseous carbon fluxes in an intermittent stream. *Biogeochemistry*, *155*(3), 381–400.

Arce, M. I., Mendoza-Lera, C., Almagro, M., Catalán, N., Romaní, A. M., Martí, E., Gómez, R., Bernal, S., Foulquier, A., Mutz, M., Marcé, R., Zoppini, A., Gionchetta, G., Weigelhofer, G., del Campo, R., Robinson, C. T., Gilmer, A., Rulik, M., Obrador, B., … von Schiller, D. (2019). A conceptual framework for understanding the biogeochemistry of dry riverbeds through the lens of soil science.

Earth-Science Reviews, *188*, 441–453.

Battin, T. J., Kaplan, L. A., Findlay, S., Hopkinson, C. S., Marti, E., Packman, A. I., Newbold, J. D., & Sabater, F. (2008). Biophysical controls on organic carbon fluxes in fluvial networks. *Nature Geoscience*, *1*(2), 95–100.

Birch, H. F. (1958). The effect of soil drying on humus decomposition and nitrogen availability. *Plant and Soil*, *10*(1), 9–31.

Blaurock, K., Garthen P., da Silva, M.P., Burkhard B., Gilfedder, B.S., Fleckenstein, J.H., Peiffer, S., Lechtenfeld, O.J., & Hopp, L. 2022. Riparian Microtopography Affects Event-Driven Stream DOC Concentrations and DOM Quality in a Forested Headwater Catchment. *Journal of Geophysical Research: Biogeosciences*, *127(12)*. https://doi.org/10.1029/2022JG006831

Bogan, M. T., Chester, E. T., Datry, T., Murphy, A. L., Robson, B. J., Ruhi, A., Stubbington, R., & Whitney, J. E. (2017). Chapter 4.8 - Resistance, Resilience, and Community Recovery in Intermittent Rivers and Ephemeral Streams. In T. Datry, N. Bonada, & A. Boulton (Eds.), *Intermittent Rivers and Ephemeral Streams* (pp. 349–376). Academic Press.

Bretz, K. A., Jackson, A. R., Rahman, S., Monroe, J. M., & Hotchkiss, E. R. (2021). Integrating ecosystem patch contributions to stream corridor carbon dioxide and methane fluxes. *Journal of Geophysical Research: Biogeosciences*, *126*(9). https://doi.org/10.1029/2021jg006313

Bretz, K. A., Murphy, N., and Hotchkis, E. R. (2022). Bretz, K., N. Murphy, E. R. Hotchkiss (2022). C_Biogeo&Export_NonPStream_Data, HydroShare, http://www.hydroshare.org/resource/5b7b84dc99a244598d5e996b6d51edbf

Buffam, I., Galloway, J. N., Blum, L. K., & McGlathery, K. J. (2001). A stormflow/baseflow comparison of dissolved organic matter concentrations and bioavailability in an Appalachian stream. *Biogeochemistry*, *53*(3), 269–306.

Burt, T. P., Ford Miniat, C., Laseter, S. H., & Swank, W. T. (2018). Changing patterns of daily precipitation totals at the Coweeta Hydrologic Laboratory, North Carolina, USA. *International Journal of Climatology*, *38*(1), 94–104.

Butturini, A., & Sabater, F. (2000). Seasonal variability of dissolved organic carbon in a Mediterranean stream. *Biogeochemistry*, *51*(3), 303–321.

Casas-Ruiz, J. P., Tittel, J., von Schiller, D., Catalán, N., Obrador, B., Gómez-Gener, L., Zwirnmann, E., Sabater, S., & Marcé, R. (2016). Drought-induced discontinuities in the source and degradation of dissolved organic matter in a Mediterranean river. *Biogeochemistry*, *127*(1), 125–139.

Catalán, N., Casas-Ruiz, J. P., von Schiller, D., Proia, L., Obrador, B., Zwirnmann, E., & Marcé, R. (2017). Biodegradation kinetics of dissolved organic matter chromatographic fractions in an intermittent river. *Journal of Geophysical Research: Biogeosciences*, *122*(1), 131–144.

Costigan, K. H., Daniels, M. D., & Dodds, W. K. (2015). Fundamental spatial and temporal disconnections in the hydrology of an intermittent prairie headwater network. *Journal of Hydrology*, *522*, 305–316.

Crabot, J., Polášek, M., Launay, B., Pařil, P., & Datry, T. (2021). Drying in newly intermittent rivers leads to higher variability of invertebrate communities. *Freshwater Biology*, *66*(4), 730–744.

Crawford, J. T., Stanley, E. H., Dornblaser, M. M., & Striegl, R. G. (2017). CO2 time series patterns in contrasting headwater streams of North America. *Aquatic Sciences*, *79*, 473–486.

Dinsmore, K. J., Wallin, M. B., Johnson, M. S., Billett, M. F., Bishop, K., Pumpanen, J., & Ojala, A. (2013). Contrasting CO_2 concentration discharge dynamics in headwater streams: A multi-catchment comparison. *Journal of Geophysical Research: Biogeosciences*, *118*(2), 445–461.

Downing, B. D., Pellerin, B. A., Bergamaschi, B. A., Saraceno, J. F., & Kraus, T. E. C. (2012). Seeing the light: The effects of particles, dissolved materials, and temperature on in situ measurements of DOM fluorescence in rivers and streams. *Limnology and Oceanography Methods*, *10*(10), 767–775.

Drake, T. W., Tank, S. E., Zhulidov, A. V., Holmes, R. M., Gurtovaya, T., & Spencer, R. G. M. (2018). Increasing alkalinity export from large Russian Arctic rivers. *Environmental Science & Technology*, 52(15), 8302–8308. https://doi.org/10.1021/acs.est.8b01051

Gómez-Gener, L., Hotchkiss, E. R., Laudon, H., & Sponseller, R. A. (2021). Integrating discharge-concentration dynamics across carbon forms in a boreal landscape. *Water Resources Research*, *57*(8). https://doi.org/10.1029/2020wr028806

Gómez-Gener, L., Obrador, B., Marcé, R., Acuña, V., Catalán, N., Casas-Ruiz, J. P., Sabater, S., Muñoz, I., & von Schiller, D. (2016). When Water Vanishes: Magnitude and Regulation of Carbon Dioxide Emissions from Dry Temporary Streams. *Ecosystems* , *19*(4), 710–723.

Gómez-Gener, L., Siebers, A. R., Arce, M. I., Arnon, S., Bernal, S., Bolpagni, R., Datry, T., Gionchetta, G., Grossart, H.-P., Mendoza-Lera, C., Pohl, V., Risse-Buhl, U., Shumilova, O., Tzoraki, O., von Schiller, D., Weigand, A., Weigelhofer, G., Zak, D., & Zoppini, A. (2021). Towards an improved understanding of biogeochemical processes across surface-groundwater interactions in intermittent rivers and ephemeral streams. *Earth-Science Reviews*, *220*, 103724.

Granados, V., Arias-Real, R., Gutiérrez-Cánovas, C., Obrador, B., & Butturini, A. (2022). Multiple drying aspects shape dissolved organic matter composition in intermittent streams. *The Science of the Total Environment*, *852*, 158376.

Granados, V., Gutiérrez-Cánovas, C., Arias-Real, R., Obrador, B., Harjung, A., & Butturini, A. (2020). The interruption of longitudinal hydrological connectivity causes delayed responses in dissolved organic matter. *The Science of the Total Environment*, *713*, 136619.

Guasch, H., Armengol, J., Martí, E., & Sabater, S. (1998). Diurnal variation in dissolved oxygen and carbon dioxide in two low-order streams. *Water Research*, *32*(4), 1067–1074.

Halbedel, S. (2015). Updates of the headspace equilibration technique often used for CO_2 sampling in water. *Protocol Exchange*. https://doi.org/10.1038/protex.2015.085

Hall, R. O., & Hotchkiss, E. R. (2017). Chapter 34 - Stream Metabolism. In G. A. Lamberti & F. R. Hauer (Eds.), *Methods in Stream Ecology (Third Edition)* (pp. 219–233). Academic Press.

Harjung, A., Sabater, F., & Butturini, A. (2018). Hydrological connectivity drives dissolved organic matter processing in an intermittent stream. *Limnologica* , *68*, 71–81.

Harjung, A., Ejarque, E., Battin, T.J., Butturini, A., Sabater, F., Stadler, M., & Schelker, J. 2019. *Limnology and Oceanography, 64(1),* 46-60. https://doi.org/10.1002/lno.11018

Horgby, Å., Segatto, P. L., Bertuzzo, E., Lauerwald, R., Lehner, B., Ulseth, A. J., Vennemann, T. W., & Battin, T. J. (2019). Unexpected large evasion fluxes of carbon dioxide from turbulent streams draining the world's mountains. *Nature Communications*, *10*(1), 4888.

Hotchkiss, E. R., Hall, R. O., Jr, Sponseller, R. A., Butman, D., Klaminder, J., Laudon, H., Rosvall, M., & Karlsson, J. (2015). Sources of and processes controlling CO_2 emissions change with the size of streams and rivers. *Nature Geoscience*, *8*(9), 696–699.

Ice, G. G., Hale, V. C., Light, J. T., Muldoon, A., Simmons, A., & Bousquet, T. (2021). Understanding dissolved oxygen concentrations in a discontinuously perennial stream within a managed forest. *Forest Ecology and Management*, *479*, 118531.

Jensen, C. K., McGuire, K. J., Shao, Y., & Dolloff, C. A. (2018). Modeling wet headwater stream networks across multiple flow conditions in the Appalachian Highlands. *Earth Surface Processes*

and Landforms, 43(13), 2762-2778. https://doi.org/10.1002/esp.4431

Johnson, E. R., Inamdar, S., Kan, J., & Vargas, R. (2018). Particulate Organic Matter Composition in Stream Runoff Following Large Storms: Role of POM Sources, Particle Size, and Event Characteristics. *Journal of Geophysical Research: Biogeosciences*, *123*(2), 660–675.

Jones, J. B., & Mulholland, P. J. (1998). Carbon dioxide variation in a hardwood forest stream: An integrative measure of whole catchment soil respiration. *Ecosystems* , *1*(2), 183–196.

Keller, P. S., Catalán, N., von Schiller, D., Grossart, H. P., Koschorreck, M., Obrador, B., Frassl, M. A., Karakaya, N., Barros, N., Howitt, J. A., Mendoza-Lera, C., Pastor, A., Flaim, G., Aben, R., Riis, T., Arce, M. I., Onandia, G., Paranaíba, J. R., Linkhorst, A., … Marcé, R. (2020). Global CO2 emissions from dry inland waters share common drivers across ecosystems. *Nature Communications*, *11*(1). https://doi.org/10.1038/s41467-020-15929-y

Koenig, L. E., Shattuck, M. D., Snyder, L. E., Potter, J. D., & McDowell, W. H. (2017). Deconstructing the effects of flow on DOC, nitrate, and major ion interactions using a high-frequency aquatic sensor network. *Water Resources Research*, *53*(12), 10655–10673.

Kokic, J., Sahlée, E., Sobek, S., Vachon, D., & Wallin, M. B. (2018). High spatial variability of gas transfer velocity in streams revealed by turbulence measurements. *Inland Waters*, *8*(4), 461–473.

Lapierre, J. F., F. Guillemette, M. Berggren, and P. A. del Giorgio (2013), Increases in terrestrially derived carbon stimulate organic carbon processing and CO_2 emissions in boreal aquatic ecosystems, *Nature Communications*, 4, 2972. https://doi.org/10.1038/ncomms3972.

Leith, F. I., Dinsmore, K. J., Wallin, M. B., Billett, M. F., Heal, K. V., Laudon, H., Öquist, M. G., & Bishop, K. H. (2015). Carbon dioxide transport across the hillslope–riparian–stream continuum in a boreal headwater catchment. *Biogeosciences* , *12*(6), 1881–1892.

Liu, B., Tian, M., Shih, K., Chan, C. N., Yang, X., & Ran, L. (2021). Spatial and temporal variability of pCO_2 and CO_2 emissions from the Dong River in south China. *Biogeosciences* , *18*(18), 5231–5245.

Looman, A., Maher, D. T., Pendall, E., Bass, A., & Santos, I. R. (2017). The carbon dioxide evasion cycle of an intermittent first-order stream: contrasting water–air and soil–air exchange. *Biogeochemistry*, *132*(1-2), 87–102.

Lupon, A., Denfeld, B. A., Laudon, H., Leach, J., Karlsson, J., & Sponseller, R. A. (2019). Groundwater inflows control patterns and sources of greenhouse gas emissions from streams. *Limnology and Oceanography, 64*(4), 1545-1557. https://doi.org/10.1002/lno.11134

Marcé, R., Obrador, B., Gómez-Gener, L., Catalán, N., Koschorreck, M., Arce, M. I., Singer, G., & von Schiller, D. (2019). Emissions from dry inland waters are a blind spot in the global carbon cycle. *Earth-Science Reviews*, *188*, 240–248.

Marin-Spiotta, E., Gruley, K.G., Crawford, J., Atkinson, E.E., Miesel, J.R., Greene, S., Cardona-Correa, C., & Spencer, R.G.M. (2014). Paradigm shifts in soil organic matter research affect interpretations of aquatic carbon cycling: transcending disciplinary and ecosystem boundaries. *Biogeochemistry* 117, 279-297. https://doi.org/10.1007/s10533-013-9949-7

Martinsen, K. T., Kragh, T., & Sand-Jensen, K. (2019). Carbon dioxide fluxes of air-exposed sediments and desiccating ponds. *Biogeochemistry*, *144*(2), 165–180.

Messager, M. L., Lehner, B., Cockburn, C., Lamouroux, N., Pella, H., Snelder, T., Tockner, K., Trautmann, T., Watt, C., & Datry, T. (2021). Global prevalence of non-perennial rivers and streams. *Nature*, *594*(7863), 391–397.

Moore, R. D. (2005). Slug injection using salt in solution. *Streamline Watershed Management Bulletin*, *8*(2), 1–6.

Nadeau, T.-L., & Rains, M. C. (2007). Hydrological connectivity between headwater streams and downstream waters: How science can inform Policy1. *Journal of the American Water Resources Association*, *43*(1), 118–133.

Peter, H., Singer, G. A., Preiler, C., Chifflard, P., Steniczka, G., & Battin, T. J. (2014). Scales and drivers of temporal pCO_2 dynamics in an Alpine stream. *Journal of Geophysical Research: Biogeosciences*, 119(6), 1078–1091. https://doi.org/10.1002/2013JG002552

Piggott, A. R., Moin, S., & Southam, C. (2005). A revised approach to the UKIH method for the calculation of baseflow / Une approche améliorée de la méthode de l'UKIH pour le calcul de l'écoulement de base. *Hydrological Sciences Journal*, *50*(5). https://doi.org/10.1623/hysj.2005.50.5.911

Plont, S., Riney, J., & Hotchkiss, E. R. (2022). Integrating perspectives on dissolved organic carbon removal and whole-stream metabolism. *Journal of Geophysical Research: Biogeosciences*, *127*(3), e2021JG006610.

Raymond, P. A., Hartmann, J., Lauerwald, R., Sobek, S., McDonald, C., Hoover, M., Butman, D., Striegl, R., Mayorga, E., Humborg, C., Kortelainen, P., Dürr, H., Meybeck, M., Ciais, P., & Guth, P. (2013). Global carbon dioxide emissions from inland waters. *Nature*, *503*(7476), 355–359.

Raymond, P. A., Zappa, C. J., Butman, D., Bott, T. L., Potter, J., Mulholland, P., Laursen, A. E., McDowell, W. H., & Newbold, D. (2012). Scaling the gas transfer velocity and hydraulic geometry in streams and small rivers. *Limnology and Oceanography: Fluids and Environments*, *2*(1), 41–53.

Raymond, P. A., Saiers, J. E., & Sobczak W. V. (2016). Hydological and biogeochemical controls on watershed dissolved organic matter transport: pulse-shunt concept. *Ecology*, *97*(1), 5-16. https://doi.org/10.1890/14-1684.1

Romaní, A.M., Chauvet, E., Febria, C., Mora-Gómez, J., Risse-Buhl, U., Timoner, X., Weitere, M., Zeglin, L. (2017). The biota of intermittent rivers and ephemeral streams: prokaryotes, fungi, and protozoans. In: Datry T, Bonada N, Boulton A (eds) *Intermittent Rivers and Ephemeral Streams*. Academic Press, Massachusetts, pp 161–188.

Schimel, J. P., Wetterstedt, J. Å. M., Holden, P. A., & Trumbore, S. E. (2011). Drying/rewetting cycles mobilize old C from deep soils from a California annual grassland. *Soil Biology & Biochemistry*, *43*(5), 1101–1103.

Schreckinger, J., Mutz, M., & Mendoza-Lera, C. (2022). When water returns: Drying history shapes respiration and nutrients release of intermittent river sediment. *The Science of the Total Environment*, *838*, 155950.

Strohmeier, S., Knorr, K.-H., Reichert, M., Frei, S., Fleckenstein, J. H., Peiffer, S., & Matzner, E. (2013). Concentrations and fluxes of dissolved organic carbon in runoff from a forested catchment: Insights from high-frequency measurements. *Biogeosciences*, *10(2)*, 905–916. https://doi.org/10.5194/bg-10-905-2013

Triska, F. J., Duff, J. H., & Avanzino, R. J. (1990). Influence of exchange flow between the channel and hyporheic zone on nitrate production in a small mountain stream. *Canadian Journal of Fisheries and Aquatic Sciences*, *47*(11), 2099–2111.

Turmel, M. C., Turgeon, J. M. L., Cloutier-Hurteau, B., & Courchesne, F. (2005). Seasonal variations of the transport of dissolved organic carbon in the intermittent stream draining the Hermine headwater catchment on the Canadian Shield. *Revue Des Sciences de L'Eau*, *18*(3), 353–380.

Ulseth, A. J., Hall, R. O., Boix Canadell, M., Madinger, H. L., Niayifar, A., & Battin, T. J. (2019). Distinct air–water gas exchange regimes in low- and high-energy streams. *Nature Geoscience*, *12*(4),

259–263.
Valett, H. M., Fisher, S. G., & Stanley, E. H. (1990). Physical and chemical characteristics of the hyporheic zone of a sonoran desert stream. *Journal of the North American Benthological Society*, *9*(3), 201–215.
Vazquez, E., Amalfitano, S., Fazi, S., & Butturini, A. (2011). Dissolved organic matter composition in a fragmented Mediterranean fluvial system under severe drought conditions. *Biogeochemistry*, *102*(1), 59–72.
Virginia Division of Mineral Resources. (1993). Geologic map of Virginia, Scale 1:500,000. Virginia Division of Mineral Resources.
von Schiller, D., Datry, T., Corti, R., Foulquier, A., Tockner, K., Marcé, R., García-Baquero, G., Odriozola, I., Obrador, B., Elosegi, A., Mendoza-Lera, C., Gessner, M. O., Stubbington, R., Albariño, R., Allen, D. C., Altermatt, F., Arce, M. I., Arnon, S., Banas, D., … Zoppini, A. (2019). Sediment respiration pulses in intermittent rivers and ephemeral streams. *Global Biogeochemical Cycles*, *33*(10), 1251–1263.
von Schiller, D., Graeber, D., Ribot, M., Timoner, X., Acuña, V., Martí, E., Sabater, S., & Tockner, K. (2015). Hydrological transitions drive dissolved organic matter quantity and composition in a temporary Mediterranean stream. *Biogeochemistry*, *123*(3), 429–446.
von Schiller, D., Marcé, R., Obrador, B., Gómez-Gener, L., Casas-Ruiz, J. P., Acuña, V., & Koschorreck, M. (2014). Carbon dioxide emissions from dry watercourses. *Inland Waters*, *4*(4), 377–382.
Ward, J. V. (1994). Ecology of alpine streams. *Freshwater Biology*, *32*(2), 277–294.
Wilson, H. F., Saiers, J. E., Raymond, P. A., & Sobczak, W. V. (2013). Hydrologic Drivers and Seasonality of Dissolved Organic Carbon Concentration, Nitrogen Content, Bioavailability, and Export in a Forested New England Stream. *Ecosystems*, *16*(4), 604–616.
Wondzell, S. M., & Ward, A. S. (2022). The channel-source hypothesis: Empirical evidence for in-channel sourcing of dissolved organic carbon to explain hysteresis in a headwater mountain stream. *Hydrological Processes*, *36*(5). https://doi.org/10.1002/hyp.14570
Yu, Z., Wang, G., & Marschner, P. (2014). Drying and rewetting – Effect of frequency of cycles and length of moist period on soil respiration and microbial biomass. *European Journal of Soil Biology*, *62*, 132–137.
Zhang, T., Li, J., Pu, J., & Wu, F. (2021). Physical and chemical control on CO2 gas transfer velocities from a low-gradient subtropical stream. *Water Research*, *204*, 117564.
Zipper, S. C., Hammond, J. C., Shanafield, M., Zimmer, M., Datry, T., Nathan Jones, C., Kaiser, K. E., Godsey, S. E., Burrows, R. M., Blaszczak, J. R., Busch, M. H., Price, A. N., Boersma, K. S., Ward, A. S., Costigan, K., Allen, G. H., Krabbenhoft, C. A., Dodds, W. K., Mims, M. C., … Allen, D. C. (2021). Pervasive changes in stream intermittency across the United States. *Environmental Research Letters*, *16*(8), 084033.

Chapter 4: Metabolic patterns of non-perennial stream pools

Kristen A. Bretz, J.P. Gannon, and Erin R. Hotchkiss

In preparation for submission, target journal: *Limnology and Oceanography*

Key points

1) Hypoxia and anoxia are common in persistent, isolated pools of non-perennial streams, but dissolved oxygen dynamics differ among pools and streams.
2) Carbon dioxide and methane concentrations in non-perennial stream pools are influenced by water level and low-oxygen environments that facilitate anaerobic respiration.
3) Ecosystem respiration varied by stream, but gross primary production was similar in both streams and higher when pools were isolated.

Abstract

Non-perennial streams are increasingly common in the southeastern United States as precipitation regimes cause longer, more intense periods of drying. Despite growing interest in non-perennial stream hydrology and biogeochemistry, we have few estimates of how prolonged disconnections in surface water flow alters ecosystem processes, including in-stream productivity and metabolism of terrestrially-derived organic matter. We studied isolated pools in two non-perennial streams draining opposite sides of a mountain ridge in southwestern Virginia, USA, during an unusually dry 7-month span. We measured dissolved oxygen (DO) continuously in three pools of each stream. We also took monthly samples of dissolved carbon dioxide and methane from each pool. Prolonged spans of surface water disconnection and times of zero discharge occurred in both streams, though flow was almost always lower in one stream (BST) compared to the other (MDH). All pools experienced hypoxia as a result of stream surface water disconnection, but to varying degrees. One pool from each stream spent approximately 50% of the study period below 50% DO saturation. These lower-DO pools had the highest

concentrations of CO_2 and CH_4 compared to the other pools grouped together. Grouping streams however, CO_2 and CH_4 concentrations were overall higher in the lower flow BST stream (17.5 μg CH_4 L^{-1} compared to 2.5 and 8 mg L^{-1} CO_2 compared to 5.4). We used pool DO data to model rates of gross primary production (GPP) and ecosystem respiration (ER). Metabolism daily estimates were difficult to obtain due to the frequent lack of diel patterns in DO concentrations (n=29 out of 209). We found that GPP was low, ranging from 0.01 - 0.78 g O_2 m^{-2} d^{-1} and increased after pools had been briefly connected by flow. ER ranged from -1.21 to -19.6 g O_2 m^{-2} d^{-1} but did not vary with flow. Non-perennial stream pools occupy unusual conceptual space in the spectrum of aquatic ecosystems where flow, typically the governor of all stream processes, can barely register for weeks only to return in force at a moment's notice. Given the increasing duration of dry periods in many ecosystems due to climate change, understanding the role of isolated pools will help fill knowledge gaps regarding carbon cycling and ecosystem processes in non-perennial systems.

1 Introduction

Stream flow governs the exchange of essential bioenergetic constituents in aquatic ecosystems. When flow disruption occurs, oxygen and carbon dynamics shift in the water remaining in non-perennial stream networks. Non-perennial streams experiencing drastic flow changes occur frequently in many landscapes. Streams integrate biogeochemical signals from their surrounding valleys, but the strength of that signal relies on the connectivity and continuity of water leaving the system. Lack of flow and subsequent reconnection have direct consequences on downstream water quality (Datry et al., 2018). Climate change is affecting precipitation patterns in many ways that will impact streamflow depending on the region; in the southeastern

United States where our study took place, precipitation is expected to fall in less frequent but more intense bursts (Burt et al., 2018). Already, streams across the United States are ceasing flow earlier and for longer periods of time (Zipper et al., 2021). Persistently receding surface waters reshape the physical stream environment and will thus alter biologic activity.

When flow ceases within a reach, the remaining surface water diminishes until only persistent pools are left behind. Just as "the natural flow regime" emerged as a paradigm from investigations of how changes in hydrology affect ecological functions (Poff et al., 1997), non-perennial streams have characteristic drying regimes that drive many ecological and biogeochemical responses (Price et al., 2021). The transition from flowing stream to isolated pools is caused when evapotranspiration exceeds precipitation and/or by flow reduction and eventual surface water contraction after the end of a precipitation event (Shanafield et al., 2021). Headwater stream flow is especially responsive to changes in precipitation over both short (Barefoot et al., 2019; Godsey & Kirchner, 2014; Jensen et al., 2017) and long terms (Ward et al., 2020). The rate of water level recession within a particular pool accounts for the extent of change in physical and chemical parameters, which can be highly variable in pools within and among different streams (Yu et al., 2022). Isolated pools experience a recognizable increase in nutrients, salts, and temperature along with declines in dissolved oxygen (DO) concentration (Gasith & Resh, 2003).

DO in streams is derived from primary producers and turbulence. Short-term hypoxia is common in rivers globally, though it is more typical in warmer, low-gradient and/or urban streams (Blaszczak et al., 2022). Without persistent flow into a stream reach, hypoxia can result from the cessation of turbulent mixing and consumption of remaining DO by aerobic microbes (Ice et al., 2021). Groundwater and hyporheic water, both more prevalent in non-perennial

streams and in sustaining isolated pools, tend to be depleted in DO. Hypoxia in fluvial environments shifts biogeochemical processes, leading to higher production of CH_4 (Gómez-Gener et al., 2020) and N_2O (Venkiteswaran et al., 2014). Prolonged or more frequent oxygen stress is harmful for aquatic organisms (Jewett et al., 2010) and downstream water quality (Whitworth et al., 2012).

Continuous DO data are increasingly used to estimate aquatic metabolism (e.g., Rodríguez-Castillo et al., 2019), but few studies have modeled gross primary productivity (GPP) and ecosystem respiration (ER) in non-perennial systems and their frequently disconnected pools with hypoxic waters. Stream metabolism is tightly coupled to the landscape through terrestrially-derived organic inputs, light availability through the canopy, and topographical- and climate-driven influences on flow permanence (Bernhardt et al., 2018; Sabater et al., 2016). GPP and ER are influenced by factors that fluctuate during flow changes - temperature, gas exchange, organic carbon availability (for ER) - as well as by flow itself (Battin et al., 2023). Dry periods in non-perennial streams lead to the accumulation of organic matter, which stimulated ER when flow resumed in one intermittent stream (Acuna et al., 2004). Rates of organic matter processing remain high in hyporheic sediments when surface water is absent, suggesting that respiration from dry sections of non-perennial streams continues with flow cessation, and may even be stimulated by shifting redox conditions (Burrows et al., 2017; Von Schiller et al., 2019). Perennial pools that emerge from non-perennial streams are host to swings in microbial community assemblage and function (Sabater et al., 2016). Microbes continually adjusting to the changing environments of isolated pools thus create a series of locations with intense biogeochemical activity within the stream channel (Vazquez et al., 2011). Some studies have investigated stream metabolism during flowing phases in non-perennial streams (Acuna et al.,

2004; Bernal et al., 2022; Sabater et al., 2016), but we know little about the metabolic patterns occurring in the water that remains in isolated pools.

Our central goal for this project was to characterize oxygen dynamics in isolated pools with distinctive channel characteristics to determine how flow fragmentation affects metabolic processes in non-perennial streams. Our objectives were to (1) determine how the effects of flow disruption on DO levels of isolated pools varies within and among streams; (2) test how patterns in CO_2 and CH_4 track changes in DO and hydrology during periods of low and no streamflow; and (3) investigate to what extent flow variability affects stream metabolism in persistent pools. We focused on two nearby watersheds, deploying DO sensors and sampling greenhouse gas concentrations in persistent pools of two non-perennial streams draining opposite sides of a mountain. Having previously observed that the south-facing stream had higher, somewhat more persistent surface flow than the north-facing stream, we predicted that contrasting reach-scale hydrology would result in distinct biogeochemical responses in pools of the two streams.

2 Methods

2.1 Study site and hydrology

Our study focused on two non-perennial streams draining opposite sides of Brush Mountain near Blacksburg, Virginia, USA – one draining the southern slope (MDH) and one draining the northern slope (BST; Figure 1a). Brush Mountain is part of the Valley and Ridge physiographic province, where long narrow ridges of the Appalachian Mountains lie parallel running southwest to northeast. Bedrock below the study streams dips to the south (Prince, 2019) and is made of Devonian shales, siltstones, and sandstones (Virginia Division of Mineral Resources, 1993). The area receives 98-103 cm of precipitation yearly; low temperatures in January are around 1 °C and July highs reach 22 °C (Arguez et al., 2010). Rain gauges deployed

for 3 months along each stream, during the winter, showed that the two slopes receive similar precipitation (+/- 3 mm) (Supplemental Table 1). Daily precipitation data were collected from a research weather station approximately 1 mile from the study sites (Ambient Weather WS-2902; Supplemental Table 2). The watersheds of both streams are entirely forested with mature (>60y) hardwood trees. Rhododendrons are present in both watersheds, growing heavily along the banks of the MDH stream but occurring at low denisities along BST.

Along each stream we selected a study reach that included 3 persistent pools (Figure 1b), meaning that even at the lowest flow times there would almost always be water a few centimeters deep. At MDH the distance between the farthest downstream (MDH-down) and farthest upstream pool (MDH-up) was 130 m, with the center pool (MDH-mid) located 90 m upstream of MDH-down. At BST, the distance between the most downstream pool (BST-down) and most upstream (BST-up) was 65 m, and the center pool (BST-mid) was 35 m upstream of BST-down. Riffle sections between the pools on both sides were mostly underlain by large cobbles.

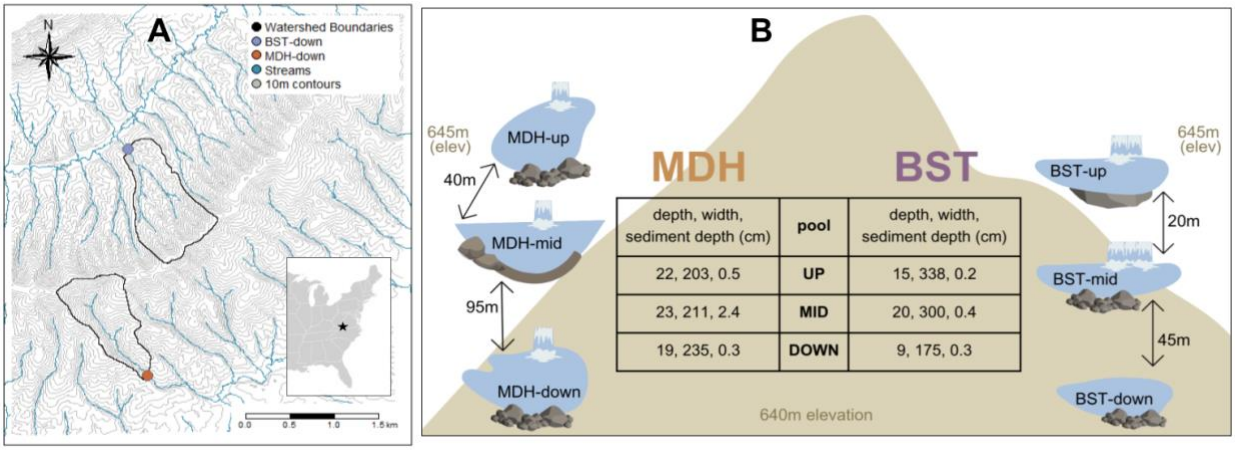

Figure 1. (A) Map showing BST and MDH watersheds relative to each other in southwestern Virginia, USA. The colored dots represent the farthest downstream pool of each study reach (blue/light for BST [37.265 N, 80.48549 W], orange/darker for MDH [37.240715 N, 80.482818 W]. (B) Site sketch of 6 persistent pools from BST and MDH streams. Icons at base of pools show substrate type (small rocks = medium cobbles, large rock = pool over a bedrock outcrop, thick line = layer of fine sediment over large cobbles). Waterfall icon indicates a step pool with presence of a jet when the stream is flowing. Chart gives average pool dimensions for base flow conditions.

We characterized pool morphology by surveying bed material and pool dimensions under different flow conditions. We measured cross sections of the study reach every 10 m repeated every other week for 16 weeks from July to September, and then again every week from December to January to determine when the streams are fully surface reconnected (n = 14 measurement dates total). We installed a pressure transducer (Onset HOBO U20L-04) in BST-down to measure water stage at 30-minute intervals. At MDH, a pressure transducer was permanently installed on a sonde in MDH-down (LevelTR400). We carried out salt (NaCl) dilution gauging to estimate stream travel time and discharge for each stream on six different days. We added NaCl in pulses into mid- and upstream pools of each stream where we placed two conductivity sensors (Onset HOBO U24-001) recording every 10 sec. During pulse additions, we measured channel width and depth every 5 m. We used data from salt additions and high-frequency stage data to create a stream-specific stage-discharge relationship (R^2 = 0.94

for BST and 0.97 for MDH; Supplemental Figure 1). The highest discharge we calculated at MDH was 1.74 and at BST was 1.51 L s^{-1}; flow calculations that were extrapolated above that curve accounted for the upper 17 and 0.1% of discharge estimates, respectively. At MDH, a camera (Moultrie Delta) took hourly photographs of MDH-down from late June until September 20. We checked each photograph for the presence of water falling over the step gradient into MDH-down to determine when there was no flow entering the pool. We used camera images to match "no flow" times with estimated discharge to determine a limit below which we could establish that discharge into/out of isolated pools was effectively zero.

2.2.1 DO sensor deployments

Oxygen sensors (miniDOT, PME) were deployed in 5 of the 6 study pools (all but MDH-down; see below) and programmed to log DO and water temperature measurements at 10 min intervals. We checked the calibration of miniDOTs in the lab before deployment, after 3 months (September 2021), and at the end of the study using bubbling, yeast, and Winkler titrations to inspect high and low calibration points (Hall & Hotchkiss, 2017). At MDH-down, a permanently installed sonde recorded DO every 10 min (Aqua TROLL 500NV, In Situ). The DO sensor in the sonde was calibrated according to manufacturer instructions using a saturated sponge before installation and in September 2021. We used instrument-specific calibration curves and assumed linear drift between calibrations when correcting sensor data using calibration check data.

We analyzed pool-specific DO patterns using exceedance probability (P), which compares the distribution of DO % saturation measurements without regard to when they occurred in the time series dataset. A pool having a low 50% exceedance value means it spends more time with less oxygen than a pool with a high 50% exceedance. We calculated the time that a certain DO % saturation level was equaled or exceeded using Equation 1:

Eq. 1 $$P = 100 \cdot \left[\frac{M}{n+1}\right]$$

where M is the ranked position of the DO % saturation measurement and n is the number of total observations made in a pool.

2.2.2 Ecosystem metabolism modeling

We used DO and water temperature time series data, with modeled light and gas exchange, to estimate daily metabolism in pools of both streams. We used the single-station method (Odum, 1956) due to the frequent lack of surface water connectivity between pools. Light was modeled at 10 min intervals based on site-specific photosynthetic photon flux density (PPFD, mmol m^{-2} s^{-1}; (Yard et al., 2005)). We used an inverse modeling approach with non-linear minimization (*nlm* in R) of the -log likelihood of parameters to estimate GPP and ER (Hall & Hotchkiss, 2017). This model iteratively finds the combination of GPP, ER and air-water gas exchange (K, d^{-1}) that minimizes the difference between measured and modeled oxygen. We let the model estimate K for days when the stream was flowing, noting that K can be higher than expected in step pools (Botter et al., 2022). On days with no flow through pools, we estimated K based on k_{600} (m d^{-1}) previously measured within a range of different discharge values in BST (Bretz et al., in revision) and the temperature normalized gas exchange coefficient. We visually inspected all model fits for every daily estimation, removing days with poor fit or impossible results (i.e., negative GPP and positive ER) and with a negative log likelihood of -110 or greater (Supplemental Tables 3-4).

2.3 CO_2 and CH_4 measurements

We measured dissolved CO_2 and CH_4 from each pool on a monthly basis. We collected triplicate water samples from each pool using the syringe headspace method (Halbedel, 2015). We drew 80 mL of bubble-free water and 40 mL of ambient air into a 120 mL syringe (JMS JS-

S00L) with an attached 3-way stopcock valve (Kimble). We shook each syringe sample vigorously for 3 minutes, after which we ejected the water and injected the headspace into a sealed 20 mL vial (Wheaton MicroLiter 20 mm), displacing ambient air with the sample using a vent needle (Bretz et al., 2021). We measured the headspace concentration of CO_2 and CH_4 using gas chromatography (Shimadzu Nexis GC-2030) fitted with a thermal conductivity and flame ionization detector. We used Equation 2 to estimate the partial pressure of CO_2 and CH_4 in pool water.

Eq. 2

$$C_{gas_i}\ water = BP \cdot \frac{vol_{air}\ (ppmv_{gasi}\ eq - ppmv_{gasi}\ air)}{\left(R \cdot T \cdot vol_{H_2O}\right) + H^{\theta} \cdot e^{\left(\frac{-\Delta_{sol} \cdot H}{R}\left(\frac{1}{T} - \frac{1}{298.15}\right)\right)} \cdot ppmv_{gas_i}eq}$$

The dissolved concentration of Cgasi, either CO2 or CH_4, is a function of barometric pressure (*BP*, kPa), volume of air in the headspace (vol_{air}, m^{-3}), measured concentration of gas_i in the equilibrated headspace (after mixing air and water, accounting for the volume and temperature of the sample water using Henry's law constant for CO_2 or CH_4 at water temperature and partial pressure of the gas in the air) ($ppmv_{gas\ eq}$, ppm), the concentration of the gas in the air used as headspace ($ppmv_{gas\ air}$, ppm), the universal gas constant (*R*, m^3 kPa K^{-1} mol^{-1} [converted from L atm K^{-1} mol^{-1}]), headspace temperature (*T*, K), the volume of water equilibrated (vol_{H20}, m^3), and Henry's law constant H^{Θ} at a standard temperature (298.15 K) for CO_2 and CH_4 converted to headspace temperature ($-\Delta_{sol} \cdot H/R$) (Henry's law constants for CO_2 and CH_4 from Sander, 2015; method adapted from Demarty et al., 2011).

2.4 Statistical analyses

We performed all data exploration and statistical analyses using base R (version 3.6.1; R Core Team, 2021). To test for variability in DO concentrations within each pool, we calculated

the standard deviation (s.d.) from the mean; then we used the F-test to see if s.d. differed among pools. To test for differences between stream and pool mean DO, CO_2, and CH_4, we used a one-way analysis of variance (ANOVA; (*aov()*). We used the Tukey Honest Significant Difference test to compare means within groups with significant differences (streams, pools, recent surface water reconnection).

3 Results

The study watersheds were very dry during the sampling campaign compared to typical conditions. Typical precipitation from June to January is 706 mm (NOAA NWS 1991-2020), but from June 2021 to Jan 2022 was only 368 mm (Figure 2a; Supplemental Table 1). Ongoing work is constraining flow estimations from the study reaches using camera data to identify no flow days. So far, we estimate that days with calculated flow less than 0.27 L s^{-1} at MDH and 0.15 L s^{-1} at BST are in fact "zero flow" days (Figure 2b). Discharge was so low in both streams that this changes over 53% of calculated flows to 0 in the MDH stream and 92% in BST. Mean discharge was higher in MDH, 1.28 L s^{-1}, compared to 0.06 L s^{-1} in BST (Figure 2b). Median BST flow was 0 L s^{-1} after implementing the no flow cutoff; this is lower than the median of 0.3 for a similar time period from the previous year (Bretz et al., in revision). Median stream temperature in BST was 13.9 °C (range 2.3 - 19.0 °C) and in MDH was 13.3 (1 - 20.2 °C) (Figure 2c).

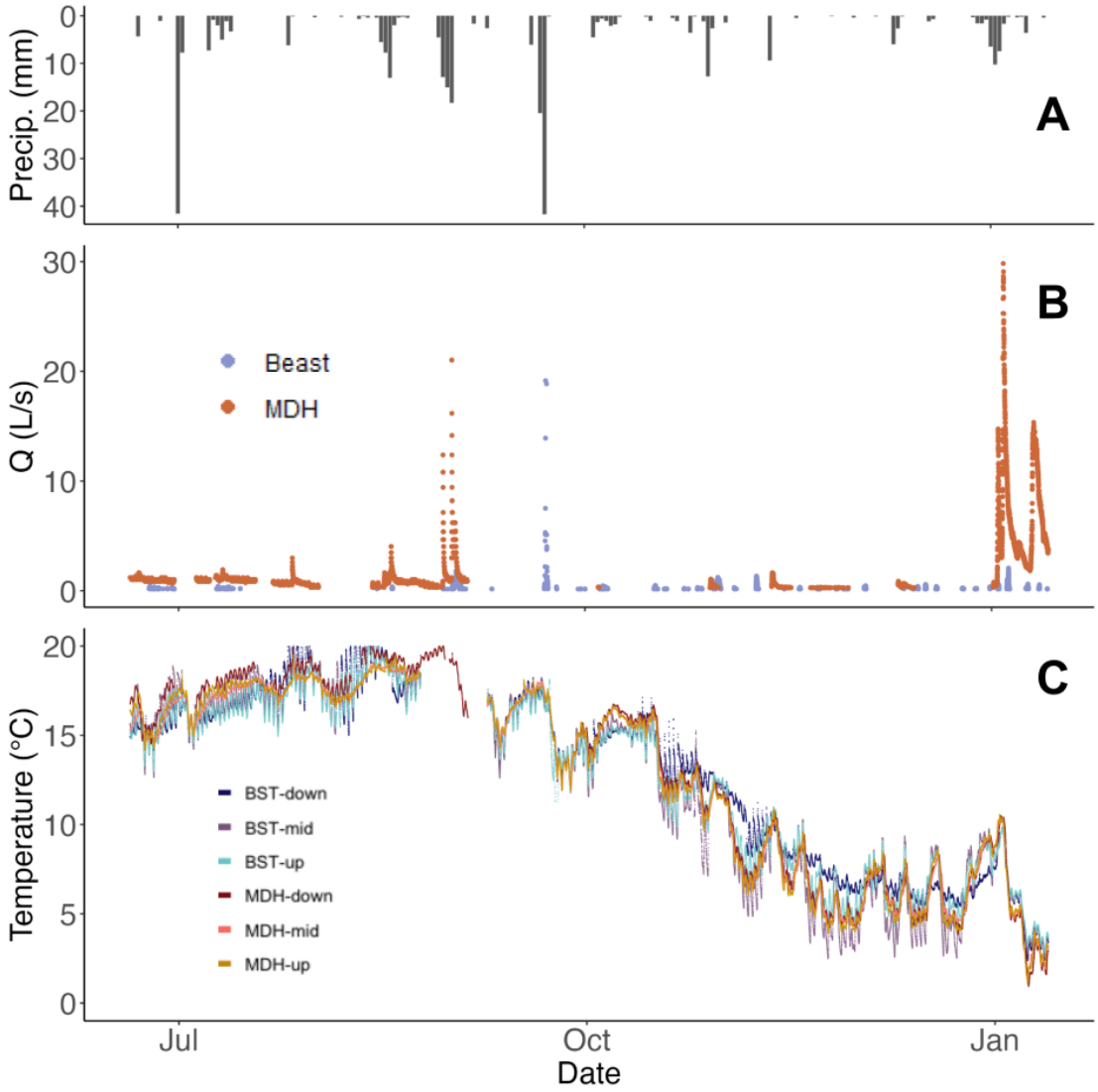

Figure 2. Time series of (A) local precipitation, (B) discharge, and (C) pool water temperature. Gaps in discharge (B) depict times of no flow through persistent pools. Gaps in temperature data (C) are times when sensors were removed from the stream for lab calibration (all pools) or data loss from temporary malfunction (MDH-down, red).

3.1 DO concentration

Patterns of DO concentration were distinct among streams and pools. Low oxygen conditions (<50% DO saturation) were common in all pools prior to October 2021 and concentrations remained under 75% for most pools until the stream fully reconnected in January

2022 (Figure 3a, b). Average DO in BST was lower than that of MDH (60% compared to 66% DO saturation, $p < 0.0001$). Pool average DO concentrations were all different from each other ($p < 0.0001$) except for BST-mid and MDH-up ($p = 0.99$). The standard deviation of DO concentrations were highest for BST-down (s.d. = 3.1) than other pools (s.d. < 3), but pool s.d.s were all different from each other ($p < 0.001$ for every pair of pools). BST-down and MDH-mid also had the lowest mean DO concentrations with 53% and 51% DO saturation, respectively. The divergent DO dynamics of BST-down and MDH-mid compared to the other 4 pools are evident from the pool DO exceedance curves: BST-down and MDH-mid both experienced hypoxic conditions (less than 30% DO saturation) for around 40% of the study period (Figure 3c). BST-down and MDH-mid had 50% exceedance values of 37-40 DO% saturation compared to 62% saturation for BST-up and over 75% saturation for BST-mid and MDH-down and -up.

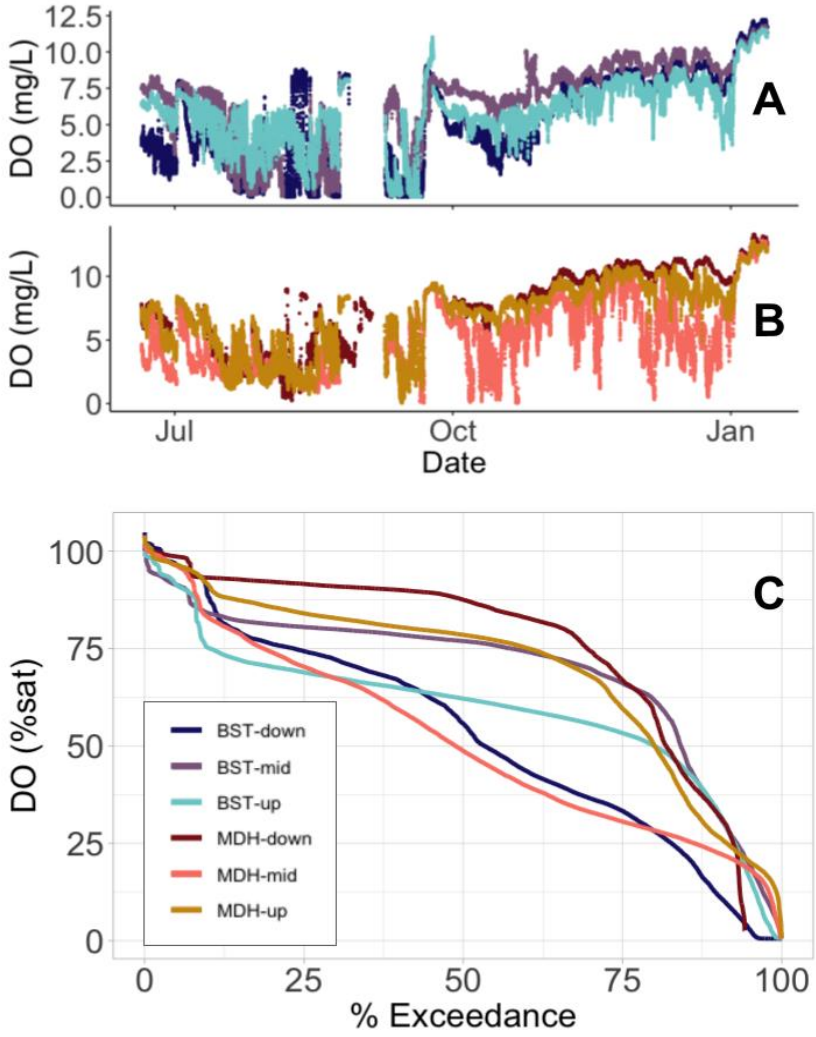

Figure 3. (A, B) Time series of DO concentrations in persistent pools of BST (A) and MDH (B) streams. Data gaps are times when sensors were removed for calibration (all pools) or data loss from temporary malfunction (MDH-down). (C) Exceedance probability curves of DO% saturation for each persistent pool.

3.2 Metabolism

We obtained daily metabolism estimates for 52 observations across 29 days from all 6 pools during the study period (209 days total). We obtained more estimates from BST (38) compared to MDH (14; Figure 5). ER was higher in BST pools, with a median of -5.7 g O_2 m^{-2} d^{-1} (range -1.2 to -19.6) compared to -4.7 g O_2 m^{-2} d^{-1} for MDH (range -1.4 to -8.2; $p = 0.03$, $F_{1, 50} = 5.1$). GPP was low and did not vary by stream ($p = 0.8$), with a median of 0.1 g O_2 m^{-2} d^{-1} for

both streams (range for BST 0.01-0.7 and for MDH 0.01-0.5 g O_2 m^{-2} d^{-1}). Rates of ER were the same over time and flow conditions, i.e., regardless of whether pools were connected or isolated in both streams ($p = 0.92$). GPP was higher in isolated pools of both streams ($p = 0.007$, $F_{1, 50} = 7.9$), with a median of 0.16 g O_2 m^{-2} d^{-1} compared to 0.05 when the pools were connected.

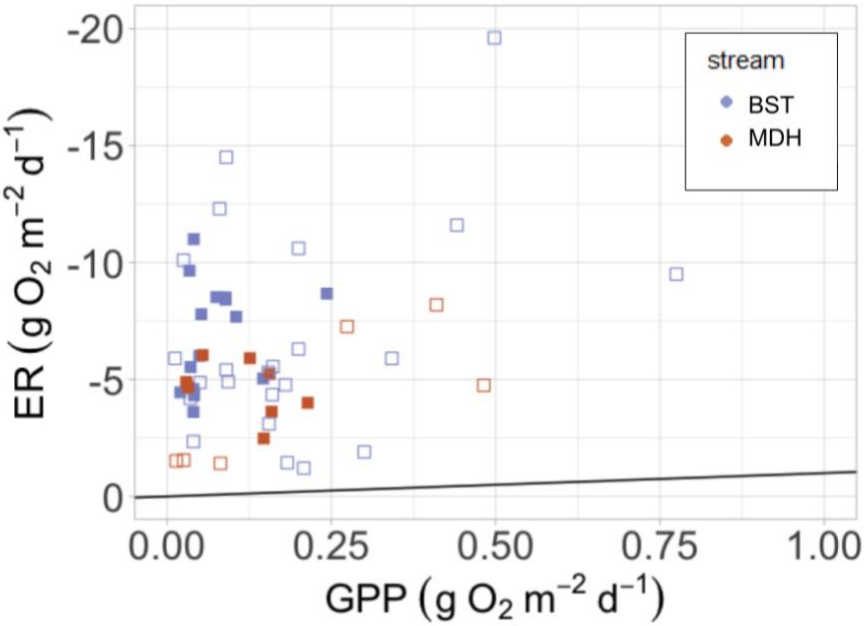

Figure 4. Gross primary production (GPP) and ecosystem respiration (ER) estimates from persistent pools of two non-perennial streams, with the BST stream represented by lighter blue squares and MDH by darker orange squares. Open squares indicate estimates from isolated pools, and filled squares indicated pools had recently reconnected. Note y-axis is reversed to emphasize more negative ER is a larger oxygen consumption flux.

3.3 CH_4 and CO_2 concentrations

CH_4 and CO_2 concentrations were higher in pools of BST than in those of MDH, but concentrations varied by individual pool. CH_4 concentrations were small in pools (median for both streams < 2 μg L^{-1}), with a few hot moments of high CH_4 observed in both streams but higher overall levels in BST ($p = 0.02$, $F_{1,95} = 5.2l$; Figure 4). In BST, CH_4 ranged from 0.07 -

193 μg L^{-1} with a median of 1.97 μg L^{-1}, while in MDH pools the range was 0.04 - 13.7 μg L^{-1} with a median of 0.7 μg L^{-1}. The highest median CH4 for any single pool came from MDH-mid (4.5 μg L^{-1}, range 0.07 - 13.7), with the other two MDH pools both having median concentrations less than 1 μg L^{-1} the difference among MDH pools was not significant ($p = 0.9$ for MDH-mid compared to both -down and -up). Median CH_4 concentrations in lower, middle, and upper BST pools were 1.3, 1.5, and 2.2 μg L^{-1} respectively. The highest CH_4 concentrations observed during the study were from BST-down, which were statistically higher than BST-mid and -down ($p < 0.01$ for both). CO_2 concentrations were higher in BST than MDH ($p < 0.001$, $F_{1,174} = 11.7$) with a median of 6.38 mg L^{-1} (range 1.1 - 30 mg L^{-1}) in BST compared to 5.4 (range 0.7 - 12 mg L^{-1}) in MDH. The highest median CO_2 concentrations were in BST-down (12 mg L^{-1}) compared to other BST pools ($p < 0.001$). MDH-mid had elevated concentrations compared to MDH-down and -up (median 7.3 mg L^{-1} compared to 5.3 and 5.9, respectively; $p = 0.03$).

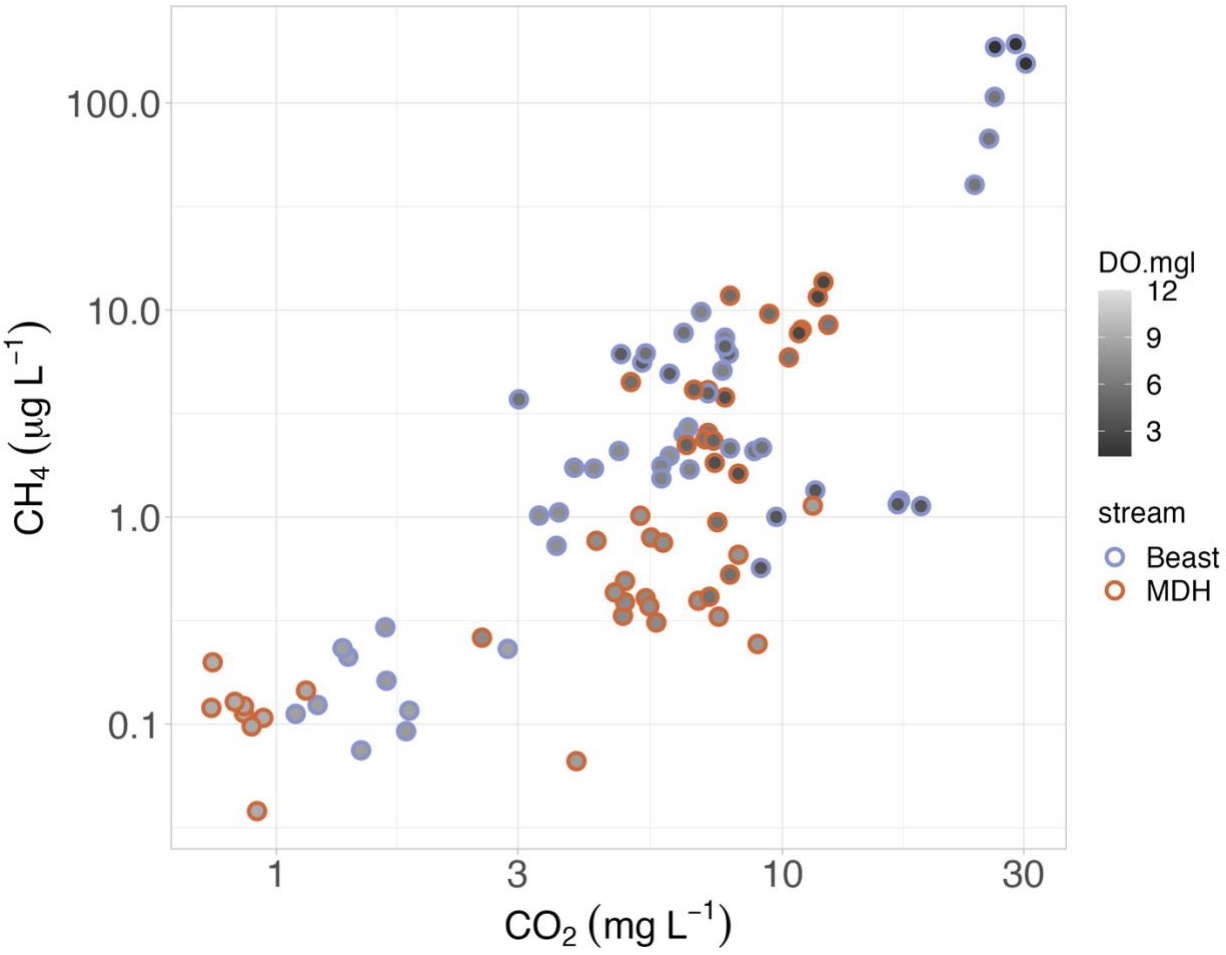

Figure 5. CO_2 and CH_4 concentrations in all 6 pools of both streams, with BST pools represented by lighter blue points outlines and MDH by darker orange points. Point fill corresponds to DO concentration. Note log scale axes.

4 Discussion

We characterized continuous DO dynamics, CO_2 and CH_4 concentrations, and metabolism of two non-perennial streams during a period where they experienced frequent, prolonged surface water disconnection. The study period from June 2021 to January 2022 was unusually dry, especially in the fall months. Dry conditions led to frequent hypoxia within stream pools, especially in the BST stream which had both lower flow and lower oxygen levels than MDH. Pool CO_2 and CH_4 were also influenced by low flow and DO, with higher concentrations

associated with surface water disconnection and lower DO. ER was greater in BST than MDH and did not differ between periods of channel connection/disconnection, while GPP did not vary by stream but was lower in pool measurement sites when they were surface water connected.

While the patterns of DO drawdown in the persistent pools of our study streams were consistent with previous studies (e.g., Gómez-Gener et al. 2021), we were surprised to find that DO dynamics were so different among pools of the same stream. Our observations of DO saturation were lower but within range of low order streams during dry conditions (Diamond et al. 2021; Blaszczak et al. 2019) as well as with small ephemeral ponds (Martinsen, Kragh, and Sand-Jensen 2019). Given the influence of flow level on DO supply (Garvey, Whiles, and Streicher 2007), we expected that MDH, our higher discharge stream, would have less severe DO depletion. While this was true for MDH-up and MDH-down, the MDH-mid pool stood out for its consistently low DO environment. MDH-mid was the deepest of the pools we monitored. Oddly, the shallowest pool (BST-down) was the other standout pool with more frequent hypoxia. The varying responses of pool DO to dry down within streams have many ecological implications. Anoxic pools have outsize significance to ecological processes within a catchment (Bernhardt et al., 2017) with respect to biogeochemical activity as well as nutrient and contaminant cycling (Blaszczak et al., 2019; Iles et al., 2022). The reactions within hypoxic and anoxic isolated pools influence how rewetting events may cause hypoxia to permeate downstream with flow as pools reconnect (Hladyz et al., 2011).

While CO_2 and CH_4 concentrations differed by stream, pool location was also an important factor. Low DO when pools were isolated was associated with high CH_4 concentrations, consistent with DO-CH_4 relationships in many aquatic ecosystems (Stanley et al. 2016; Peacock et al. 2021; Burke et al. 2019). The highest CO_2 and CH_4 concentrations occurred

in the more frequently anoxic pools, MDH-mid and BST-down. That carbon gas concentrations would be more variable from pool to pool is expected given many previous reports of CO_2 and CH_4 heterogeneity in both perennial (Bretz et al. 2021; Crawford et al. 2017; Clow, Striegl, and Dornblaser 2021) and non-perennial (Granados et al. 2020; Looman et al. 2017) streams. CO_2 build-up in isolated pools has been recorded previously in the BST watershed; the BST-down pool was repeatedly observed to begin accumulating CO_2 after a rain event during periods of surface water fragmentation (Bretz et al., in revision). Here we found evidence that as no-flow periods are prolonged, high CO_2 and reducing conditions yield hot moments of CH_4 production. Anaerobic respiration can be a significant source of greenhouse gasses but is most often observed in flatter, warmer streams (DelVecchia et al., 2022). While the channels in this study would not be characterized as low-gradient, the isolated pools essentially have no gradient during zero-flow periods; further, within a season, pool temperature increases with time since the last precipitation event. This shift in conceptualizing the site—from a high-gradient flowing stream to zero-gradient isolated pools—overlaps with the influence of geomorphically-induced habitat heterogeneity on stream CO_2 and CH_4. For example, Lupon et al. (2019) found that the location of OM source material into the stream drove CO_2 and CH_4 concentrations, and Smits et al. (2017) identified channel physical drivers such as slope, bed roughness, and hydraulic geometry. Isolated pools form along the stream channel at places where some geomorphic drivers will take on enhanced local importance (e.g., a pool in a deep, sedimented bowl like MDH-mid) and others will diminish (e.g., the last remnant of a riffle where slope no longer matters like BST-down).

Different causes may be behind the similar biogeochemical responses of MDH-mid and BST-down. BST-down was the only persistent pool not immediately below a step gradient and

was the first pool to isolate during the drying phase; therefore, its low DO may have resulted from less upstream supply and earlier depletion of remaining oxygen by aerobic respiration. Similarly, since it is not directly over or below a bedrock outcrop, BST-down likely has a stronger connection to the hyporheic zone of the reach lying just upstream, and hyporheic zones often serve as sources of CO_2 and CH_4 to stream surface waters (Dinsmore et al., 2013; Rasilo et al., 2017; Schindler & Krabbenhoft, 1998). MDH-mid had the thickest layer of benthic sediment, which may have enabled higher oxygen demand by benthic heterotrophic organisms compared to the other pools. When inflow is very low or absent, the pool may behave like a pond where high sediment and edge to water ratios promote CH_4 production and anoxia disallows CH_4 oxidation (Holgerson & Raymond, 2016).

GPP and ER estimates from pools in this study were within range of others for small (Rodríguez-Castillo et al. 2019) and forested (Roberts, Mulholland, and Hill 2007; Bernot et al. 2010; (Northington et al., 2013)) streams. Our estimates of ER were more variable from pools, both when isolated and when connected, than both a nearby, lower-gradient second-order stream (O'Donnell & Hotchkiss, 2019) as well as from flowing phases of a non-perennial Mediterranean stream (Bernal et al. 2022). Some of the variability in metabolism is likely introduced by uncertainty in our estimates of K. However, it is notable that there was no pattern in this variation in ER by pool, stream, or hydrologic condition. We expected rewetting cycles would be followed by relatively large pulses of ER due to the build up of organic matter in the channel, as in a non-perennial Mediterranean stream (Acuna et al., 2004). Drying affects the delivery and quality of organic matter substrates available for ER and is variable across different habitats of the stream (Ylla et al., 2011). Our findings of no change to ER and lower GPP after surface water reconnection is thus in contrast to a recent study comparing non-perennial and perennial

stream metabolism where GPP was not different between the two environments but ER was higher in the perennial stream (Bernal et al., 2022).

The limited spatial and temporal extent of this study limits broader characterizations of non-perennial stream metabolism. However, the difficulty of modeling metabolism in challenging watersheds or periods (i.e., low flow, high groundwater inputs, disturbance events) creates a hole in network-scale perspectives of GPP and ER (Diamond et al. 2021). Noisy DO signals are common in many freshwaters of interest, for instance ephemeral ponds (Martinsen, Kragh, and Sand-Jensen 2019) and urban streams (Blaszczak et al., 2019). Metabolism is a useful metric of ecosystem function, but its drivers can be both numerous and competing. For instance, metabolism drives the drawdown of DO, but the intensity of this decline in isolated pools makes actually measuring metabolism in them difficult. Several factors that influence both stream metabolic activity and the means we use to estimate metabolism are also central to lingering questions surrounding the dynamics of hydro-biogeochemical responses of non-perennial systems. The locations and magnitudes of groundwater inputs along the stream channel affect dry-down speed and extent (Shanafield et al., 2021) as well as what method is most appropriate for estimating metabolism (Hall et al., 2016). The rate of exchange between dissolved stream gasses and the air is central to the metabolism model (Hall & Hotchkiss, 2017); it is also one of the most difficult parameters to accurately measure or estimate from perennial streams (Raymond et al., 2012), much less streams that are constantly fluctuating between intense turbulence and stagnation. Gathering metabolism estimates from diverse watersheds, especially those with emerging hydrologic regime shifts due to global change, will improve our ability to apply metabolism as a management tool (Jankowski et al., 2021)

Biogeochemical activity in non-perennial streams is affected by the extent and duration of surface water disconnection. We studied isolated pools in two non-perennial streams during an unusually dry 7-month period, but often non-perennial streams in this region and many temperate forests oscillate more frequently between flowing and non-slowing states (e.g., Bretz et al., in revision; Jensen et al. 2017). Our goal was to determine to what degree overall higher flow and anticipated shorter duration of fragmentation into pools (in MDH) would affect stream metabolism. Instead the drought kept the pools of both streams from fully reconnecting for much of the study period, and we learned more about the distinct DO depletion regimes of individual pools. Frequent hypoxia and anoxia in pools resulted in a shift to anaerobic respiration and resulting higher CO_2 and CH_4 concentrations. Geomorphic heterogeneity and variable flow-mediated responses are central concepts for understanding patterns and drivers of biogeochemical cycling in river networks, and non-perennial stream pools are at the intersection of these concepts. The interaction of spatial and temporal hydrologic complexity in non-perennial ecosystems present a formidable challenge to understanding carbon and oxygen cycling. Studying isolated pools is an opportunity to observe many processes at an accessible spatial scale that may become increasingly relevant to network and regional biogeochemistry as non-perennial streams become more common across many landscapes.

Acknowledgements
This work was supported by the Virginia Water Resources Research Center, NSF DEB 1655996, and the Virginia Tech Department of Biological Sciences. Thank you to Kelly Crum, Morgan Wood, Felicity Detoll, and Rooster Snyder for assistance in the field; Kelly Crum and Carmen Curry helped with data processing. Many thanks to Bobbie Niederlehner for her support and assistance in the analytical lab. Thank you to the United States Forest Service and the town of Blacksburg, Virginia for access to the two study streams.

References

Acuna, V., Adonis, G., Munoz, I., Uehlinger, U., & Sabater, S. (2004). Flow extremes and benthic organic matter shape the metabolism of a headwater Mediterranean stream. *Freshwater Biology*, *49*, 960–971. https://login.ezproxy.lib.vt.edu/login?qurl=https%3A%2F%2Fonlinelibrary.wiley.com%2Fdoi%2Fpdfdirect%2F10.1111%2Fj.1365-2427.2004.01239.x

Arguez, A., Durre, I., Applequist, S., Squires, M., Vose, R., Yin, X., & Bilotta, R. (2010). *NOAA's U.S. Climate Normals (1981-2010)*. National Centers for Environmental Information. DOI:10.7289/V5PN93JP

Barefoot, E., Pavelsky, T. M., Allen, G. H., Zimmer, M. A., & McGlynn, B. L. (2019). Temporally Variable Stream Width and Surface Area Distributions in a Headwater Catchment. *Water Resources Research*, 2018WR023877. https://doi.org/10.1029/2018WR023877

Battin, T. J., Lauerwald, R., Bernhardt, E. S., Bertuzzo, E., Gener, L. G., Hall, R. O., Jr, Hotchkiss, E. R., Maavara, T., Pavelsky, T. M., Ran, L., Raymond, P., Rosentreter, J. A., & Regnier, P. (2023). River ecosystem metabolism and carbon biogeochemistry in a changing world. *Nature*, *613*(7944), 449–459. https://doi.org/10.1038/s41586-022-05500-8

Bernal, S., Cohen, M. J., Ledesma, J. L. J., Kirk, L., Martí, E., & Lupon, A. (2022). Stream metabolism sources a large fraction of carbon dioxide to the atmosphere in two hydrologically contrasting headwater streams. *Limnology and Oceanography*, *67*(12), 2621–2634. https://doi.org/10.1002/lno.12226

Bernhardt, E. S., Blaszczak, J. R., Ficken, C. D., Fork, M. L., Kaiser, K. E., & Seybold, E. C. (2017). Control Points in Ecosystems: Moving Beyond the Hot Spot Hot Moment Concept. *Ecosystems* , *20*(4), 665–682. https://doi.org/10.1007/s10021-016-0103-y

Bernhardt, E. S., Heffernan, J. B., Grimm, N. B., Stanley, E. H., Harvey, J. W., Arroita, M., Appling, A. P., Cohen, M. J., McDowell, W. H., Hall, R. O., Read, J. S., Roberts, B. J., Stets, E. G., & Yackulic, C. B. (2018). The metabolic regimes of flowing waters. *Limnology and Oceanography*, *63*(S1), S99–S118. https://doi.org/10.1002/lno.10726

Blaszczak, J. R., Delesantro, J. M., Urban, D. L., Doyle, M. W., & Bernhardt, E. S. (2019). Scoured or suffocated: Urban stream ecosystems oscillate between hydrologic and dissolved oxygen extremes. *Limnology and Oceanography*, *64*(3), 877–894. https://doi.org/10.1002/lno.11081

Blaszczak, J. R., Koenig, L. E., Mejia, F. H., Gómez-Gener, L., Dutton, C. L., Carter, A. M., Grimm, N. B., Harvey, J. W., Helton, A. M., & Cohen, M. J. (2022). Extent, patterns, and drivers of hypoxia in the world's streams and rivers. *Limnology and Oceanography Letters*. https://doi.org/10.1002/lol2.10297

Botter, G., Carozzani, A., Peruzzo, P., & Durighetto, N. (2022). Steps dominate gas evasion from a mountain headwater stream. *Nature Communications*, 13, 7803. https://doi.org/10.1038/s41467-022-35552-3

Bretz, K. A., Jackson, A. R., Rahman, S., Monroe, J. M., & Hotchkiss, E. R. (2021). Integrating ecosystem patch contributions to stream corridor carbon dioxide and methane fluxes. *Journal of Geophysical Research. Biogeosciences*, *126*(9). https://doi.org/10.1029/2021jg006313

Bretz, K.A., Murphy, N.M, and Hotchkiss, E.R. Carbon Biogeochemistry and Export Governed by Flow in a Non-perennial Stream. In Revision at *Water Resources Research.*

Burrows, R. M., Rutlidge, H., Bond, N. R., Eberhard, S. M., Auhl, A., Andersen, M. S., Valdez, D. G., & Kennard, M. J. (2017). High rates of organic carbon processing in the hyporheic zone of intermittent streams. *Scientific Reports*, *7*(1), 13198. https://doi.org/10.1038/s41598-017-12957-5

Burt, T. P., Ford Miniat, C., Laseter, S. H., & Swank, W. T. (2018). Changing patterns of daily precipitation totals at the Coweeta Hydrologic Laboratory, North Carolina, USA. *International Journal of Climatology*, *38*(1), 94–104. https://doi.org/10.1002/joc.5163

Datry, T., Boulton, A. J., Bonada, N., Fritz, K., Leigh, C., Sauquet, E., Tockner, K., Hugueny, B., & Dahm, C. N. (2018). Flow intermittence and ecosystem services in rivers of the Anthropocene. *The Journal of Applied Ecology*, *55*(1), 353–364. https://doi.org/10.1111/1365-2664.12941

DelVecchia, A. G., Rhea, S., Aho, K. S., Stanley, E. H., Hotchkiss, E. R., Carter, A., & Bernhardt, E. S. (2022). Variability and drivers of CO_2, CH_4, and N_2O concentrations in streams across the United States. *Limnology and Oceanography*. https://doi.org/10.1002/lno.12281

Dinsmore, K. J., Billett, M. F., & Dyson, K. E. (2013). Temperature and precipitation drive temporal variability in aquatic carbon and GHG concentrations and fluxes in a peatland catchment. *Global Change Biology*, *19*(7), 2133–2148. https://doi.org/10.1111/gcb.12209

Gasith, A., & Resh, V. H. (2003). *Streams in Mediterranean Climate Regions: Abiotic Influences and Biotic Responses to Predictable Seasonal Events*. https://doi.org/10.1146/annurev.ecolsys.30.1.51

Godsey, S. E., & Kirchner, J. W. (2014). Dynamic, discontinuous stream networks: hydrologically driven variations in active drainage density, flowing channels and stream order. *Hydrological Processes*, *28*(23), 5791–5803. https://doi.org/10.1002/hyp.10310

Gómez-Gener, L., Lupon, A., Laudon, H., & Sponseller, R. A. (2020). Drought alters the biogeochemistry of boreal stream networks. *Nature Communications*, *11*(1), 1795. https://doi.org/10.1038/s41467-020-15496-2

Halbedel, S. (2015). Updates of the Headspace Equilibration Technique often used for CO2 Sampling in water. *Protocol Exchange*. https://doi.org/10.1038/protex.2015.085

Hall, R. O., & Hotchkiss, E. R. (2017). Chapter 34 - Stream Metabolism. In G. A. Lamberti & F. R. Hauer (Eds.), *Methods in Stream Ecology (Third Edition)* (pp. 219–233). Academic

Press. https://doi.org/10.1016/B978-0-12-813047-6.00012-7
Hall, R. O., Tank, J. L., Baker, M. A., Rosi-Marshall, E. J., & Hotchkiss, E. R. (2016). Metabolism, Gas Exchange, and Carbon Spiraling in Rivers. *Ecosystems , 19*(1), 73–86. https://doi.org/10.1007/s10021-015-9918-1
Hladyz, S., Watkins, S. C., Whitworth, K. L., & Baldwin, D. S. (2011). Flows and hypoxic blackwater events in managed ephemeral river channels. *Journal of Hydrology*, *401*(1), 117–125. https://doi.org/10.1016/j.jhydrol.2011.02.014
Holgerson, M. A., & Raymond, P. A. (2016). Large contribution to inland water CO2 and CH4 emissions from very small ponds. *Nature Geoscience*, *9*(3), 222–226. https://doi.org/10.1038/ngeo2654
Ice, G. G., Hale, V. C., Light, J. T., Muldoon, A., Simmons, A., & Bousquet, T. (2021). Understanding dissolved oxygen concentrations in a discontinuously perennial stream within a managed forest. *Forest Ecology and Management*, *479*, 118531. https://doi.org/10.1016/j.foreco.2020.118531
Iles, J. A., Pettit, N. E., Donn, M. J., & Grierson, P. F. (2022). Phosphorus sorption characteristics and interactions with leaf litter-derived dissolved organic matter leachate in iron-rich sediments of a sub-tropical ephemeral stream. *Aquatic Sciences*, *84*(4), 56. https://doi.org/10.1007/s00027-022-00888-x
Jankowski, K. J., Mejia, F. H., Blaszczak, J. R., & Holtgrieve, G. W. (2021). Aquatic ecosystem metabolism as a tool in environmental management. *WIREs. Water*, *8*(4). https://doi.org/10.1002/wat2.1521
Jensen, C. K., McGuire, K. J., & Prince, P. S. (2017). Headwater stream length dynamics across four physiographic provinces of the Appalachian Highlands. *Hydrological Processes*, *31*(19), 3350–3363. https://doi.org/10.1002/hyp.11259
Jewett, E. B., Kidwell, D. M., Lopez, C. B., Bricker, S. B., Burke, M. K., Walbridge, M. R., Eldridge, P. M., Greene, R. M., Hagy, J. D., Buxton, H. T., & Diaz, R. J. (2010). *Scientific Assessment of Hypoxia in U.S. Coastal Waters*. National Oceanic and Atmospheric Administration.
NOAA. National Weather Service National Online Weather Data (NOWData) 1991-2020. https://www.weather.gov/wrh/Climate?wfo=rnk
Northington, R. M., Webster, J. R., Benfield, E. F., Cheever, B. M., & Niederlehner, B. R. (2013). Ecosystem function in Appalachian headwater streams during an active invasion by the hemlock woolly adelgid. *PloS One*, *8*(4), e61171. https://doi.org/10.1371/journal.pone.0061171
O'Donnell, B., & Hotchkiss, E. R. (2019). Coupling concentration- and process-discharge relationships integrates water chemistry and metabolism in streams. *Water Resources Research*, *55*(12), 10179–10190. https://doi.org/10.1029/2019wr025025
Odum, H. T. (1956). Primary Production in Flowing Waters1. *Limnology and Oceanography*, *1*(2), 102–117. https://doi.org/10.4319/lo.1956.1.2.0102
Poff, N. L., Allan, J. D., Bain, M. B., Karr, J. R., Prestegaard, K. L., Richter, B. D., Sparks, R.

E., & Stromberg, J. C. (1997). The Natural Flow Regime. *Bioscience*, *47*(11), 769–784. https://doi.org/10.2307/1313099

Price, A. N., Jones, C. N., Hammond, J. C., Zimmer, M. A., & Zipper, S. C. (2021). The drying regimes of non-perennial rivers and streams. *Geophysical Research Letters*, *48*(14). https://doi.org/10.1029/2021gl093298

Prince, P. 2019. *Geologic Map of the Newport Quadrangle, Virginia*. Virginia Department of Mines, Minerals, and Energy. https://energy.virginia.gov/commercedocs/OFR_19_10.pdf

Rasilo, T., Hutchins, R. H. S., Ruiz-González, C., & del Giorgio, P. A. (2017). Transport and transformation of soil-derived CO2, CH4 and DOC sustain CO2 supersaturation in small boreal streams. *The Science of the Total Environment*, *579*, 902–912. https://doi.org/10.1016/j.scitotenv.2016.10.187

Raymond, P. A., Zappa, C. J., Butman, D., Bott, T. L., Potter, J., Mulholland, P., Laursen, A. E., McDowell, W. H., & Newbold, D. (2012). Scaling the gas transfer velocity and hydraulic geometry in streams and small rivers. *Limnology and Oceanography: Fluids and Environments*, *2*(1), 41–53. https://doi.org/10.1215/21573689-1597669

Rodríguez-Castillo, T., Estévez, E., González-Ferreras, A. M., & Barquín, J. (2019). Estimating Ecosystem Metabolism to Entire River Networks. *Ecosystems* , *22*(4), 892–911. https://doi.org/10.1007/s10021-018-0311-8

Sabater, S., Timoner, X., Borrego, C., & Acuña, V. (2016). Stream Biofilm Responses to Flow Intermittency: From Cells to Ecosystems. *Frontiers of Environmental Science & Engineering in China*, *4*. https://doi.org/10.3389/fenvs.2016.00014

Schindler, J. E., & Krabbenhoft, D. P. (1998). The hyporheic zone as a source of dissolved organic carbon and carbon gases to a temperate forested stream. *Biogeochemistry*, *43*(2), 157–174. https://doi.org/10.1023/A:1006005311257

Shanafield, M., Bourke, S. A., Zimmer, M. A., & Costigan, K. (2021). An overview of the hydrology of non-perennial rivers and streams. *WIREs Water*, *8*(e1504). https://doi.org/10.1002/wat2.1504

Vazquez, E., Amalfitano, S., Fazi, S., & Butturini, A. (2011). Dissolved organic matter composition in a fragmented Mediterranean fluvial system under severe drought conditions. *Biogeochemistry*, *102*(1), 59–72. https://doi.org/10.1007/s10533-010-9421-x

Venkiteswaran, J. J., Rosamond, M. S., & Schiff, S. L. (2014). Nonlinear response of riverine N2O fluxes to oxygen and temperature. *Environmental Science & Technology*, *48*(3), 1566–1573. https://doi.org/10.1021/es500069j

Von Schiller, D., Datry, T., Corti, R., Foulquier, A., Tockner, K., Marcé, R., García-Baquero, G., Odriozola, I., Obrador, B., Elosegi, A., Mendoza-Lera, C., Gessner, M. O., Stubbington, R., Albariño, R., Allen, D. C., Altermatt, F., Arce, M. I., Arnon, S., Banas, D., … Zoppini, A. (2019). Sediment respiration pulses in intermittent rivers and ephemeral streams. *Global Biogeochemical Cycles*, *33*(10), 1251–1263. https://doi.org/10.1029/2019gb006276

Ward, A. S., Wondzell, S. M., Schmadel, N. M., & Herzog, S. P. (2020). Climate Change Causes River Network Contraction and Disconnection in the H.J. Andrews Experimental Forest,

Oregon, USA. *Frontiers in Water*, *2*. https://doi.org/10.3389/frwa.2020.00007

Whitworth, K. L., Baldwin, D. S., & Kerr, J. L. (2012). Drought, floods and water quality: Drivers of a severe hypoxic blackwater event in a major river system (the southern Murray–Darling Basin, Australia). *Journal of Hydrology*, *450-451*, 190–198. https://doi.org/10.1016/j.jhydrol.2012.04.057

Yard, M. D., Bennett, G. E., Mietz, S. N., Coggins, L. G., Stevens, L. E., Hueftle, S., & Blinn, D. W. (2005). Influence of topographic complexity on solar insolation estimates for the Colorado River, Grand Canyon, AZ. *Ecological Modelling*, *183*(2), 157–172. https://doi.org/10.1016/j.ecolmodel.2004.07.027

Ylla, I., Sanpera-Calbet, I., Muñoz, I., Romaní, A. M., & Sabater, S. (2011). Organic matter characteristics in a Mediterranean stream through amino acid composition: changes driven by intermittency. *Aquatic Sciences*, *73*(4), 523–535. https://doi.org/10.1007/s00027-011-0211-x

Yu, S., Burrows, R. M., Shanafield, M., & Kennard, M. J. (2022). Water-level recession characteristics in isolated pools within non-perennial streams. *Advances in Water Resources*, *166*, 104267. https://doi.org/10.1016/j.advwatres.2022.104267

Zipper, S. C., Hammond, J. C., Shanafield, M., Zimmer, M., Datry, T., Nathan Jones, C., Kaiser, K. E., Godsey, S. E., Burrows, R. M., Blaszczak, J. R., Busch, M. H., Price, A. N., Boersma, K. S., Ward, A. S., Costigan, K., Allen, G. H., Krabbenhoft, C. A., Dodds, W. K., Mims, M. C., … Allen, D. C. (2021). Pervasive changes in stream intermittency across the United States. *Environmental Research Letters: ERL [Web Site]*, *16*(8), 084033. https://doi.org/10.1088/1748-9326/ac14ec

Chapter 5: Synthesis

What is the purpose of studying tiny, near-pristine streams in a world where anthropogenic disturbance necessitates "big data"-driven management solutions and global carbon accounting? The importance of headwater ecosystem functions to the entire river network has been well-established (Wohl, 2017), yet headwaters have often been excluded from policy discussions and legal protections (Nadeau & Rains, 2007). To be fair, the scale of working in or managing headwaters is bewildering. Their dominance of river network total length, outnumbering of higher order streams, ubiquity across landscapes, and role in draining massive proportions of terrestrial ecosystems contrasts with their narrowness, shallowness, and individually small flow contributions. Added to this is the complexity of headwater networks constantly changing size and connective capacity to different aspects of aquatic and terrestrial ecosystems. The goal of this body of research has been to address questions surrounding small-scale biogeochemical cycles in headwaters so that we may better understand their complexity and how they may be uniquely affected by global change.

Findings and Future Directions

In Chapter 2, I found that connectivity among different habitat patches within a stream corridor affected stream corridor-scale carbon emissions; in particular, the presence of a vernal pool enhanced CO_2 and CH_4 emissions from the corridor (Bretz et al., 2021). While the bulk of this study took place during a dry summer, when we were able to observe connections between stream and pool surface waters disappearing and reforming, streams at Coweeta Hydrologic Laboratory undergo much less expansion and contraction than streams on Brush Mountain (Jensen et al., 2017), where my research presented in Chapters 3-4 took place. Incorporating

ephemeral wetlands into studies of aquatic carbon cycling has fortunately been getting more attention in recent years (Gómez-Gener et al., 2021; Looman et al., 2021). Vernal pools, ditches, and floodplain ponds all exist in the more hydrologically dynamic watersheds of the valley and ridge topography of Brush Mountain; while it was not a focus of my work at those sites, investigating the linkages among these patches and the second-order Poverty Creek as they all transition from aquatic to semi-aquatic to dry would provide valuable insight to how arrangements and hydrologic timings affects carbon export from a larger watershed.

Stream microbial communities are sensitive to the many fluctuations that occur in non-perennial streams, like emersion and desiccation, temperature changes, and shifts in DOM composition (Arce et al., 2019; Belnap et al., 2005; Duarte et al., 2017). Opening the "microbial black box" of stream ecology is an exciting avenue for better understanding stream heterogeneity in headwaters and biogeochemical responses to disturbance in expanding and contracting networks. Prior work in this area found that organic substrate heterogeneity is higher in more geomorphically complex, hydrologically isolated networks (Lynch et al., 2019). An undergraduate researcher working with us at Virginia Tech also found differences in certain substrate metabolic potentials in stream habitats during various flow levels. Using EcoPlates (Biolog), Jack Monroe exposed stream microbes to substrate options: carbohydrates, carboxylic acids, amino acids, polymers, and amines. For all substrates except polymers, the microbial assemblage from isolated pools and dry beds had higher metabolic potentials than microbes from flowing water (Figure 1). Unfortunately, associated microbial, biogeochemical, and hydrologic data are quite rare in the literature (Zimmer et al., 2022). To better assess the aggregate impacts of headwater stream drying on downstream ecosystem function and water quality, more

collaboration and expansive studies are needed to mediate different microbial metabolic pathways with the ecosystem-scale biogeochemical cycles they govern.

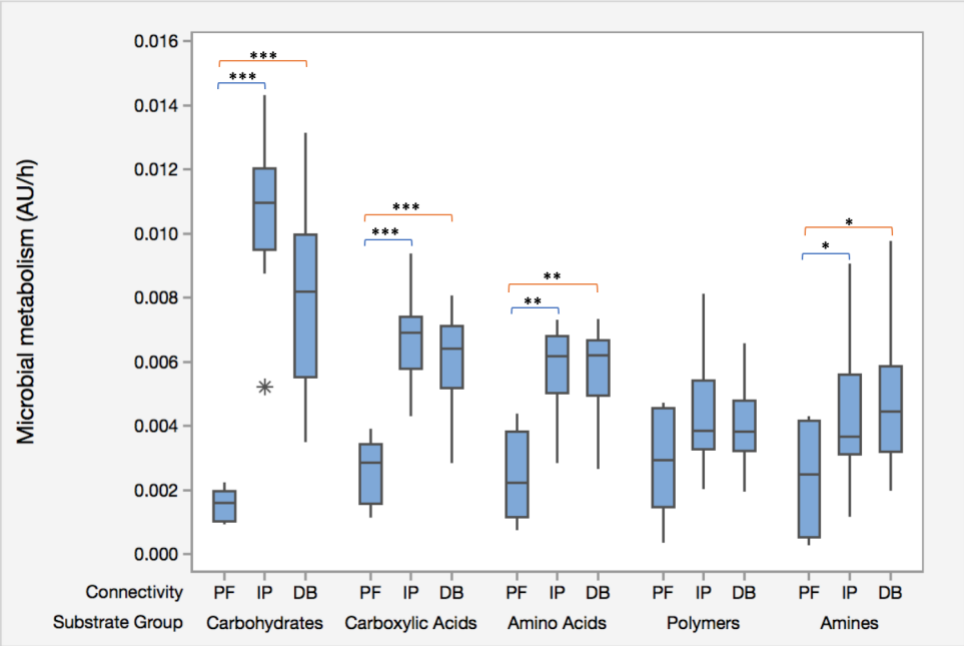

Figure 1. Microbial metabolic potential of different substrate groups from habitats in the non-perennial Beast Stream on Brush Mountain; PF = persistently flowing reach, IP = isolated pool, DB = dry bed; stars indicate significance level *** p <0.0001, ** p <0.01, * p <0.05. Source: Monroe et al., unpublished data.

Stream metabolism is increasingly being used as a tool in assessing stream health (Ferreira et al., 2020) and managing watersheds (Jankowski et al., 2021). As DO sensors decrease in cost and size, deploying them in a wider diversity of stream networks should greatly add to the utility of metabolic data. However, deriving estimates of stream metabolism using high-frequency sensor data is logistically and conceptually challenging in non-perennial systems. In theory, the geomorphic heterogeneity, low light, and groundwater influence of headwater streams would benefit from a two-station approach to modeling metabolism for a defined reach of the stream (Hall et al., 2016). In practice, the two-station approach itself has constraints that do not work well in streams with contracting surface waters. The most obvious is that streams

may fragment such that the two-stations are no longer within one continuously flowing reach. Additionally, reach length, or the spatial distance and water travel time between two DO sensors, is an important component of study design (Riley & Dodds, 2013). However, high variability in travel time between two stations in streams with dynamic flow complicates the identification of an appropriate reach length and fixed sensor deployments, and continuously flowing reaches may not be long enough to detect a change in metabolic signals. For that reason, my estimates of isolated pool metabolism in Chapter 4 used the one-station method. Models that can shift between ponded and flowing waters in the same stream would provide more comprehensive estimates of metabolism that encompass local heterogeneity and changing flow conditions. Including dynamic and hyporheic flow in metabolism models would also give context to metabolism estimates from isolated reaches (Pathak & Demars, 2023). Even with one-station modeling, metabolism estimates are very difficult in non-perennial headwaters, especially where primary production is low, because DO concentrations often do not conform to neat diel patterns with daytime highs and nighttime lows. I observed many days of flatlined or erratic DO behavior in my non-perennial study sites. I found that GPP was low but increased after pools had been briefly reconnected, while ER did not vary with flow. However I was only able to obtain metabolism estimates from 29 days out of the 209-day study period, many of them from when the pools were not fully isolated. Thus, efforts to understand GPP and ER indirectly from DO data are also worthy of future attention. For example, improving spatial coverage of comparisons of DO proxies with metabolism metrics for smaller streams (Diamond et al., 2021) as well as using analyses like DO exceedance curves (Chapter 4; Blaszczak et al., 2019) could enhance understanding of essential ecosystem processes in tandem with more frequent investigations of stream metabolism.

When facing the challenge of widespread, heterogeneous systems where small individual components have a large collective impact, it is easy to feel pulled to collect all the data all the time. With non-perennial streams, it's true that we are in some senses playing "catch-up" to the body of work already established for perennial streams. Longer term studies (Ward et al., 2020) of more diverse systems and flow states (Liu et al., 2022) will advance our understanding of how global change impacts the carbon cycle beyond episodic questions focusing only on arid environments. In Chapter 3 I contributed to this knowledge gap using high-frequency sensors in a temperate forest stream, an environment not often thought to be water-limited prior to the 2010s. By continually monitoring gas and OC concentrations at the outlet of a non-perennial headwater stream, I was able to determine that carbon biogeochemistry of intermediate flow states were indeed unique from lowest- and highest-flow environments. Despite the insight gained from these explorations, deploying high-frequency sensors to all the nooks and crevices of interesting streams remains sadly impractical. Conceptual approaches like the Net Watershed Exchange Framework (Casas-Ruiz et al., 2023), which integrates land-atmosphere and hydrologic carbon transfers, will allow for incorporating contributions from multiple habitats within a watershed when certain component habitats and fluxes are known.

Conclusions

Non-perennial and heterogenous headwater networks are significant players in transforming carbon across the landscape. This dissertation expands our understanding of biogeochemical processes at points of flow disconnection and reconnection, both within streams and among stream-adjacent habitats. Further research will provide insight into overlapping and interacting mechanisms of stream carbon cycling. As global change affects flow dynamics,

disturbance frequency, and the movement of carbon from terrestrial to aquatic ecosystems, continuing study of mechanisms and responses in headwater streams will help inform our understanding of network-wide impacts and management strategies.

References

Arce, M. I., Mendoza-Lera, C., Almagro, M., Catalán, N., Romaní, A. M., Martí, E., Gómez, R., Bernal, S., Foulquier, A., Mutz, M., Marcé, R., Zoppini, A., Gionchetta, G., Weigelhofer, G., del Campo, R., Robinson, C. T., Gilmer, A., Rulik, M., Obrador, B., … von Schiller, D. (2019). A conceptual framework for understanding the biogeochemistry of dry riverbeds through the lens of soil science. *Earth-Science Reviews*, *188*, 441–453.

Belnap, J., Welter, J. R., Grimm, N. B., Barger, N., & Ludwig, J. A. (2005). Linkages between microbial and hydrologic processes in arid and semiarid watersheds. *Ecology*, *86*(2), 298–307.

Blaszczak, J. R., Delesantro, J. M., Urban, D. L., Doyle, M. W., & Bernhardt, E. S. (2019). Scoured or suffocated: Urban stream ecosystems oscillate between hydrologic and dissolved oxygen extremes. *Limnology and Oceanography*, *64*(3), 877–894.

Bretz, K. A., Jackson, A. R., Rahman, S., Monroe, J. M., & Hotchkiss, E. R. (2021). Integrating ecosystem patch contributions to stream corridor carbon dioxide and methane fluxes. *Journal of Geophysical Research. Biogeosciences*, *126*(9). https://doi.org/10.1029/2021jg006313

Casas-Ruiz, J. P., Bodmer, P., Bona, K. A., Butman, D., Couturier, M., Emilson, E. J. S., Finlay, K., Genet, H., Hayes, D., Karlsson, J., Paré, D., Peng, C., Striegl, R., Webb, J., Wei, X., Ziegler, S. E., & Del Giorgio, P. A. (2023). Integrating terrestrial and aquatic ecosystems to constrain estimates of land-atmosphere carbon exchange. *Nature Communications*, *14*(1), 1571.

Diamond, J. S., Bernal, S., Boukra, A., Cohen, M. J., Lewis, D., Masson, M., Moatar, F., & Pinay, G. (2021). Stream network variation in dissolved oxygen: Metabolism proxies and biogeochemical controls. *Ecological Indicators*, *131*, 108233.

Duarte, S., Mora-Gómez, J., Romaní, A. M., Cássio, F., & Pascoal, C. (2017). Responses of microbial decomposers to drought in streams may depend on the environmental context. *Environmental Microbiology Reports*, *9*(6), 756–765.

Ferreira, V., Elosegi, A., D. Tiegs, S., von Schiller, D., & Young, R. (2020). Organic Matter Decomposition and Ecosystem Metabolism as Tools to Assess the Functional Integrity of Streams and Rivers–A Systematic Review. *WATER*, *12*(12), 3523.

Gómez-Gener, L., Hotchkiss, E. R., Laudon, H., & Sponseller, R. A. (2021). Integrating discharge-concentration dynamics across carbon forms in a boreal landscape. *Water*

Resources Research, *57*(8). https://doi.org/10.1029/2020wr028806
Hall, R. O., Tank, J. L., Baker, M. A., Rosi-Marshall, E. J., & Hotchkiss, E. R. (2016). Metabolism, Gas Exchange, and Carbon Spiraling in Rivers. *Ecosystems* , *19*(1), 73–86.
Jankowski, K. J., Mejia, F. H., Blaszczak, J. R., & Holtgrieve, G. W. (2021). Aquatic ecosystem metabolism as a tool in environmental management. *WIREs. Water*, *8*(4). https://doi.org/10.1002/wat2.1521
Jensen, C. K., McGuire, K. J., & Prince, P. S. (2017). Headwater stream length dynamics across four physiographic provinces of the Appalachian Highlands. *Hydrological Processes*, *31*(19), 3350–3363.
Liu, S., Kuhn, C., Amatulli, G., Aho, K., Butman, D. E., Allen, G. H., Lin, P., Pan, M., Yamazaki, D., Brinkerhoff, C., Gleason, C., Xia, X., & Raymond, P. A. (2022). The importance of hydrology in routing terrestrial carbon to the atmosphere via global streams and rivers. *Proceedings of the National Academy of Sciences of the United States of America*, *119*(11), e2106322119.
Looman, A., Maher, D. T., & Santos, I. R. (2021). Carbon dioxide hydrodynamics along a wetland-lake-stream-waterfall continuum (Blue Mountains, Australia). *The Science of the Total Environment*, *777*, 146124.
Lynch, L. M., Sutfin, N. A., Fegel, T. S., Boot, C. M., Covino, T. P., & Wallenstein, M. D. (2019). River channel connectivity shifts metabolite composition and dissolved organic matter chemistry. *Nature Communications*, *10*(1), 459.
Monroe, J.M., Bretz, K.A., and Hotchkiss, E.R. 2021. Stream Intermittency Alters Microbial Metabolism and Functional Diversity. Unpublished Data.
Nadeau, T.-L., & Rains, M. C. (2007). Hydrological connectivity between headwater streams and downstream waters: How science can inform Policy1. *Journal of the American Water Resources Association*, *43*(1), 118–133.
Pathak, D., & Demars, B. O. L. (2023). Metabolism Modeling in Rivers With Unsteady Flow Conditions and Transient Storage Zones. *Journal of Geophysical Research: Biogeosciences*, *128*(3), e2022JG007245.
Riley, A. J., & Dodds, W. K. (2013). Whole-stream metabolism: strategies for measuring and modeling diel trends of dissolved oxygen. *Freshwater Science* , *32*(1), 56–69.
Ward, A. S., Wondzell, S. M., Schmadel, N. M., & Herzog, S. P. (2020). Climate Change Causes River Network Contraction and Disconnection in the H.J. Andrews Experimental Forest, Oregon, USA. *Frontiers in Water*, *2*. https://doi.org/10.3389/frwa.2020.00007
Wohl, E. (2017). The significance of small streams. *Frontiers of Earth Science*, *11*(3), 447–456.
Zimmer, M. A., Burgin, A. J., Kaiser, K., & Hosen, J. (2022). The unknown biogeochemical impacts of drying rivers and streams. *Nature Communications*, *13*(1), 7213.

Appendix A

Supplement Chapter 2

Supporting Information for: Integrating Ecosystem Patch Contributions to Stream Corridor Carbon Dioxide and Methane Fluxes

Contents of this file

Figures S1 to S3
Tables S1 to S6

Introduction

This supporting information provides figures to visualize sites and methods, one figure with additional gas flux relationships, and statistical relationships. Figure S1 describes stream corridors at Coweeta Hydrologic Laboratory that we sampled for this study. Figure S2 shows the decline in water level from one of our study wetlands over the summer of 2019. Figure S3 is a plot of stream CO_2 flux by stream CH_4 flux. Tables S1-S7 provide extra details of statistical analyses comparing gas fluxes from different sampling sites, years, and corridors.

Table S1. Number of sampling points for each patch type in each stream corridor. Dashes (-) represent patches that were not present in a corridor, and thus, not included in sampling or upscaling estimates.

Stream corridor	Stream	Dry streambed	Hillslope	Vernal pool	Total (from all patch types)
WS55	137	4	6	-	147
TOWR	141	6	6	-	153
OLD5	44	-	-	18	70
BALL	18	-	5	41	72

Table S2. Dissolved CO_2 and CH_4 concentrations from stream and vernal pool water: numbers represent individual site means for a sampling trip

Year	Month	Corridor	Site ID or meter mark	Patch	Water temperature (°C)	Air temperature (°C)	CO_2 (mmol m^{-2} d^{-1})	CH_4 (mmol m^{-2} d^{-1})
2019	June	Ball	upstream	stream	15.1	22.2	23.5	0.012
2019	June	Ball	wetland	wetland	15.8	22.2	143.6	0.511
2019	June	Ball	downstream	stream	14.9	22.2	23.6	0.012
2019	June	Old5	61	stream	16.1	27.2	37.9	0.077

2019	June	Old5	wetland	wetland	17.2	27.2	113.7	4.300
2019	June	Old5	52	stream	16.1	27.2	26.3	0.242
2019	July	Ball	upstream	stream	16	17.7	25.5	0.011
2019	July	Ball	wetland	wetland	17.3	17.7	232.3	0.349
2019	July	Ball	downstream	stream	16	17.7	23.9	0.008
2019	July	Old5	61	stream	17.5	23.8	35.4	0.068
2019	July	Old5	wetland	wetland	19	23.8	171.7	1.577
2019	July	Old5	52	stream	17.5	23.8	61.3	0.270
2019	June	TOWR	10	stream	18.7	28.8	70.2	0.011
2019	June	TOWR	20	stream	19	28.8	17.0	0.008
2019	June	TOWR	55	stream	19	28.8	27.9	0.009
2019	June	TOWR	65	stream	19.3	28.8	20.1	0.018
2019	June	TOWR	85	stream	18.9	28.8	30.0	0.001
2019	July	TOWR	10	stream	17.7	24.4	54.4	0.018
2019	July	TOWR	20	stream	17.7	24.4	18.4	0.017
2019	July	TOWR	55	stream	18	24.4	30.3	0.007
2019	July	TOWR	65	stream	18	24.4	26.7	0.039
2019	July	TOWR	85	stream	18.4	24.4	32.4	0.007
2019	August	TOWR	10	stream	20	27.2	110.3	0.015
2019	August	TOWR	20	stream	20	27.2	18.7	0.008
2019	August	TOWR	55	stream	20	27.2	33.4	0.014
2019	August	TOWR	65	stream	20	27.2	37.6	0.041
2019	August	TOWR	85	stream	20.6	27.2	31.2	0.007
2019	June	WS55	35	stream	16.1	21.1	20.5	0.009
2019	June	WS55	57	stream	15.7	21.1	37.7	n/a
2019	June	WS55	65	stream	15.7	21.1	33.3	n/a
2019	June	WS55	68	stream	15.7	21.1	29.1	0.007
2019	June	WS55	75	stream	15.7	21.1	239.8	0.009
2019	June	WS55	110	stream	15.8	21.1	33.5	0.007
2019	July	WS55	35	stream	15.7	17.2	18.2	0.008
2019	July	WS55	57	stream	15.7	17.2	19.8	0.009

2019	July	WS55	65	stream	15.7	17.2	25.4	0.002
2019	July	WS55	68	stream	15.7	17.2	21.0	0.009
2019	July	WS55	75	stream	15.7	17.2	20.4	0.010
2019	July	WS55	110	stream	15.8	17.2	39.0	0.005
2019	August	WS55	35	stream	17.8	27.2	22.2	0.008
2019	August	WS55	57	stream	17.8	27.2	31.2	0.004
2019	August	WS55	65	stream	17.9	27.2	32.8	0.002
2019	August	WS55	68	stream	17.9	27.2	35.4	0.007
2019	August	WS55	75	stream	17.9	27.2	14.2	n/a
2019	August	WS55	110	stream	18.2	27.2	43.7	0.003
2019	August	Ball	upstream	stream	18	29.4	11.7	0.013
2019	August	Ball	downstream	stream	18	29.4	9.8	0.009
2019	August	Old5	61	stream	20.8	29.4	36.2	0.063
2019	August	Old5	52	stream	20.8	29.4	28.7	0.099
2018	August	Old5	150	stream	18	27.2	569.0	0.088
2018	August	Old5	150	stream	18	27.2	385.0	0.081
2018	August	Old5	140	stream	18	27.2	166.0	0.079
2018	August	Old5	130	stream	18	27.2	190.0	0.145
2018	August	Old5	120	stream	18	27.2	187.0	0.080
2018	August	Old5	100	stream	18	27.2	195.0	0.036
2018	August	Old5	100	stream	18	27.2	355.0	0.091
2018	August	Old5	0	stream	18	27.2	283.3	0.750
2018	August	Old5	10	stream	18	27.2	436.0	1.300
2018	August	Old5	10	stream	18	27.2		
2018	August	Old5	35	stream	18	27.2	526.5	55.900
2018	August	Old5	36	stream	18	27.2	77.2	0.754
2018	August	Old5	52	stream	18	27.2	38.0	0.252
2018	August	Old5	61	stream	18	27.2	20.4	0.309
2018	August	Old5	91	stream	18	27.2	49.4	0.258
2018	August	TOWR	90	stream	18	27.2	19.0	0.150
2018	August	TOWR	73	stream	18	27.2	40.2	0.174

2018	August	TOWR	72	stream	18	27.2	93.9	0.080
2018	August	TOWR	60	stream	18	27.2	33.3	0.212
2018	August	TOWR	59	stream	18	27.2	30.6	0.199
2018	August	TOWR	514	stream	18	27.2	55.7	0.192
2018	August	TOWR	50	stream	18	27.2	218.5	0.188
2018	August	TOWR	45	stream	18	27.2	6.1	0.051
2018	August	TOWR	43	stream	18	27.2	48.4	0.190
2018	August	TOWR	33	stream	18	27.2	56.1	0.195
2018	August	WS55	90	stream	18	27.2	16.2	0.038
2018	August	WS55	75	stream	18	27.2	2.5	0.020
2018	August	WS55	76	stream	18	27.2	30.6	0.032
2018	August	WS55	70	stream	18	27.2	13.1	0.045
2018	August	WS55	68	stream	18	27.2	10.2	0.029
2018	August	WS55	65	stream	18	27.2	8.3	0.029
2018	August	WS55	64	stream	18	27.2	9.0	0.033
2018	August	WS55	59	stream	18	27.2	142.0	0.038
2018	August	WS55	57	stream	18	27.2	9.4	0.016
2018	August	WS55	50	stream	18	27.2	6.7	0.009

Table S3. Gas exchange rates for individual stream sampling sites and collective vernal pool sites, for each corridor and month

Corridor	**Month**	**Sampling site (m)**	**$k_{600\ CO2}$ (m d^{-1})**
WS55	June	65	6.35
WS55	June	75	2.46
WS55	June	110	2.85
WS55	July	65	13.6
WS55	July	110	5.52
WS55	August	35	10.2
WS55	August	65	6.45
WS55	August	110	2.41
TOWR	June	10	2.91
TOWR	June	55	5.29
TOWR	June	85	3.15

TOWR	July	10	5.16
TOWR	July	55	3.78
TOWR	July	65	9.02
TOWR	July	85	5.31
TOWR	August	10	4.30
TOWR	August	55	4.62
TOWR	August	65	0.667
TOWR	August	85	3.34
TOWR	August	35	1.98
TOWR	August	45	1.92
TOWR	August	60	1.59
BALL	June	wetland	1.56
BALL	July	wetland	1.29
OLD5	June	wetland	4.60
OLD5	July	wetland	1.42

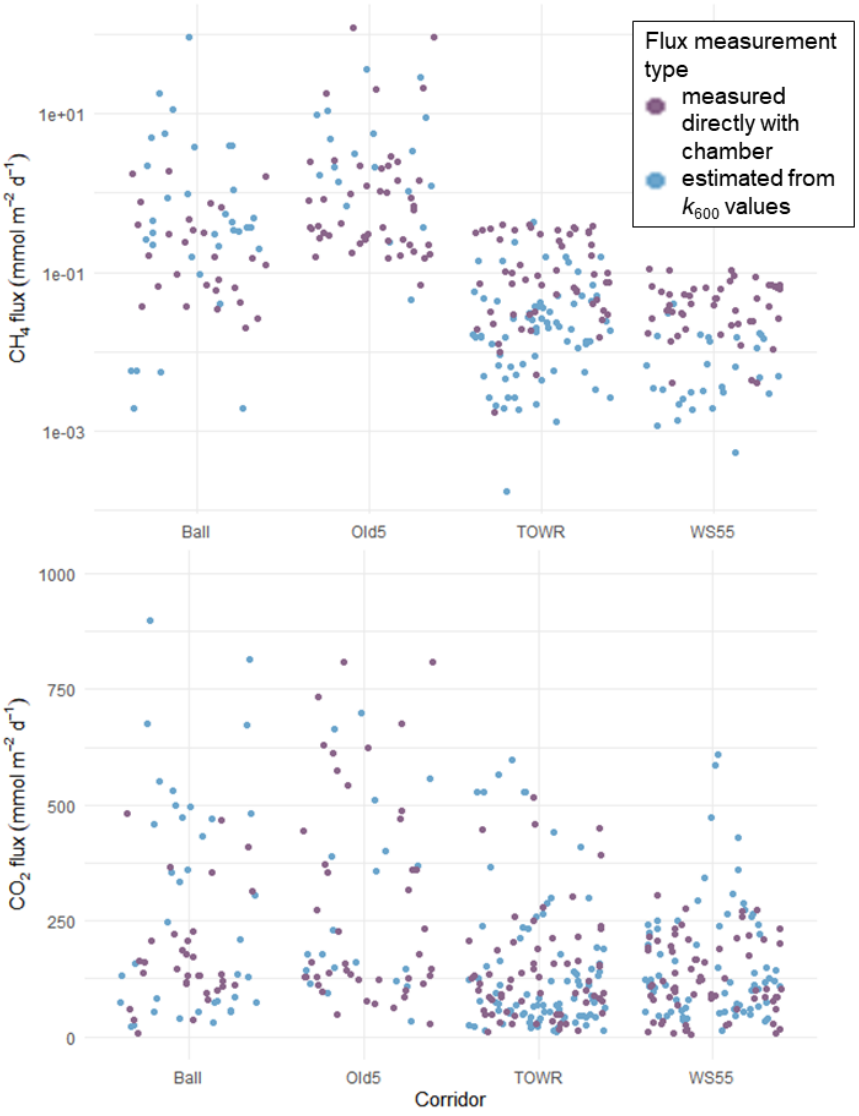

Figure S1. Comparison of measured and estimated flux values. Measured values come from chamber placements. Estimated values come from k_{600} values derived from the chambers that were then applied to dissolved gas concentrations (equation 3 in main text).

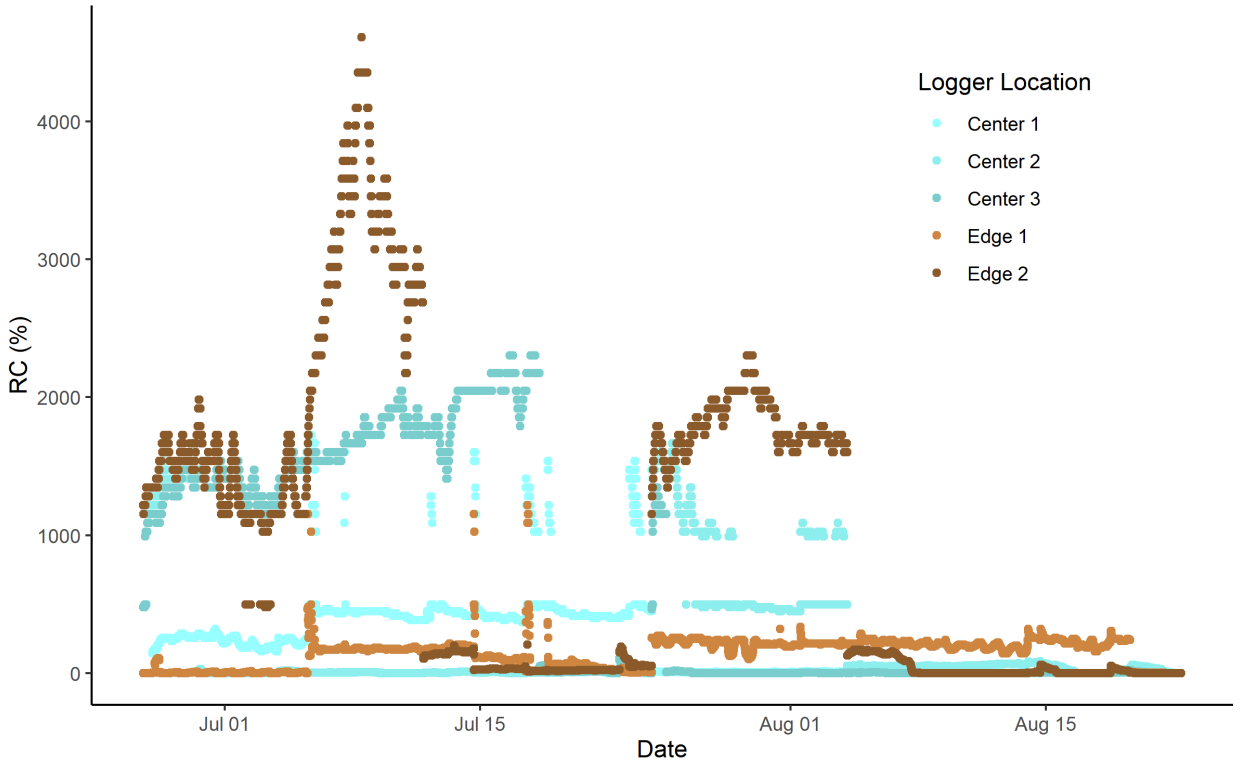

Figure S2. Relative conductivity (RC) for intermittency loggers deployed in the OLD5 vernal pool during summer 2019. Blue points reflect loggers set in the center of the wetland, and brown points are loggers that were set at opposite edges of the wetted width of the wetland in June (Figure 1b). Relative conductivity = max conductance recorded by each logger/current signal *100 as described by Chapin et al. 2014. Values below 50% RC are interpreted as lack of standing water at the sensor.

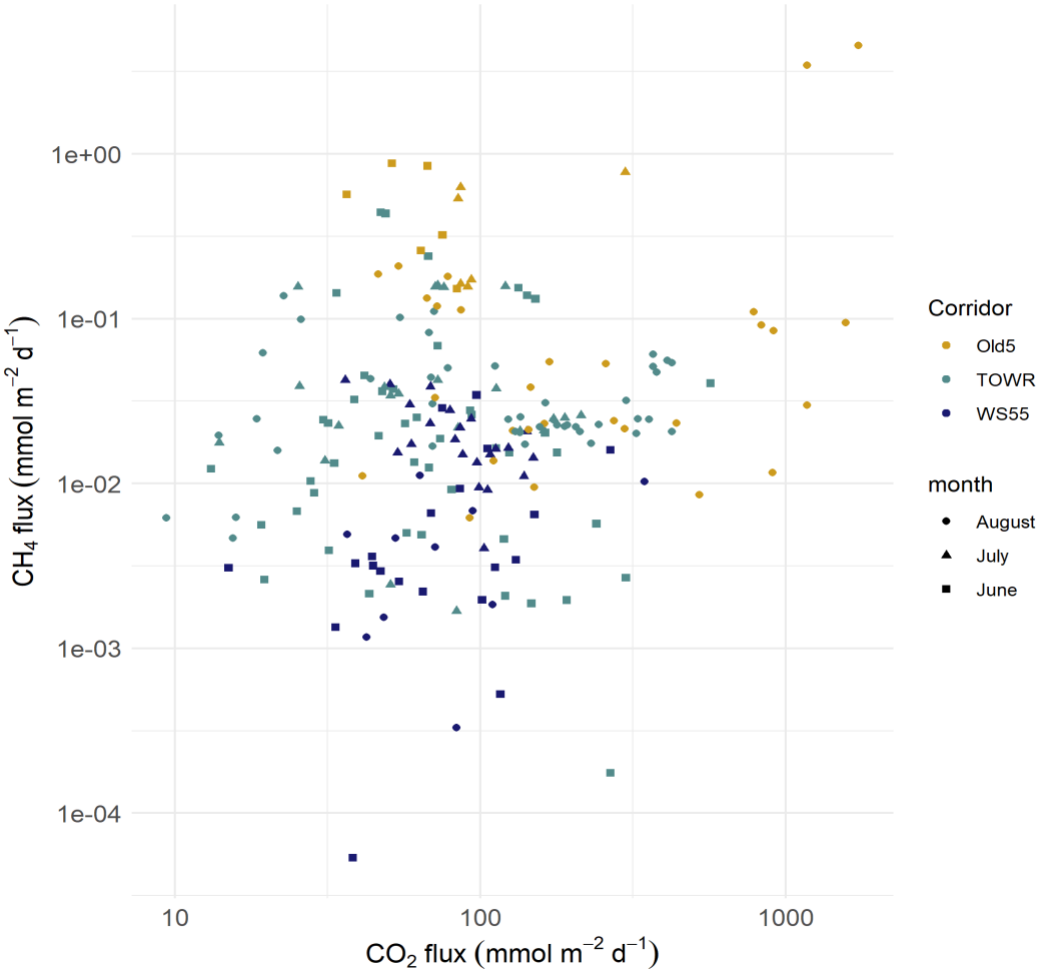

Figure S3. Comparison of CO_2 and CH_4 emissions from three first order streams in Coweeta, NC, USA. Sampling months (from 2018 and 2019) are noted with different shapes: squares (June), triangles (July), and circles (August). Shading color corresponds with the stream corridor (OLD5, TOWR, WS55). Note the log-transformed axes.

Table S4. 1-way ANOVA: Spatial variation by sampling site

CH_4

	F-value	**DF**	**Pr(>F)**
OLD5	39.58	13	0.0000
TOWR	1.847	27	0.0148
WS55	1.747	18	0.0409

CO_2

	F-value	**DF**	**Pr(>F)**
OLD5	7.895	13	0.0000
TOWR	8.17	27	0.0000
WS55	2.862	18	0.0004

*For tables S3 and S4, * denotes significant at the p>0.05 level.*

Table S3. 1-way ANOVA with Tukey HSD: Stream CH_4 and CO_2 Emissions from 4 Corridors

CH_4

F-value 14.3, Pr(>F) 0.0000

	OLD5	**TOWR**	**WS55**
BALL	0.0164*	0.9918	0.8914
OLD5		0.0000*	0.0000*
TOWR			0.7554

CO_2

F-value 12.3, Pr(>F) 0.0000

	OLD5	**TOWR**	**WS55**
BALL	0.0001*	0.9475	0.9928
OLD5		0.0000	0.0000
TOWR			0.9435

Table S4. 1-way ANOVA with Tukey HSD: Stream CH_4 and CO_2 Emissions from Patch Types

CH_4

F-value 5.227, Pr(>F) 0.0004

	Dry pool	**Hillslope**	**Stream**	**Vernal pool**
Dry bed	0.9826	1.000	1.000	0.3215
Dry pool		0.9705	0.9201	0.5804
Hillslope			1.000	0.1304
Stream				0.0001*

CO_2

F-value 11.62, Pr(>F) 0.0000

	Dry pool	**Hillslope**	**Stream**	**Vernal pool**
Dry bed	0.0463*	0.9544	0.8312	0.9862
Dry pool		0.1196	0.0000*	0.0081*
Hillslope			0.0941	0.9950
Stream				0.0029*

Table S5. 1-way ANOVA comparing corridors with vernal pools (OLD5, BALL) to those without (TOWR, WS55)

	F-value	**DF**	**Pr(>F)**
CH4 Vernal pools present	32.16	1	0.0000
CO2 Vernal pools present	20.52	1	0.0000

Table S6. 2-way ANOVA: interaction of patch type and corridor

CH4

	F-value	**DF**	**Pr(>F)**
Patch type	5.886	4	0.0001
Corridor	8.497	3	0.0000
Patch*corridor	6.550	5	0.0000

CO_2

	F-value	**DF**	**Pr(>F)**
Patch type	12.961	4	0.0000
Corridor	5.648	3	0.0008
Patch*corridor	8.127	5	0.0000

Supplement Chapter 3

Supporting Information for: Carbon Biogeochemistry and Export Governed by Flow in a Non-Perennial Stream

Contents of this file

Figures S1 to S5
Table S1 and S2

Introduction

This supporting information provides figures to help visualize analytical relationships, and provide additional visual context for discussion in the main text regarding carbon dioxide concentration relationships with emissions as well as with dissolved organic carbon. A table is also provided to compare estimated and measured gas exchange rates for CO_2 from the Beast Stream.

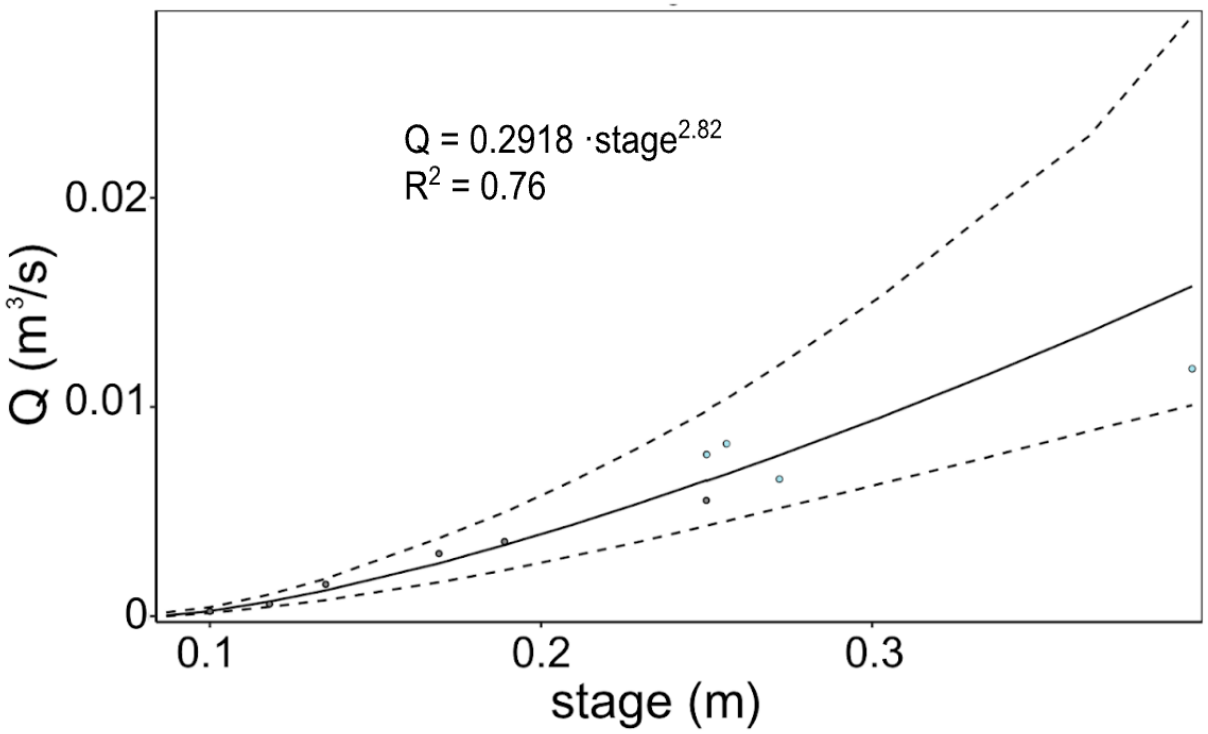

Figure S1. Rating curve showing the relationship between water stage and discharge (Q) for the Beast Stream. Grey band represents 95% confidence intervals around the linear model. Gray dots are direct measurements and blue dots are from Manning's equation.

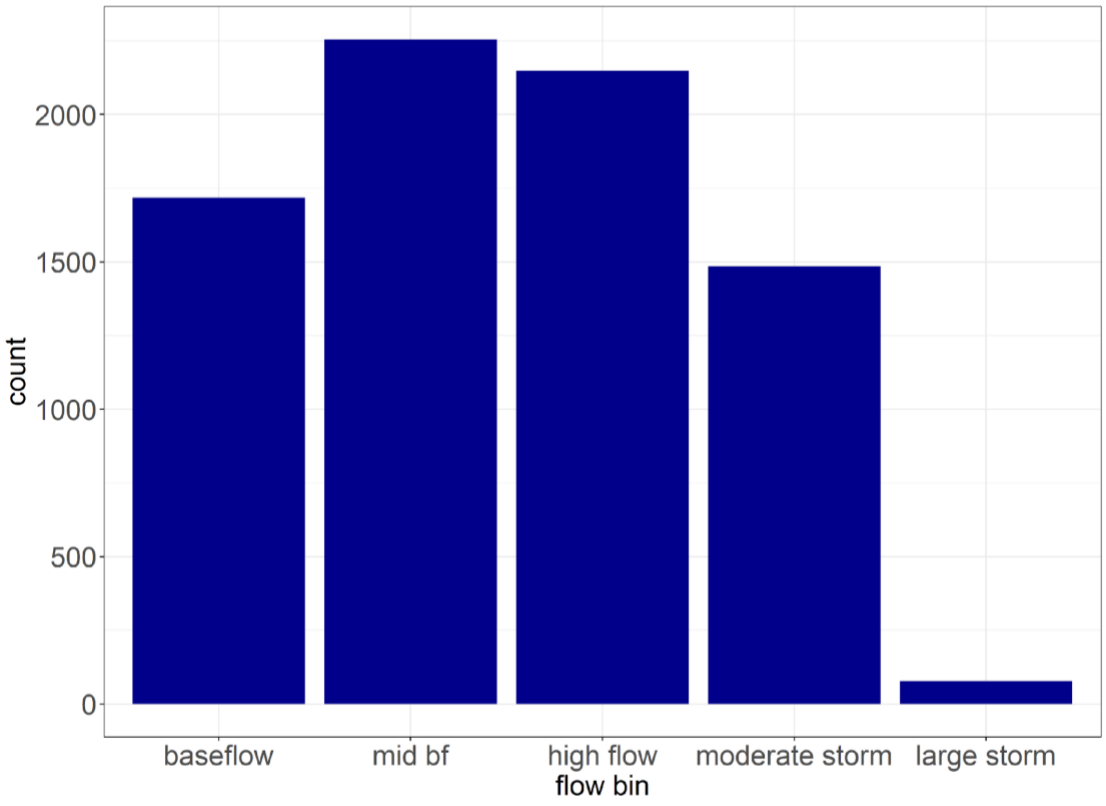

Figure S2. Distributions of discharge observations from Beast Stream during the July-December 2020 study period across the 5 flow categories: “baseflow” is low baseflow 0.073-0.23 L s-1, “mid bf” is mid-baseflow 0.23-0.37 L s-1, “high flow” is high baseflow 0.37-0.98 L s-1, moderate storm flow 0.98-7.16 L s-1, and large storms (top 1%) 7.25-31.44. L s-1.

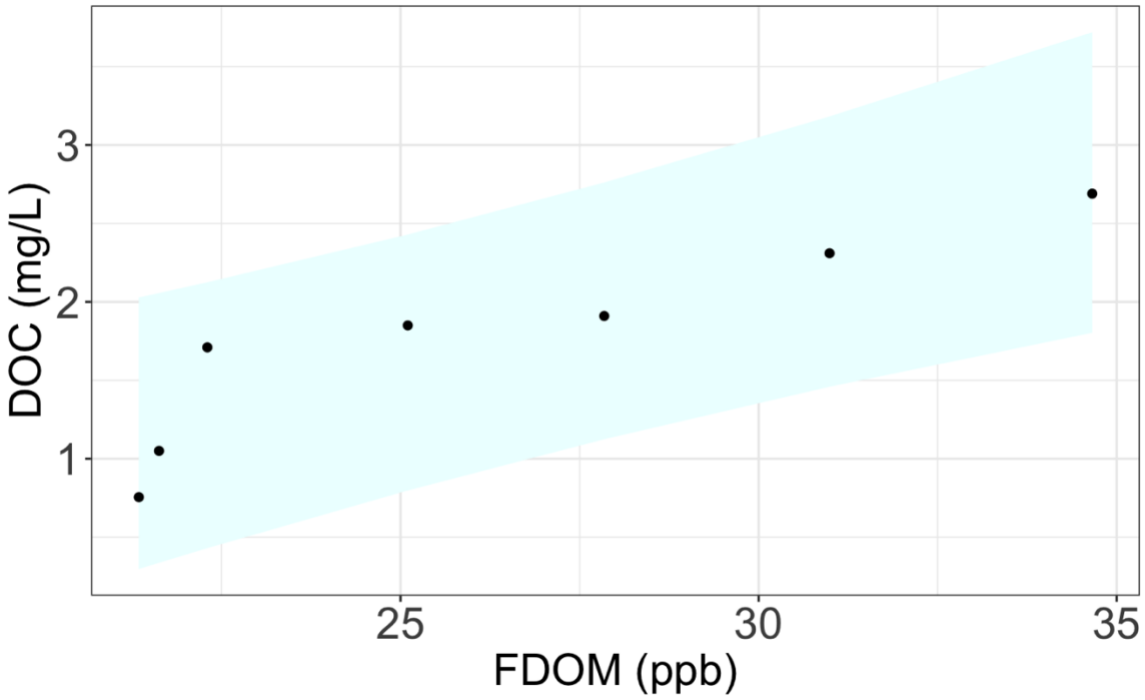

Figure S3. Relationship between grab sample dissolved organic carbon (DOC) and temperature corrected fluorescent dissolved organic matter (FDOM) sensor measurements for the Beast Stream. Blue fill represents prediction intervals (5 and 95%).

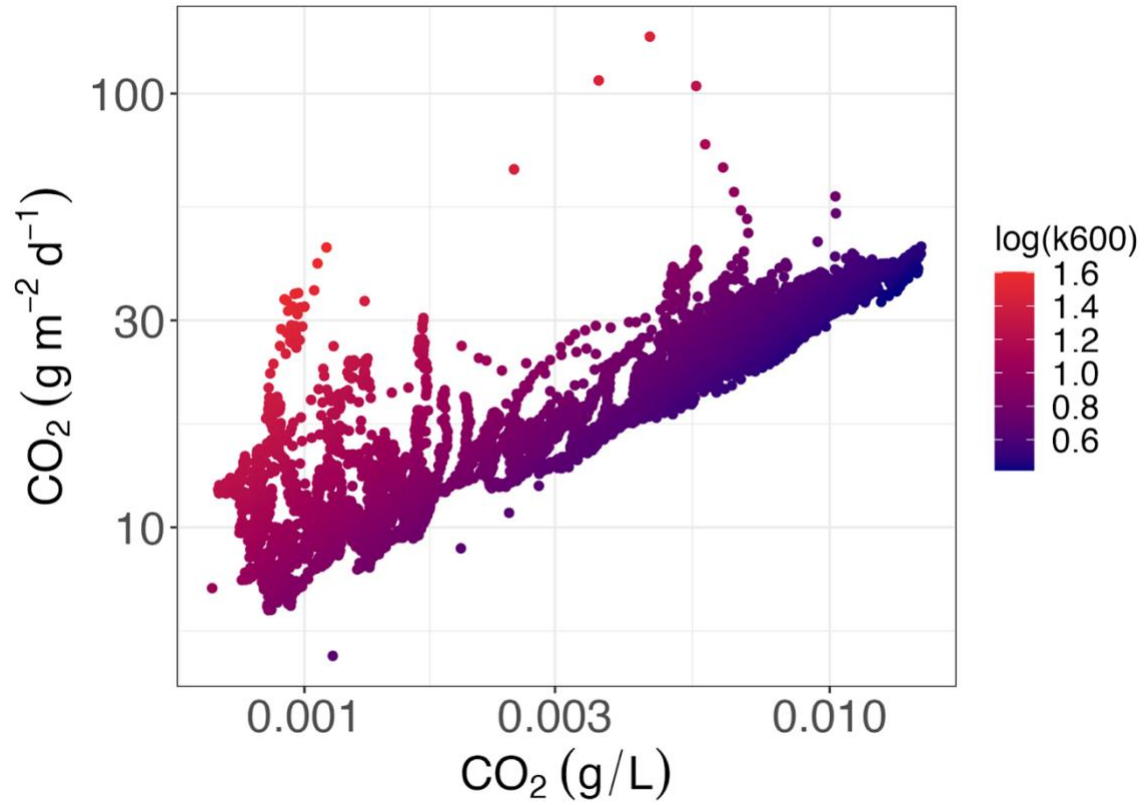

Figure S4. Carbon dioxide (CO_2) concentration versus CO_2 emission color ramped by log_{10}-transformed gas transfer velocity, k_{600} (m d^{-1}).

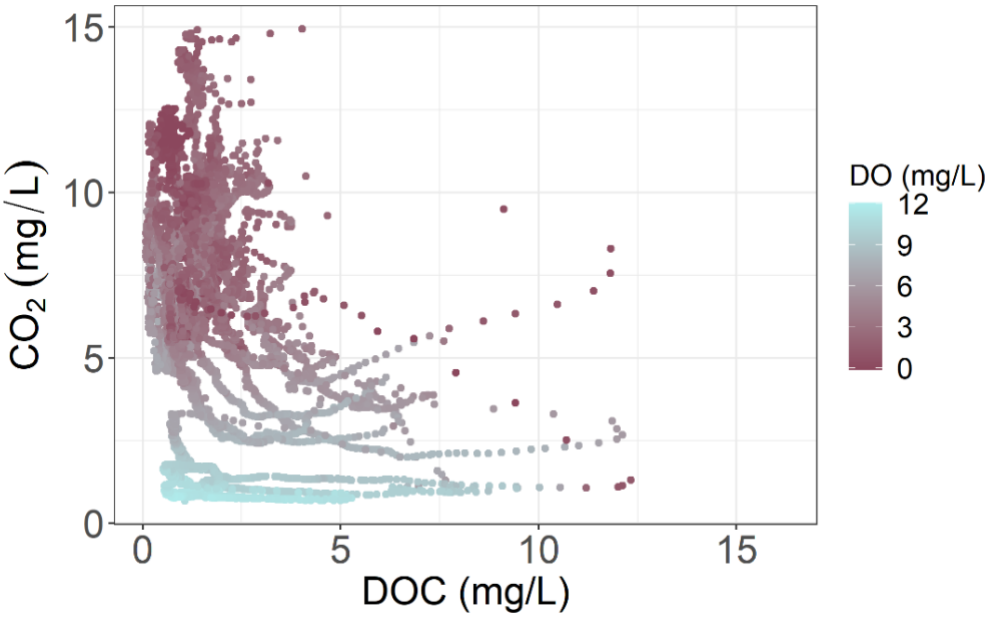

Figure S5. Dissolved organic carbon (DOC) concentration versus carbon dioxide (CO_2) concentration, colored by dissolved oxygen (DO) concentration.

Date	Location (m)	Temperature (°C)	DO (mg L^{-1})
8 July 2020	150	17.6	3.7
	250	17.3	4.0
	350	17.2	3.7
	450	18	7.1
	1000	17.5	6.8
29 July 2020	150	17.2	2.9
	500	18.4	5.7
21 August 2020	150	17.9	3.5
	250	17.5	6.2
	350	17.3	7.1
	450	17.8	7.8
	1000	17.1	5.8
2 September 2020	150	18.3	4.9
	250	17.8	6.2
	350	18.0	5.9
	450	18.4	6.9
	1000	17.5	5.2
16 September 2020	150	13.7	7.9
	250	13.3	8.1
	450	13.1	8.3
	1000	14.5	7.1
14 October 2020	150	12.7	6.9
	450	12.6	7.9

26 October 2020	150	13.0	5.0
	250	13.0	6.1
	350	12.7	6.1
	450	12.8	6.5
	1000	13.7	5.7
15 November 2020	150	7.6	9.6
	250	8.1	9.2
	350	8.2	9.3
	450	8.6	9.3
	1000	8.6	9.5
2 December 2020	150	5.9	10.1
	250	5.8	10.3
	350	6.3	10.2
	450	6.0	10.3
	1000	6.2	10.5
15 December 2020	150	6.9	10.6
	250	6.2	11.3
	350	6.2	11.4
	450	6.0	10.3
	1000	6.4	10.7

Table S1. Surface water temperature and dissolved oxygen (DO) measurements made using handheld sensors at persistent pools at or below 1000m of the Beast Stream from the July-December 2020 study period. "Location (m)" indicates meters upstream of the confluence of the Beast tributary with Poverty Creek.

Flow category	Median k_{600} from stream velocity ($m\ d^{-1}$)	Median k_{CO2} from chamber measurements in 2019 ($m\ d^{-1}$)	n
Low baseflow	2.1	1.5	4
Mid-baseflow	2.4	2.3	9
High flow	3.4	3.3	3
Moderate storms	8.9	7.2	2
Large storms	49.8	-	-

Table S2. Comparison of estimated k_{600} values based on stream velocity for the 2020 study period and k_{CO2} measured from chamber deployments in 2019. Chamber-derived measurements are matched to a flow category based on recorded discharge at the time of measurement. "-" represents no measurements from chamber deployment during/after a large storm.

Supplement Chapter 4

Supporting Information for: Metabolic Patterns of Non-perennial Stream Pools

Contents of this file
Figure S1
Tables S1-S4

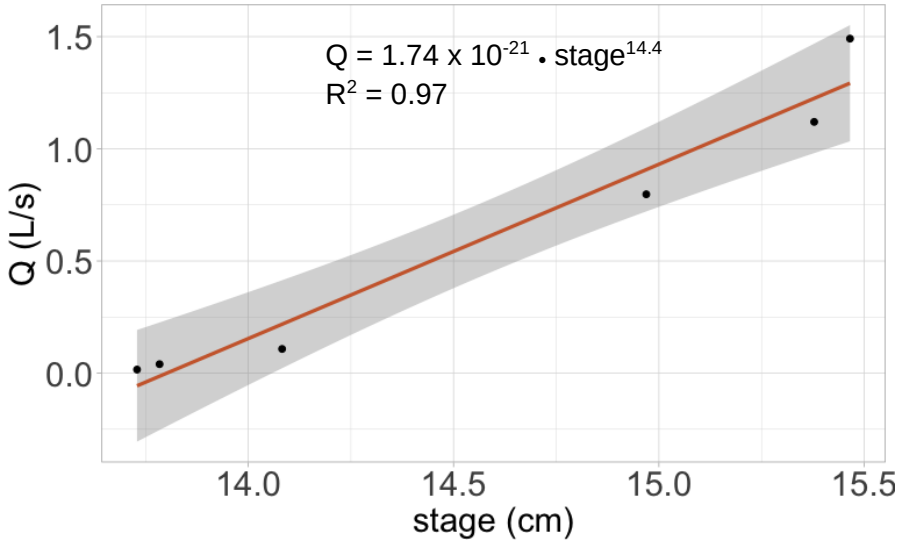

Figure S1. Rating curve showing the relationship between water stage and discharge (Q) for the MDH stream (BST curve shown in Fig S1, Supplement Chapter 3). Grey band represents 95% confidence intervals around the linear model.

Table S1. Rain gauge readings (mm) for both study streams from observations winter 2021through early spring 2022.

Date	MDH	BST
1/13/22	21	24
1/24/22	30	28
2/7/22	0.6	0.4
3/9/22	1.2	1.5
3/23/22	13.2	13

Table S2. Daily precipitation totals measured from a personal weather station near Brush Mountain in Blacksburg, VA.

date	Precipitation (mm)
6/20/21	0
6/21/21	0
6/22/21	4.343
6/23/21	0
6/24/21	0
6/25/21	0
6/26/21	0
6/27/21	1.086
6/28/21	0
6/29/21	0
6/30/21	0
7/1/21	41.572
7/2/21	7.767
7/3/21	0
7/4/21	0
7/5/21	0
7/6/21	0
7/7/21	0
7/8/21	7.298
7/9/21	0.85
7/10/21	2.008

7/11/21	5.051
7/12/21	1.157
7/13/21	3.307
7/14/21	0
7/15/21	0
7/16/21	0
7/17/21	0
7/18/21	0
7/19/21	0
7/20/21	0
7/21/21	0
7/22/21	0
7/23/21	0
7/24/21	0
7/25/21	0
7/26/21	6.212
7/27/21	0.142
7/28/21	0
7/29/21	0
7/30/21	0
7/31/21	0
8/1/21	0.307
8/2/21	0
8/3/21	0

8/4/21	0
8/5/21	0
8/6/21	0
8/7/21	0.236
8/8/21	0
8/9/21	0
8/10/21	0
8/11/21	0.685
8/12/21	0.094
8/13/21	0.401
8/14/21	0
8/15/21	0.378
8/16/21	5.527
8/17/21	7.767
8/18/21	13.06
8/19/21	1.983
8/20/21	0.378
8/21/21	0.236
8/22/21	0.449
8/23/21	0
8/24/21	0
8/25/21	0
8/26/21	0
8/27/21	0

8/28/21	0
8/29/21	4.557
8/30/21	12.899
8/31/21	15.068
9/1/21	18.3
9/2/21	0
9/3/21	0
9/4/21	0
9/5/21	0
9/6/21	1.676
9/7/21	0
9/8/21	0
9/9/21	2.62
9/10/21	0
9/11/21	0
9/12/21	0
9/13/21	0
9/14/21	0
9/15/21	0
9/16/21	0
9/17/21	0
9/18/21	0
9/19/21	6.095
9/20/21	0

9/21/21	20.467
9/22/21	41.705
9/23/21	0.142
9/24/21	0
9/25/21	0
9/26/21	0
9/27/21	0
9/28/21	0
9/29/21	0
9/30/21	0
10/1/21	0
10/2/21	0
10/3/21	4.533
10/4/21	1.324
10/5/21	0.614
10/6/21	1.086
10/7/21	2.124
10/8/21	1.794
10/9/21	0.236
10/10/21	0
10/11/21	0
10/12/21	0
10/13/21	0
10/14/21	0

10/15/21	0.213
10/16/21	1.086
10/17/21	0
10/18/21	0
10/19/21	0
10/20/21	0
10/21/21	0.472
10/22/21	1.133
10/23/21	0
10/24/21	0
10/25/21	3.588
10/26/21	0.142
10/27/21	0
10/28/21	1.18
10/29/21	12.726
10/30/21	2.644
10/31/21	0
11/1/21	0
11/2/21	1.44
11/3/21	0
11/4/21	0
11/5/21	0
11/6/21	0
11/7/21	0

11/8/21	0
11/9/21	0
11/10/21	0
11/11/21	0
11/12/21	9.423
11/13/21	0
11/14/21	0
11/15/21	0
11/16/21	0
11/17/21	0
11/18/21	0.472
11/19/21	0
11/20/21	0
11/21/21	0
11/22/21	0
11/23/21	0
11/24/21	0
11/25/21	0
11/26/21	0.094
11/27/21	0
11/28/21	0
11/29/21	0
11/30/21	0
12/1/21	0.378

12/2/21	0
12/3/21	0
12/4/21	0
12/5/21	0
12/6/21	0.142
12/7/21	0
12/8/21	0
12/9/21	0
12/10/21	5.999
12/11/21	2.669
12/12/21	0.142
12/13/21	0
12/14/21	0
12/15/21	0
12/16/21	0
12/17/21	0
12/18/21	1.18
12/19/21	0.708
12/20/21	0
12/21/21	0
12/22/21	0
12/23/21	0
12/24/21	0
12/25/21	0

12/26/21	0
12/27/21	0
12/28/21	0.307
12/29/21	1.582
12/30/21	1.605
12/31/21	0.802
1/1/22	6.496
1/2/22	10.245
1/3/22	7.458
1/4/22	1.7
1/5/22	0.236
1/6/22	0
1/7/22	0.33
1/8/22	0.236
1/9/22	3.612
1/10/22	0
1/11/22	0
1/12/22	0
1/13/22	0.378
1/14/22	0.094
1/15/22	0

Table S3. Model information for metabolism estimates. Plot table number for referencing plot table (Table S4) to GPP and ER.

plot table number	day	stream	pool	GPP	ER	neglog	K
1	8/8/21	BST	BST-mid	0.183	-1.44	-116	24
2	8/9/21	BST	BST-mid	0.208	-1.21	-92	19
3	9/27/21	BST	BST-mid	0.04	-4.59	-231	11.5
4	9/28/21	BST	BST-mid	0.146	-5.04	-155	11
5	9/29/21	BST	BST-mid	0.02	-4.45	-216	9.5
6	9/27/21	BST	BST-up	0.0356	-5.53	-194	11
7	9/28/21	BST	BST-up	0.049	-6.01	-214	11
8	9/29/21	BST	BST-up	0.0405	-11	-235	11
9	9/29/21	MDH	MDH-mid	0.147	-2.48	-203	2.5
10	9/24/21	MDH	MDH-up	0.159	-3.62	-193	24
11	9/25/21	MDH	MDH-up	0.214	-4	-180	20
12	9/26/21	MDH	MDH-up	0.156	-5.23	-237	20
13	10/4/21	BST	BST-mid	0.0354	-4.19	-153	9
14	10/12/21	BST	BST-up	0.2	-10.6	-144	10
15	10/17/21	BST	BST-up	0.498	-19.6	-115	11
16	10/1/21	MDH	MDH-down	90	-4.75	-145	9.5
17	10/2/21	MDH	MDH-down	0.41	-8.19	-173	15.5
18	11/20/21	BST	BST-down	0.16	-4.35	-280	9
19	11/21/21	BST	BST-down	0.18	-4.77	-192	9
20	11/23/21	BST	BST-down	0.04	-2.35	-186	5.5
21	11/24/21	BST	BST-down	0.155	-3.1	-294	7
22	11/20/21	BST	BST-mid	0.09	-5.41	-209	12
23	11/21/21	BST	BST-mid	0.161	-5.55	-247	12
24	11/23/21	BST	BST-mid	0.093	-4.9	-244	12
25	11/24/21	BST	BST-mid	0.05	-4.87	-195	12
26	11/20/21	BST	BST-up	0.08	-12.3	-185	19
27	11/21/21	BST	BST-up	0.2	-6.3	-167	9
28	11/23/21	MDH	MDH-up	0.274	-7.26	-154	9
29	12/24/21	BST	BST-down	0.775	-9.5	-141	9
30	12/31/21	BST	BST-down	0.441	-11.6	-124	10
31	12/23/21	BST	BST-mid	0.012	-5.9	-212	13
32	12/24/21	BST	BST-mid	0.025	-10.1	-269	15
33	12/27/21	BST	BST-mid	0.09	-14.5	-190	17
34	12/16/21	BST	BST-up	0.342	-5.9	-225	15

35	12/18/21	BST	BST-up	0.154	-5.3	-139	19
36	12/24/21	BST	BST-up	0.3	-1.9	-158	18
37	12/5/21	MDH	MDH-down	0.0252	-1.55	-255	12
38	12/8/21	MDH	MDH-down	0.0139	-1.52	-208	12
39	12/9/21	MDH	MDH-down	0.081	-1.41	-152	12
40	1/10/22	BST	BST-down	0.243	-8.67	-228	19
41	1/11/22	BST	BST-down	0.04	-3.61	-305	19
42	1/12/22	BST	BST-down	0.041	-4.32	-204	20
43	1/10/22	BST	BST-mid	0.052	-7.79	-303	19
44	1/11/22	BST	BST-mid	0.105	-7.68	-363	19
45	1/12/22	BST	BST-mid	0.089	-8.51	-248	20
46	1/10/22	BST	BST-up	0.089	-8.41	-255	20
47	1/11/22	BST	BST-up	0.075	-8.52	-283	20
48	1/12/22	BST	BST-up	0.034	-9.65	-170	20
49	1/10/22	MDH	MDH-mid	0.126	-5.91	-526	21
50	1/11/22	MDH	MDH-mid	0.054	-6.04	-314	21
51	1/10/22	MDH	MDH-mid	0.029	-4.89	-349	21
52	1/11/22	MDH	MDH-mid	0.032	-4.66	-180	21

Table S4. Plot outputs for daily metabolism estimates. Open circles represent actual DO measurements, while solid line represents modeled metabolism.

Table S3 number	Date	Pool	plot
1	8/8/21	BP-mid	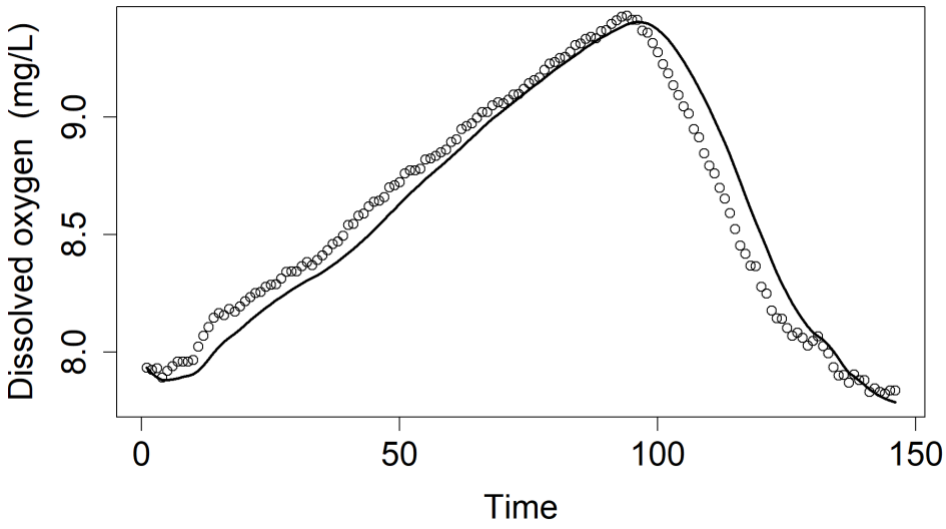

2	8/9/21	BST-mid	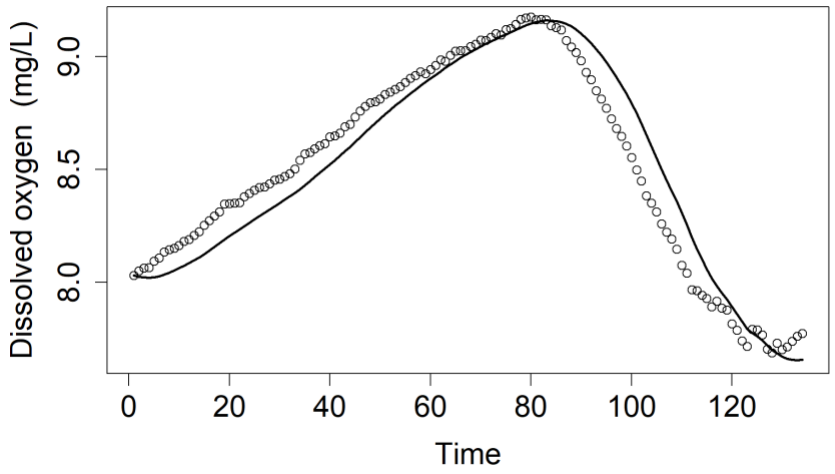
3	9/27/21	BST-mid	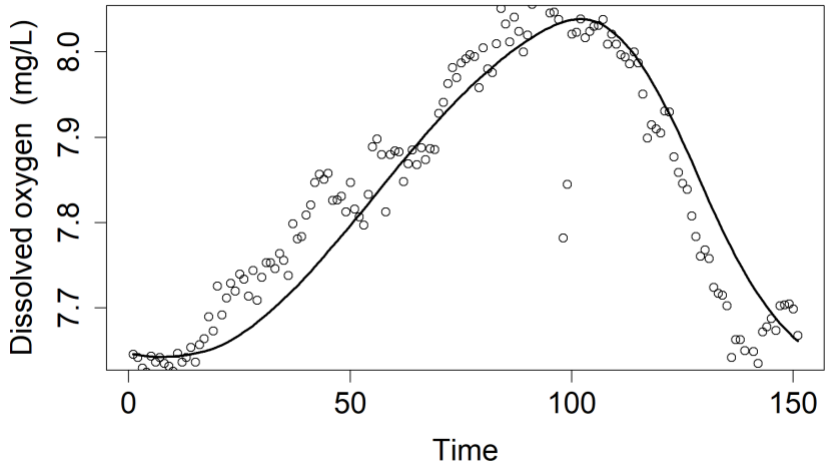

4	9/28/21	BST-mid	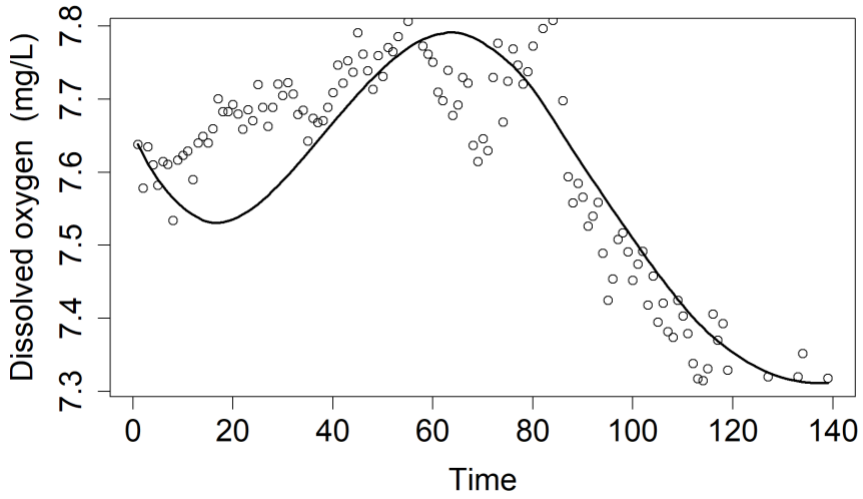
5	9/29/21	BST-mid	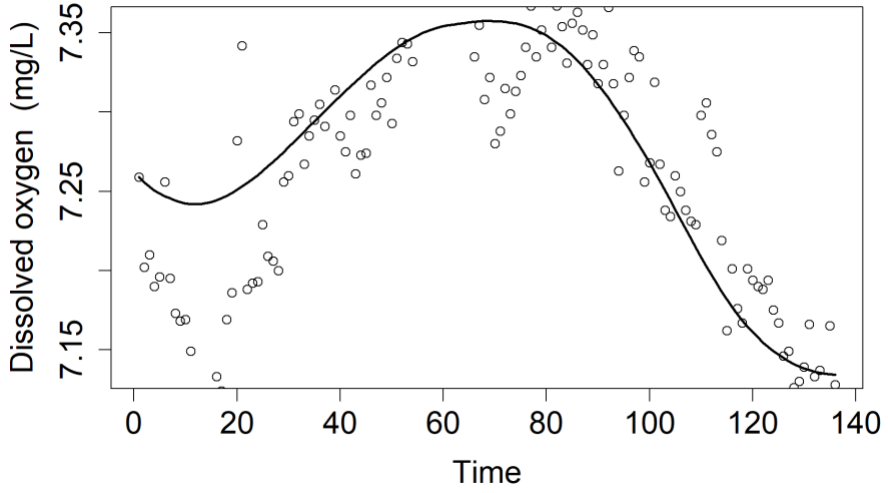

6	9/27/21	BST-mid	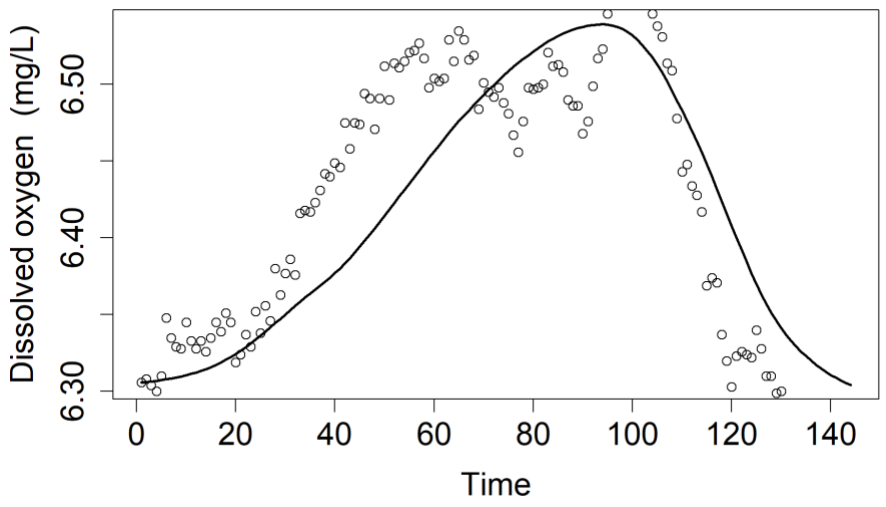
7	9/28/21	BST-up	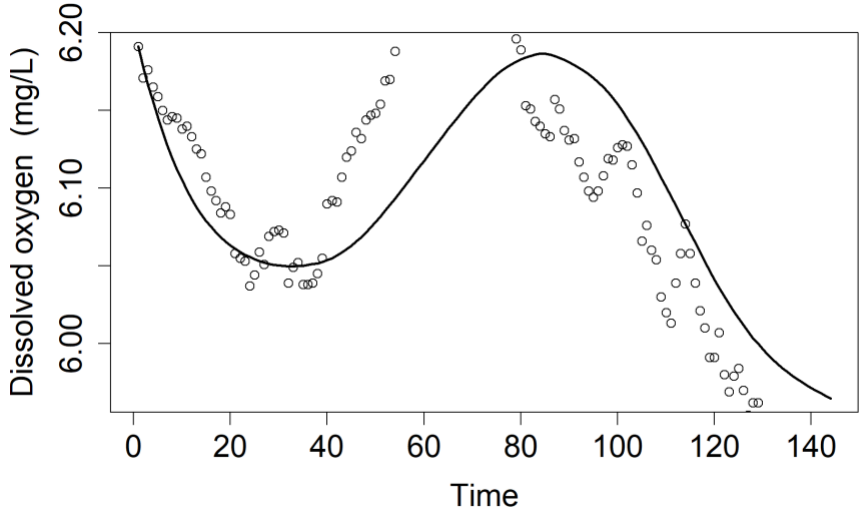

8	9/29/21	BST-up	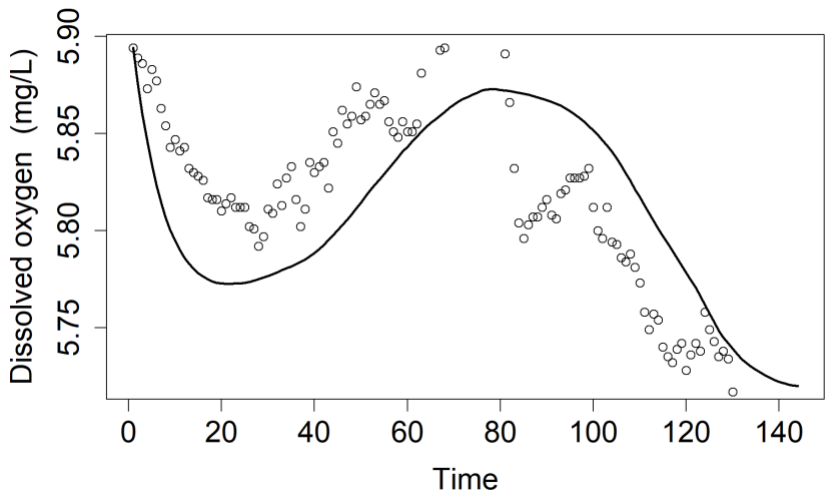
9	9/29/21	MDH-mid	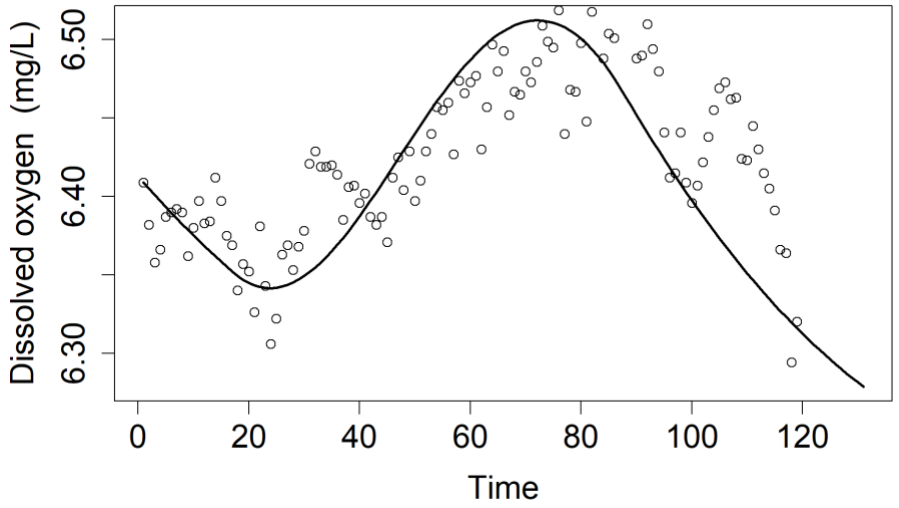

10	9/24/21	MDH-up	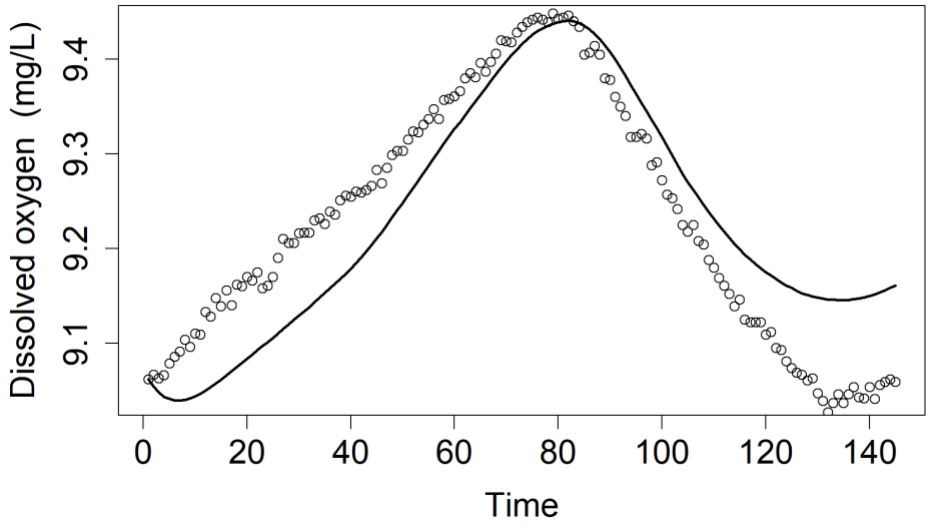
11	9/25/21	MDH-up	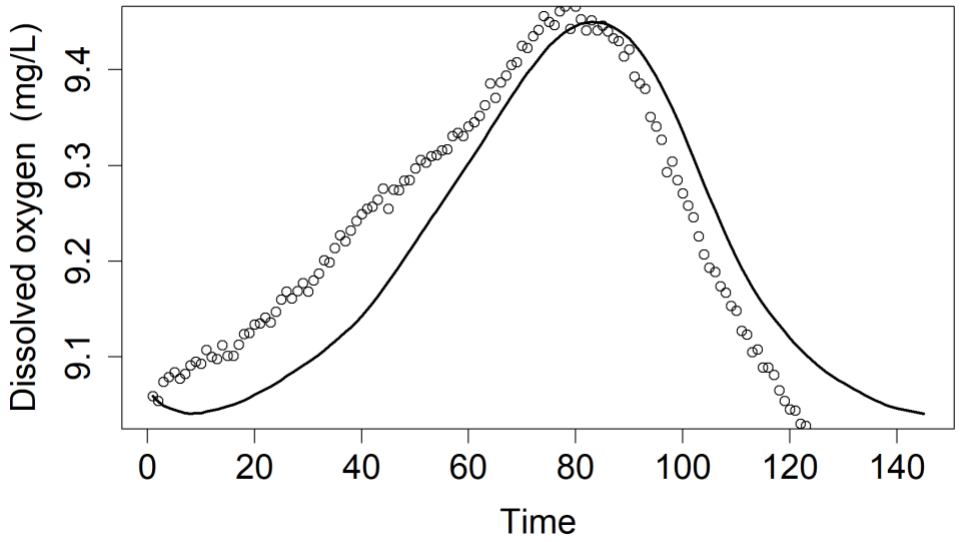

12	9/26/21	MDH-up	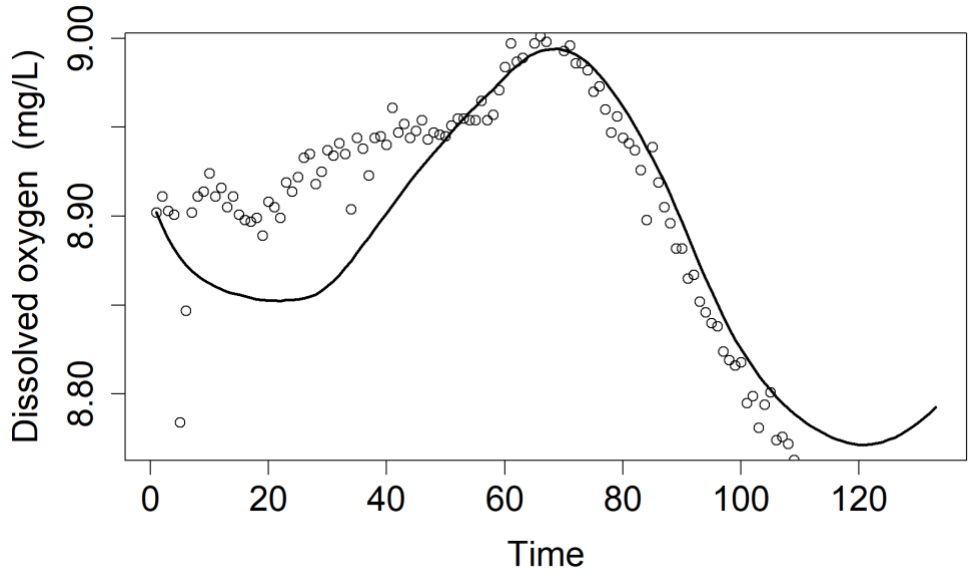
13	10/4/21	BST-mid	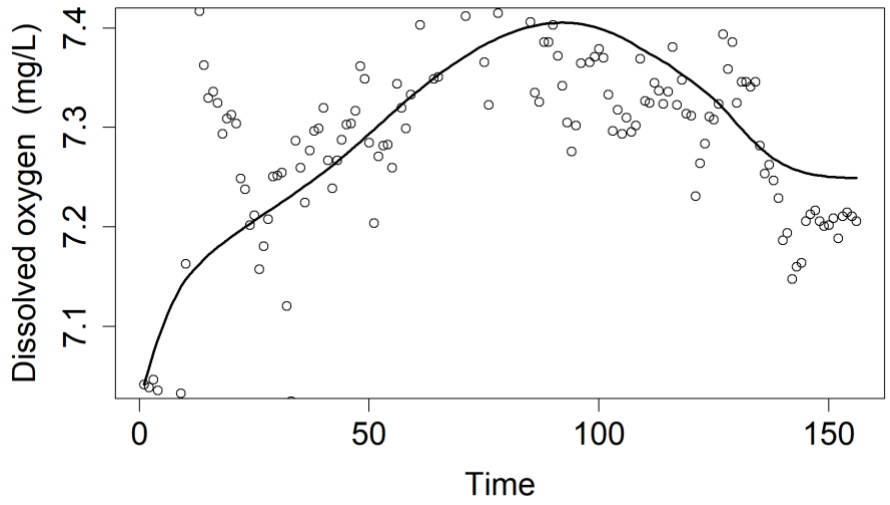

14	10/12/21	BST-up	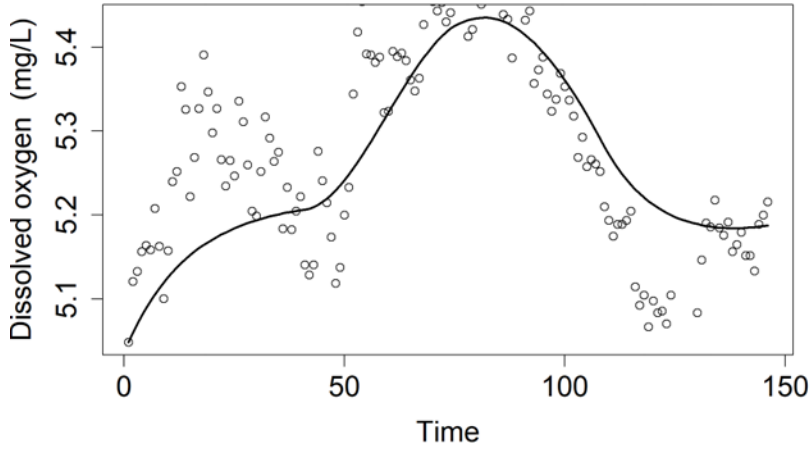
15	10/17/21	BST-up	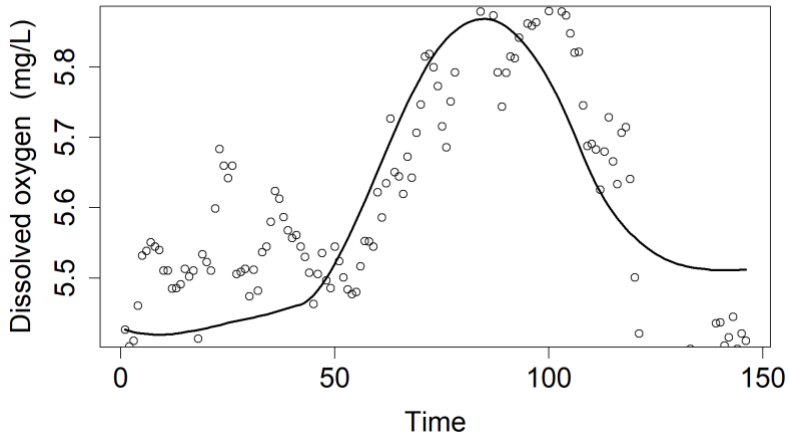

16	10/1/21	MDH-down	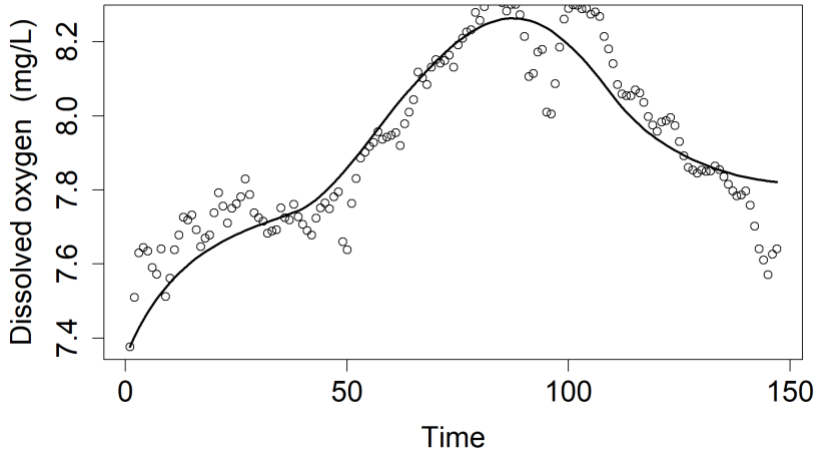
17	10/2/21	MDH-down	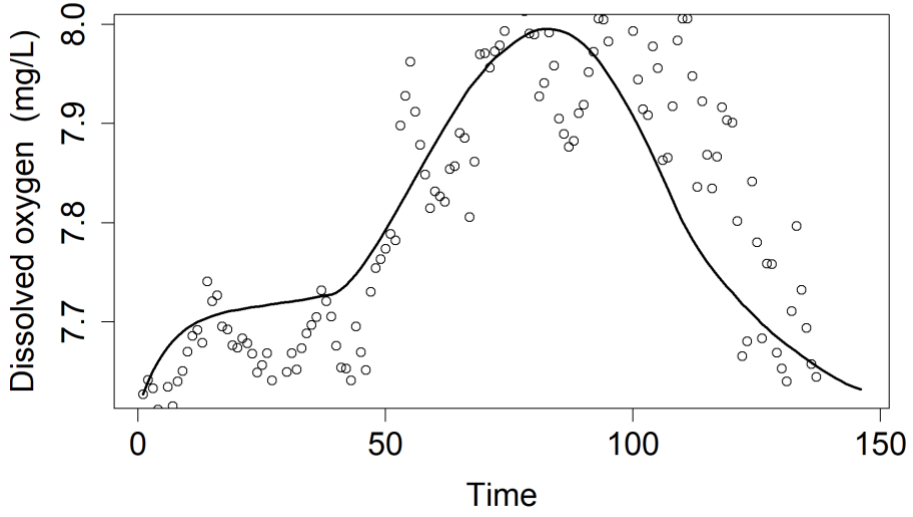

18	11/20/21	BST - down	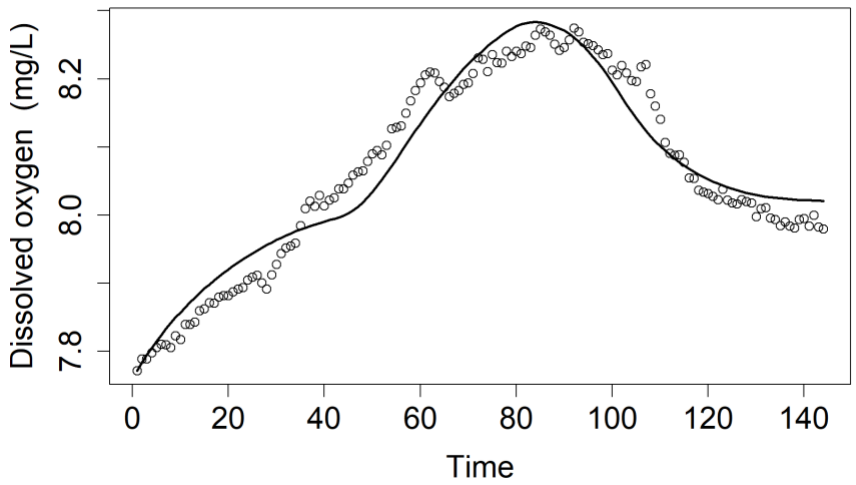
19	11/21/21	BST - down	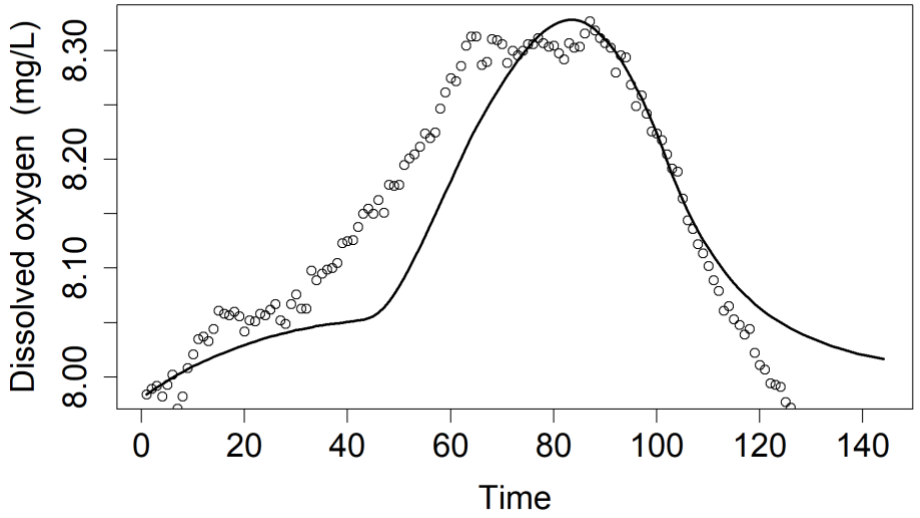

20	11/23/21	BST - down	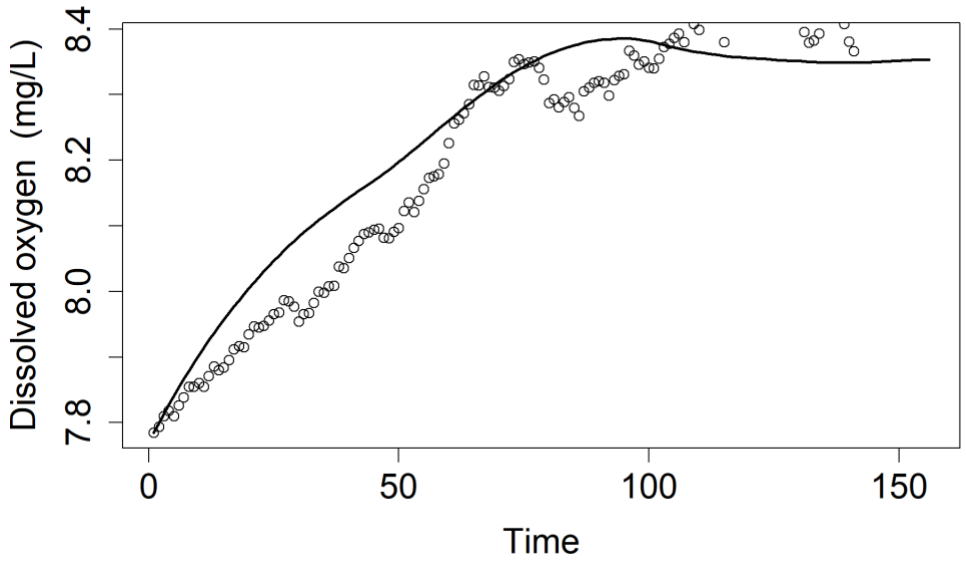
21	11/24/21	BST - down	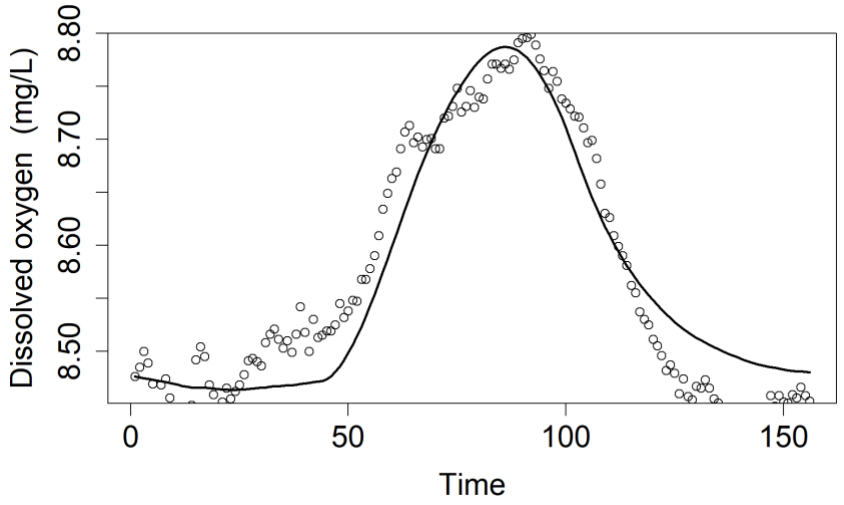

22	11/20/21	BST-mid	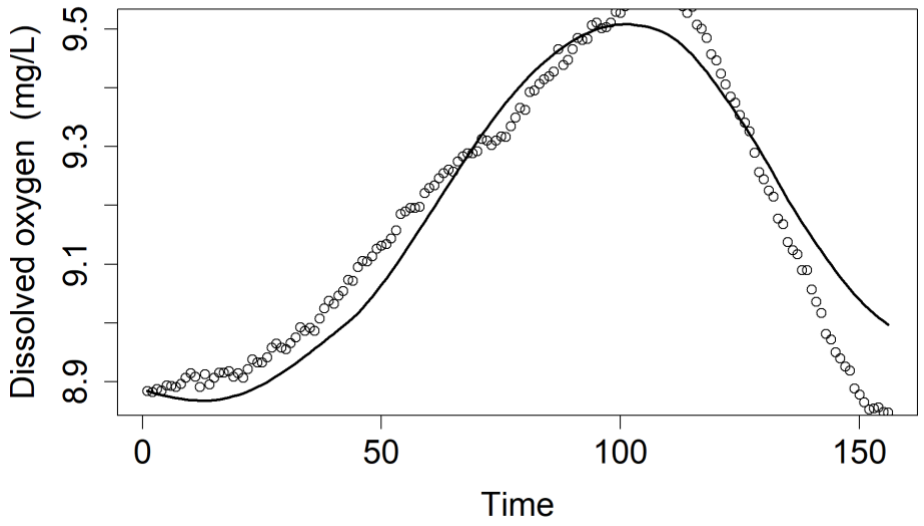
23	11/21/21	BST-mid	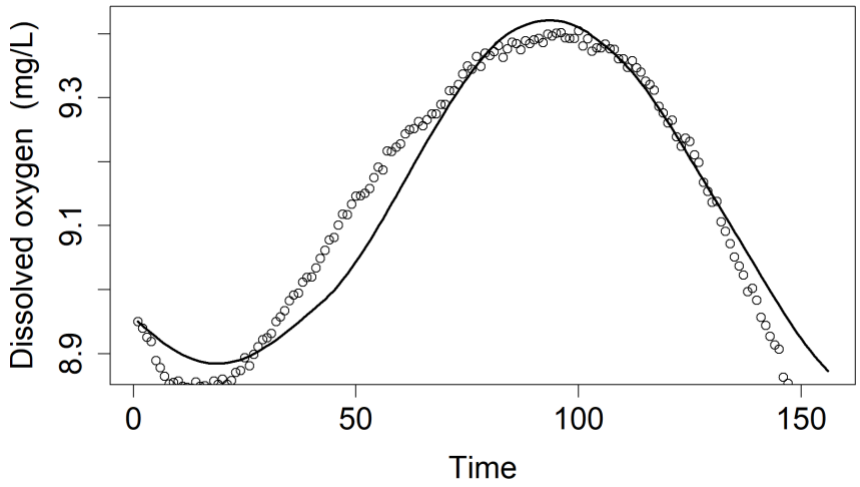

24	11/23/21	BST-mid	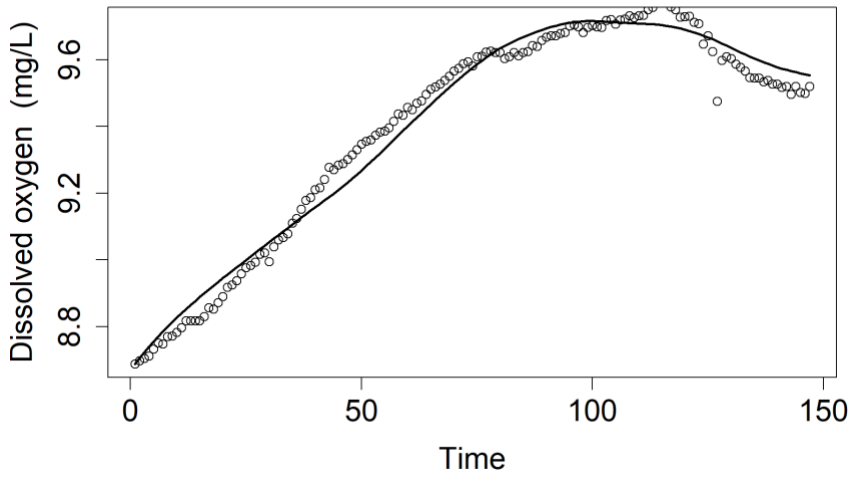
25	11/24/21	BST-mid	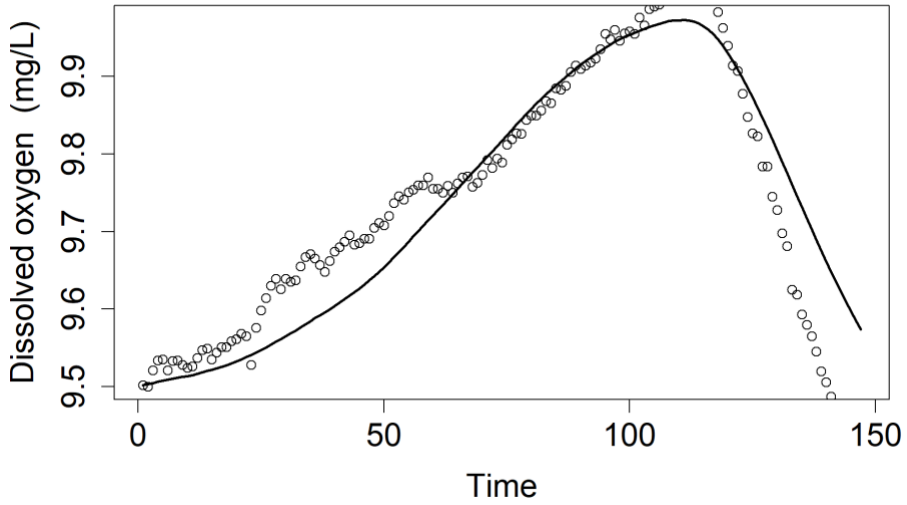

26	11/20/21	BST-up	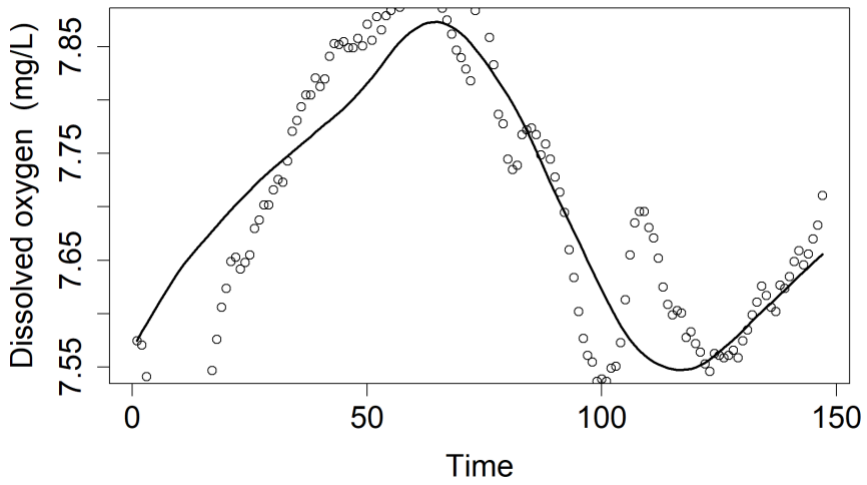
27	11/21/21	BST-up	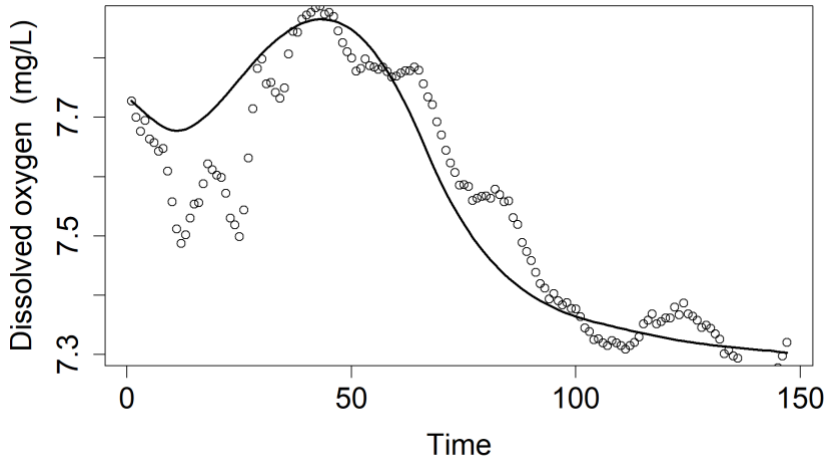

28	11/23/21	MDH-up	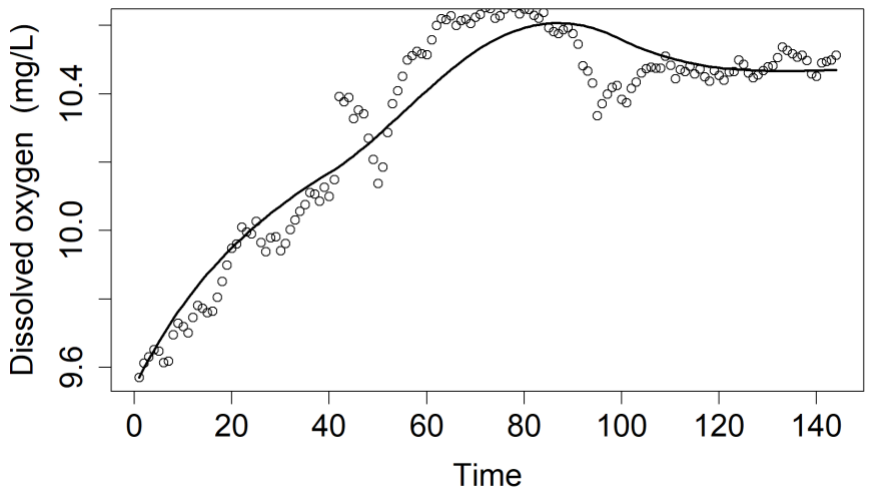
29	12/24/21	BST-down	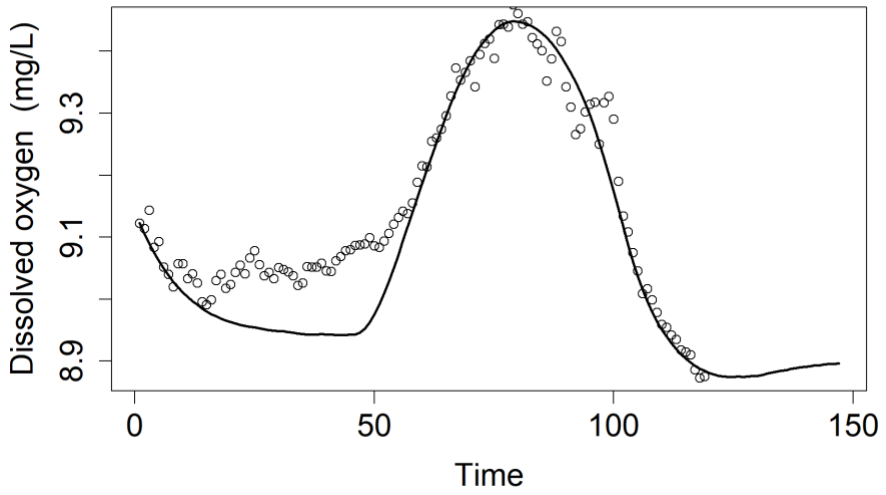

30	12/31/21	BST-down	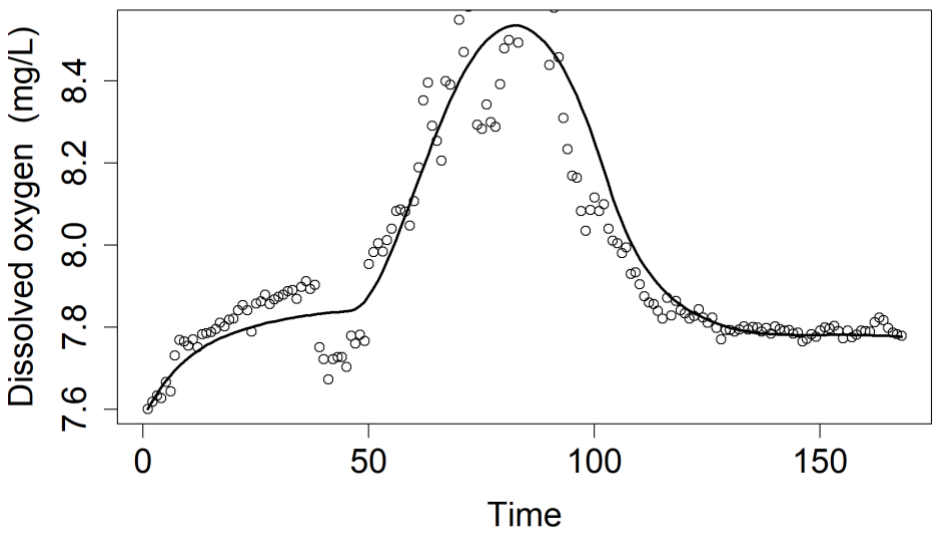
31	12/23/21	BST-mid	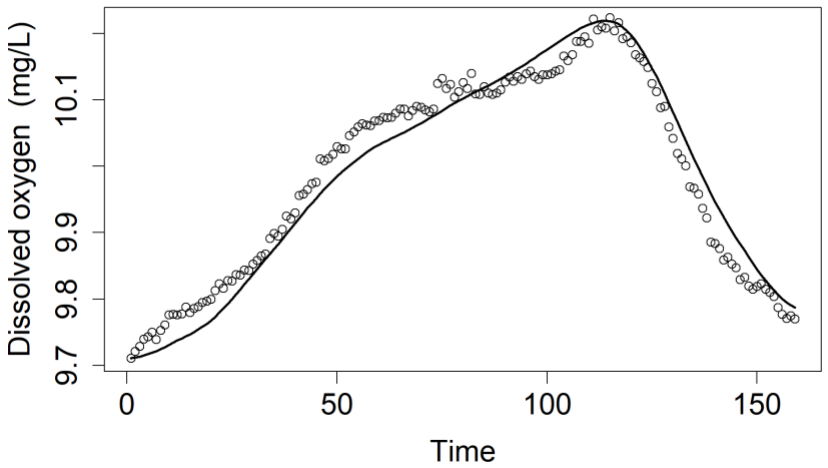

32	12/24/21	BST-mid	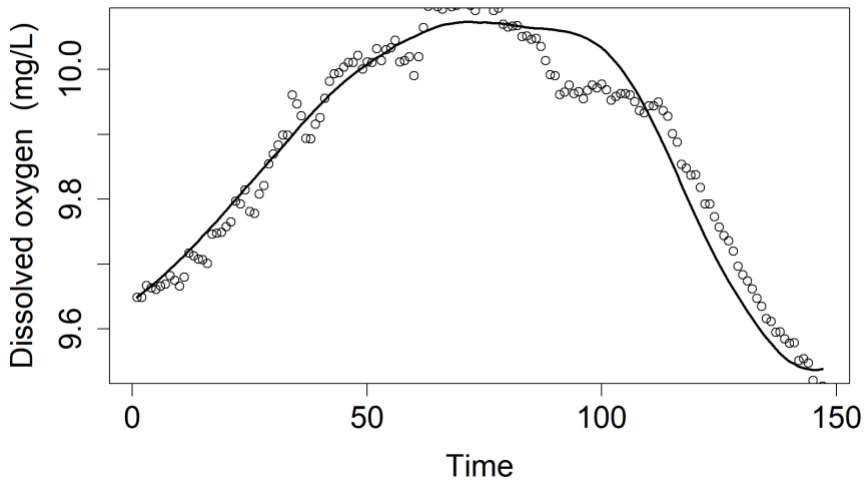
33	12/27/21	BST-mid	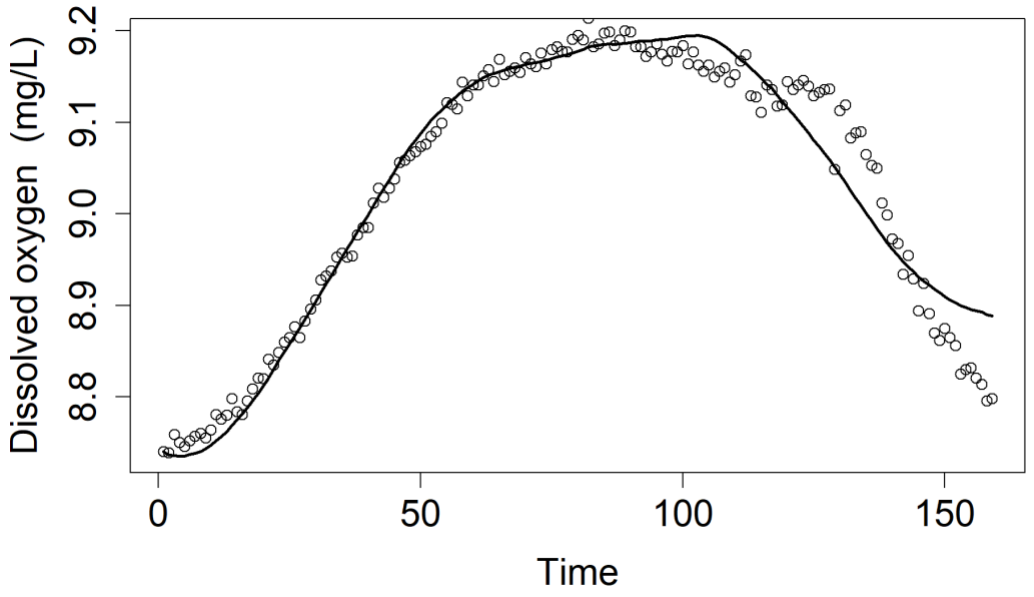

34	12/16/21	BST-up	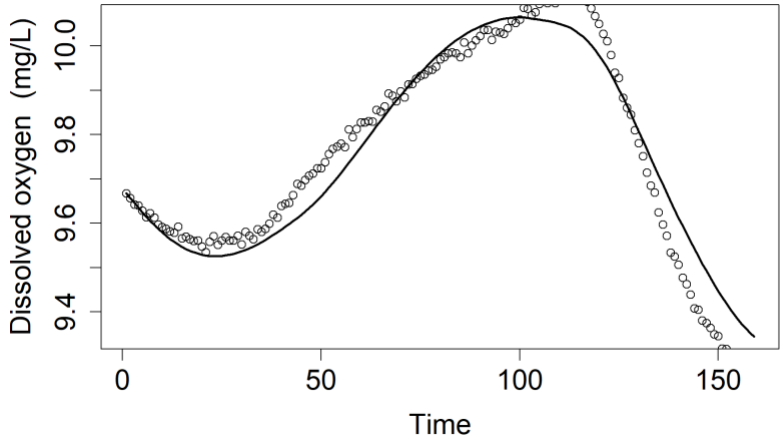
35	12/18/21	BST-up	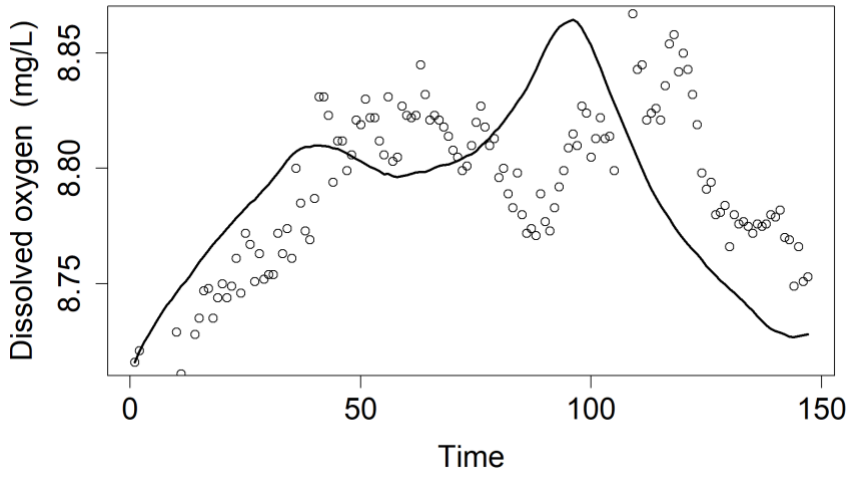

36	12/24/21	BST-up	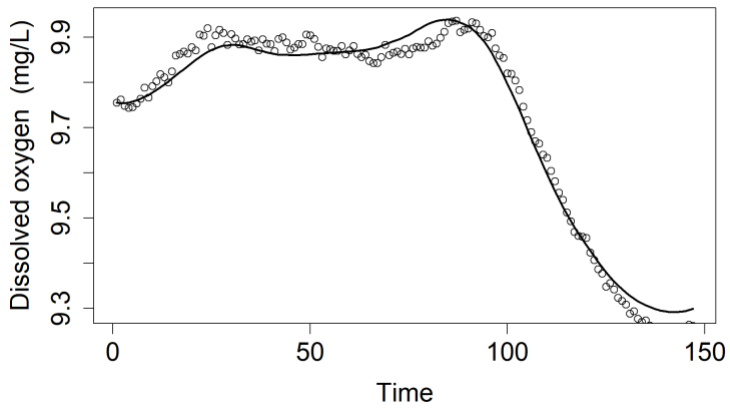
37	12/5/21	MDH-down	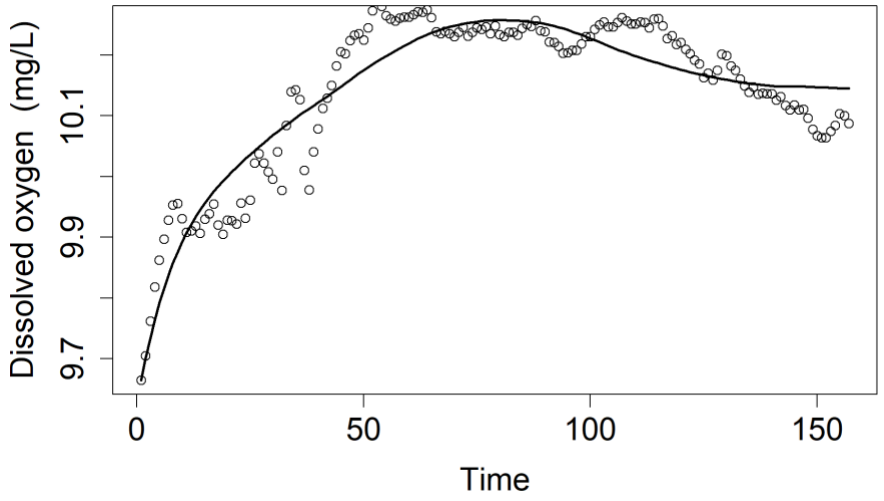

38	12/8/21	MDH-down	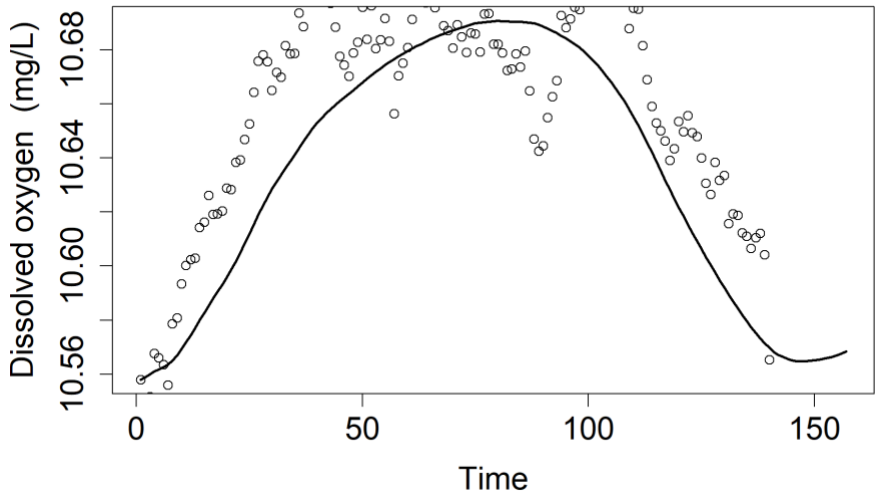
39	12/9/21	MDH-down	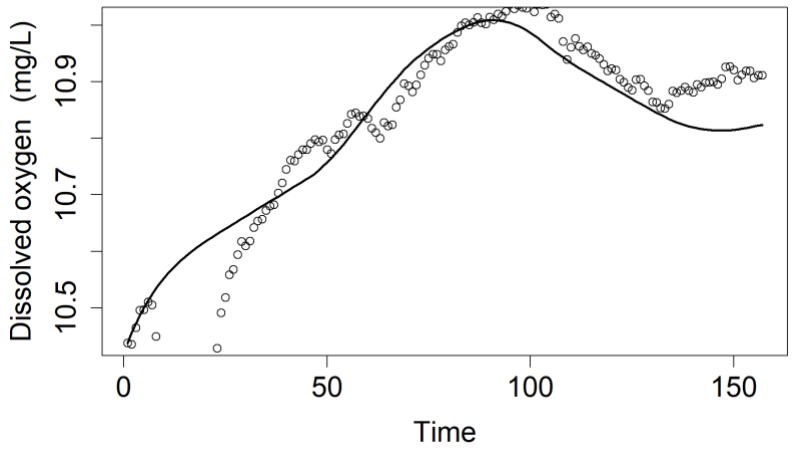

40	1/10/22	BST-down	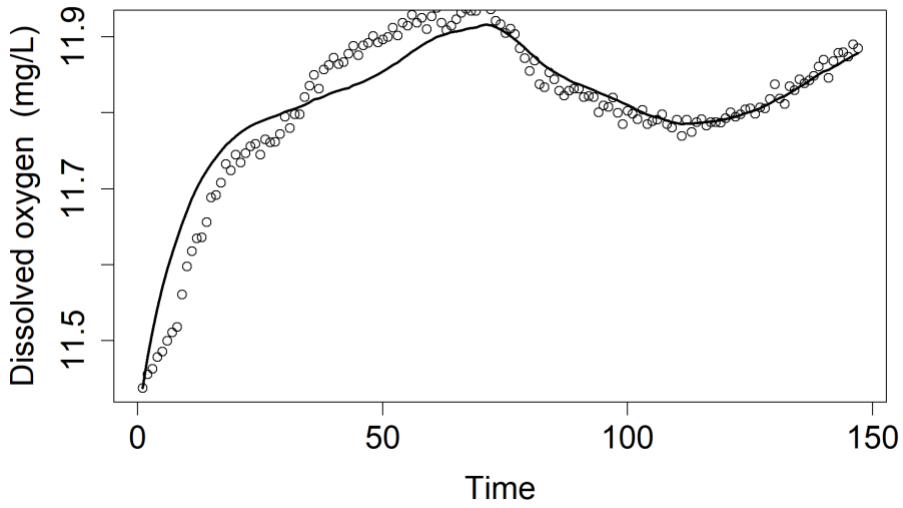
41	1/11/22	BST-down	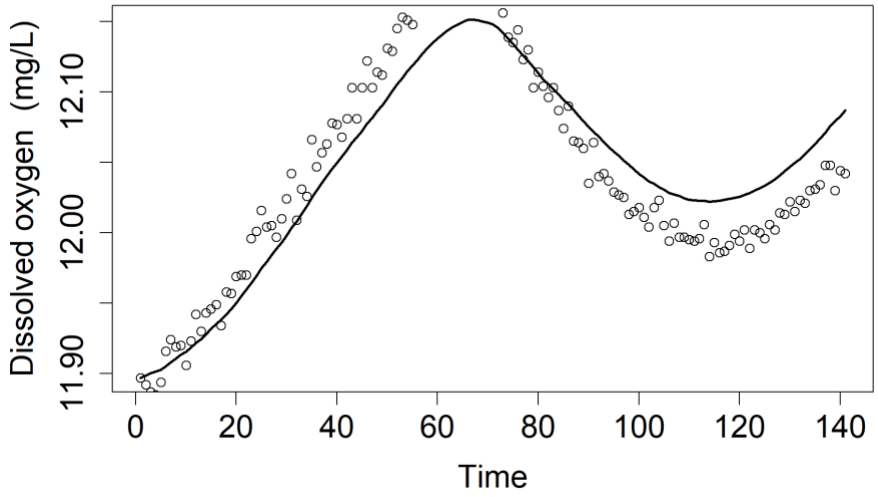

42	1/12/22	BST-down	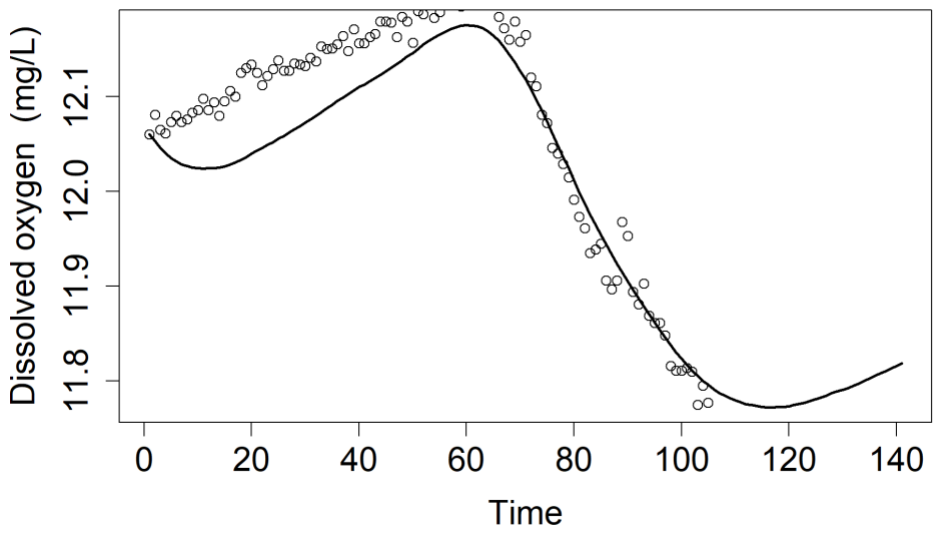
43	1/10/22	BST-mid	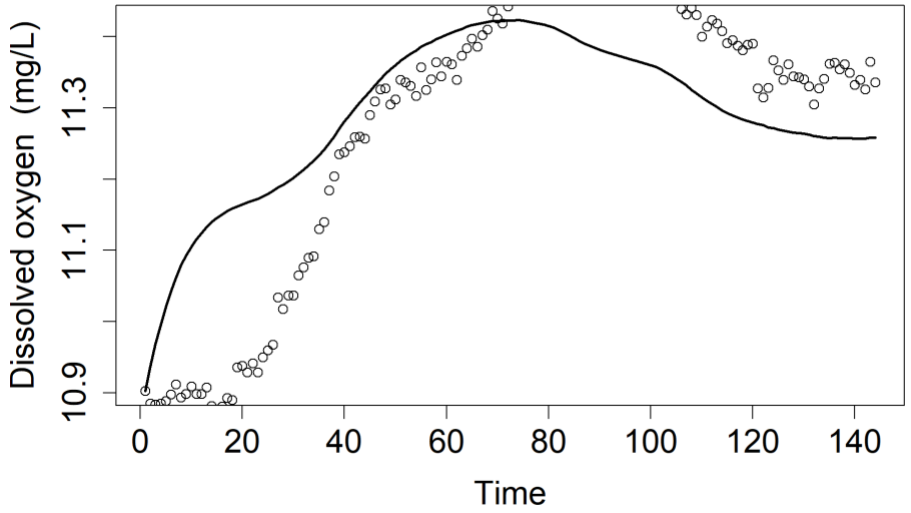

44	1/11/22	BST-mid	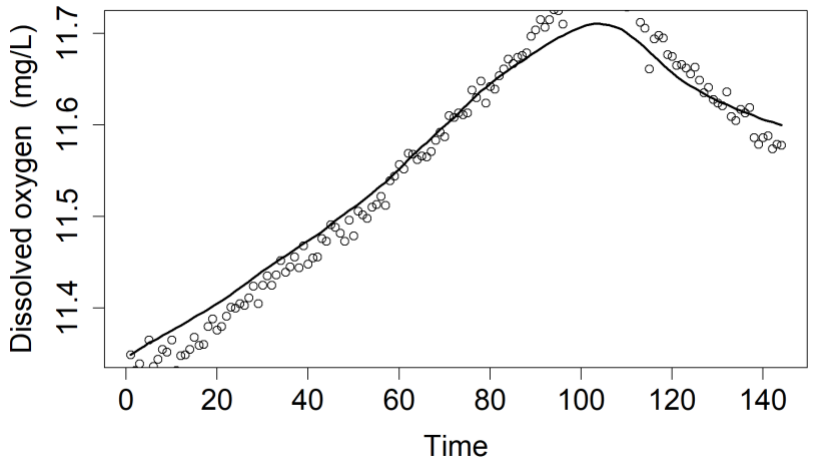
45	1/12/22	BST-mid	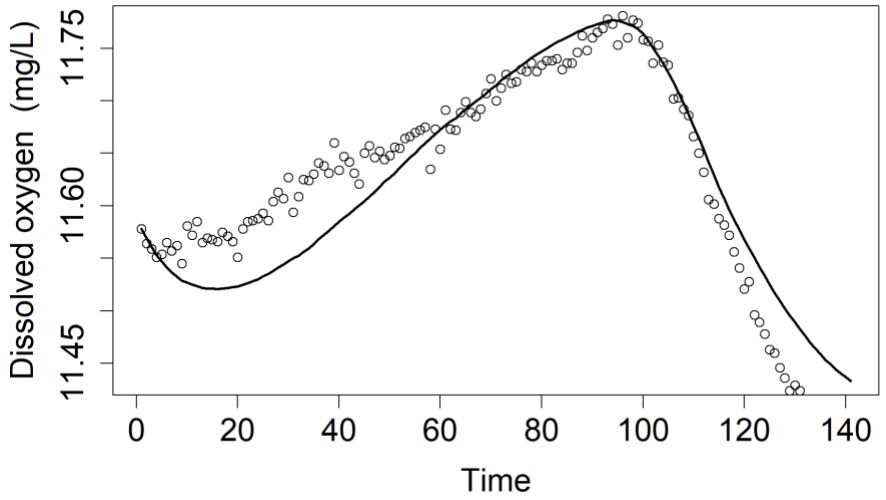

46	1/10/22	BST-up	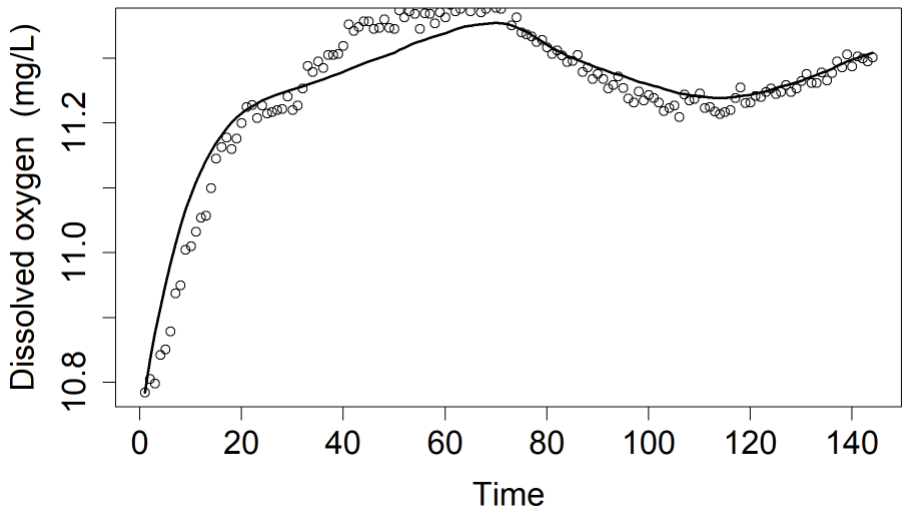
47	1/11/22	BST-up	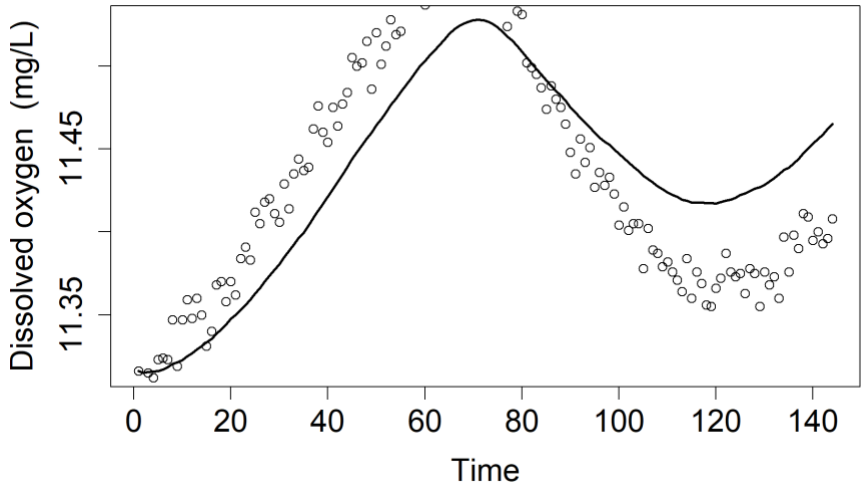

48	1/12/22	BST-up	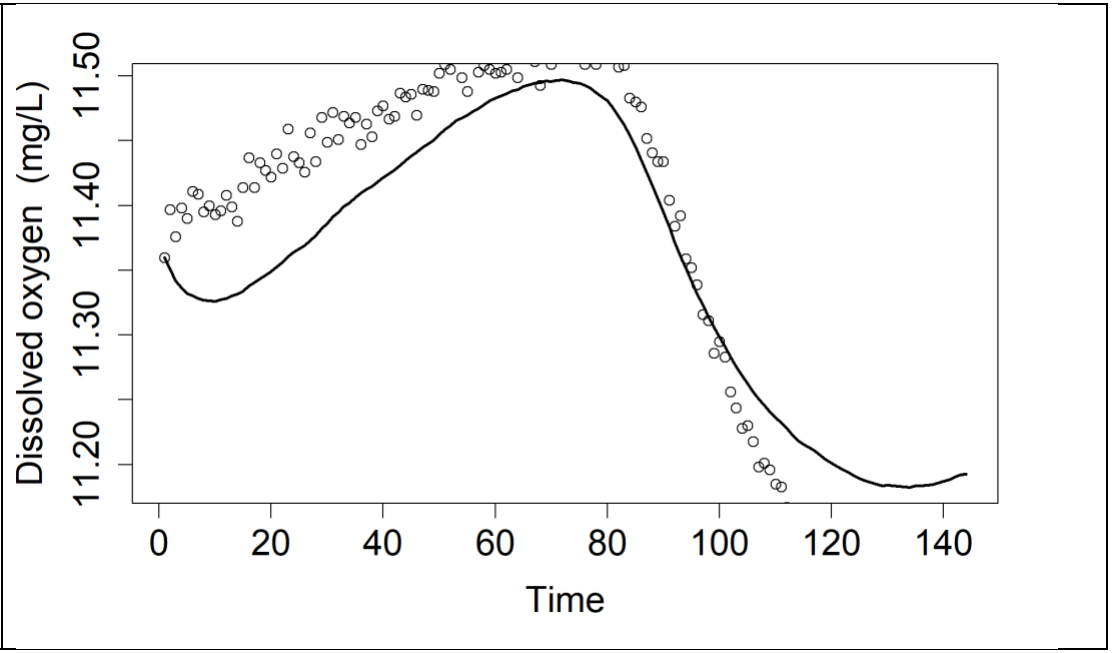

49	1/10/22	MDH-mid	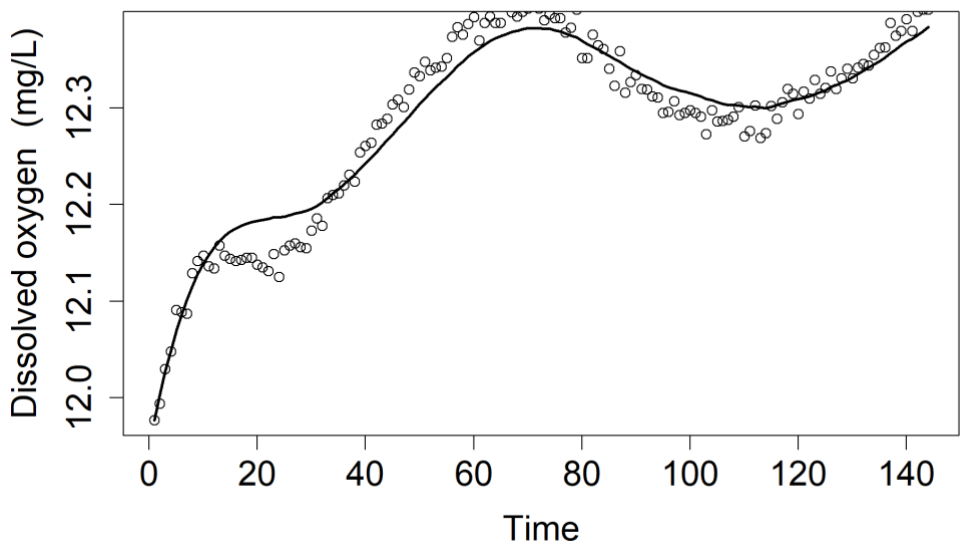

50	1/11/22	MDH-mid	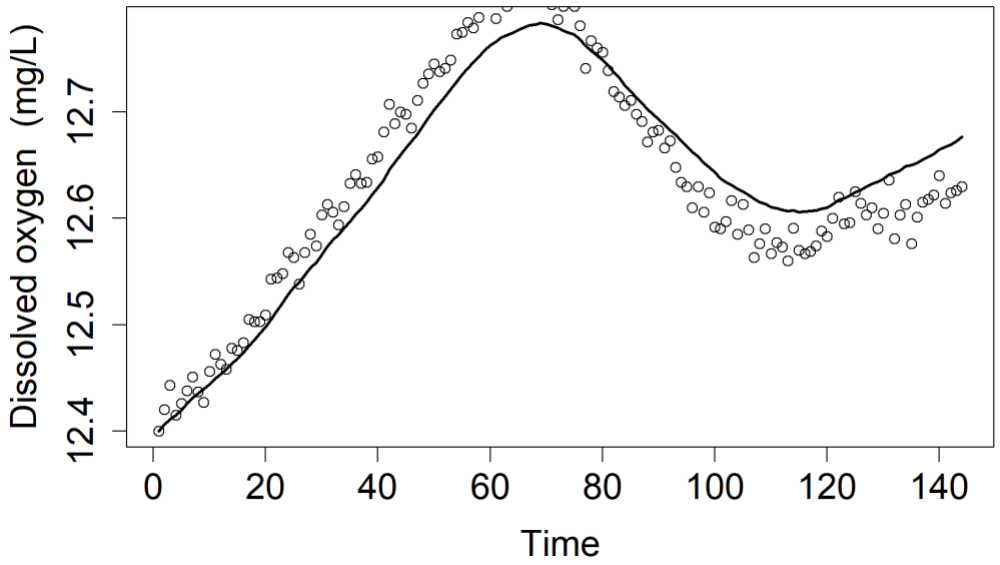
51	1/10/22	MDH-down	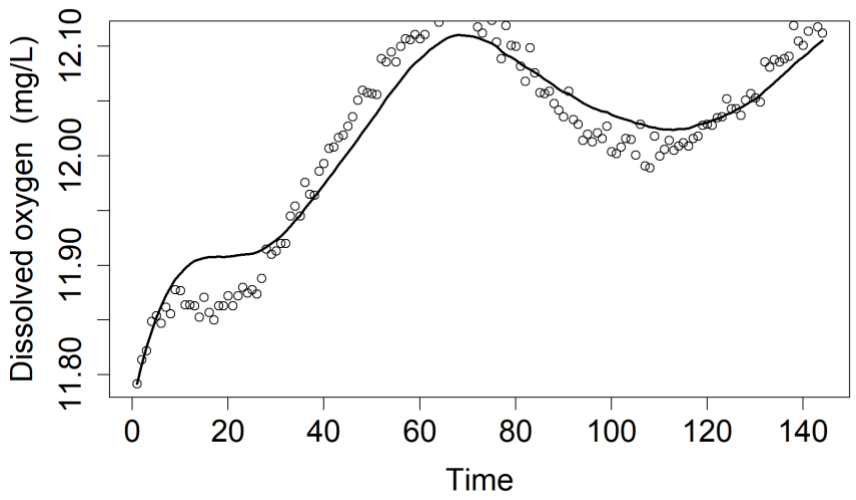

52	1/11/22	MDH-up